Chemical and Nuclear Catalysis Mediated by the Energy Localization in Hydrogenated Crystals and Quasicrystals

Vladimir Dubinko[1,3], Denis Laptev[2,3],
Valeriy Borysenko [1,3], Oleksii Dmytrenko [1,3], Klee Irwin[3]

[1]NSC Kharkov Institute of Physics and Technology, Ukraine

[2]B. Verkin Institute for Low Temperature Physics and Engineering, Ukraine

[3]Quantum Gravity Research, USA

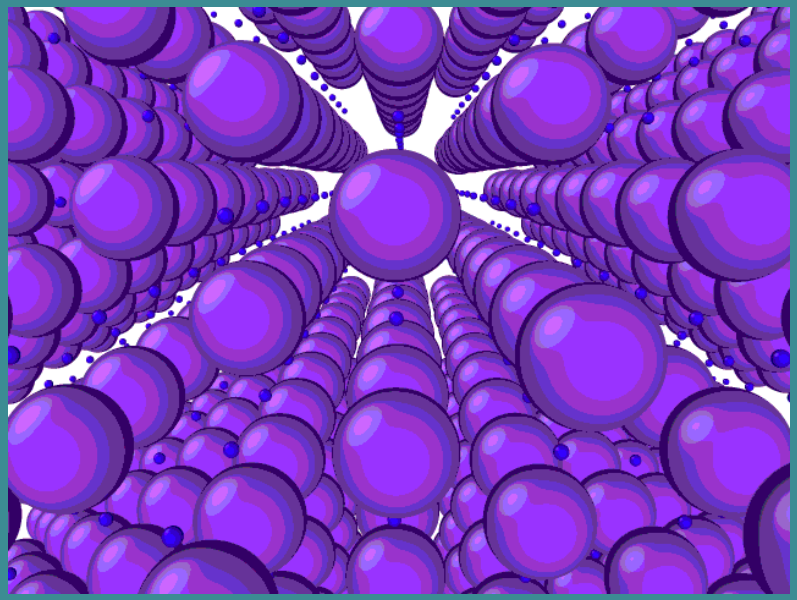

IWAHLM 2018

Outline

- Localized Anharmonic Vibrations (**LAV**) in metals
- **LAV** role in catalysis at high T (violation of Arrhenius low)
- **LAV** role in catalysis at low T (quantum tunneling)
- **LAV** induced **LENR**
- MD simulations in Ni, Pd, Ni-H, Pd-H crystals and Pd nanoclusters
- Experimental results

Energy localization in anharmonic lattices

In the summer of 1953 Enrico Fermi, John Pasta, Stanislaw Ulam, and Mary Tsingou conducted numerical experiments (i.e. computer simulations) of a vibrating string that included a non-linear term (quadratic in one test, cubic in another, and a piecewise linear approximation to a cubic in a third). They found that the behavior of the system was quite different from what intuition would have led them to expect. Fermi thought that after many iterations, the system would exhibit thermalization, an ergodic behavior in which the influence of the initial modes of vibration fade and the system becomes more or less random with all modes excited more or less equally. Instead, the system exhibited a very complicated quasi-periodic behavior. They published their results in a Los Alamos technical report in 1955.

The **FPU paradox** was important both in showing the complexity of nonlinear system behavior and the value of computer simulation in analyzing systems.

Localized Anharmonic Vibrations (LAVs)
A. Ovchinnikov (1969)

Two coupled anharmonic oscillators

$$\ddot{x}_1 + \omega_0^2 x_1 + \varepsilon\lambda x_1^3 = \varepsilon\beta x_2$$
$$\ddot{x}_2 + \omega_0^2 x_2 + \varepsilon\lambda x_2^3 = \varepsilon\beta x_1$$

$$\tau = \frac{\omega_0}{\varepsilon\beta}\int_0^{\pi/2} \frac{d\eta}{\sqrt{1-\left(\frac{3A_0\lambda}{4\beta}\right)^2 \sin^2\eta}}$$

Localization condition

$$A_0 > \frac{4\beta}{3\lambda} \Rightarrow \tau \to \infty$$

Phase diagram

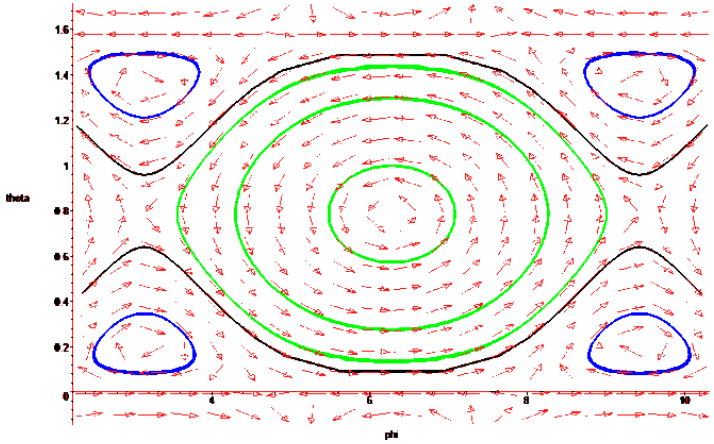

1D crystal — Hirota lattice model
(nonlinear telegraph equations, 1973)

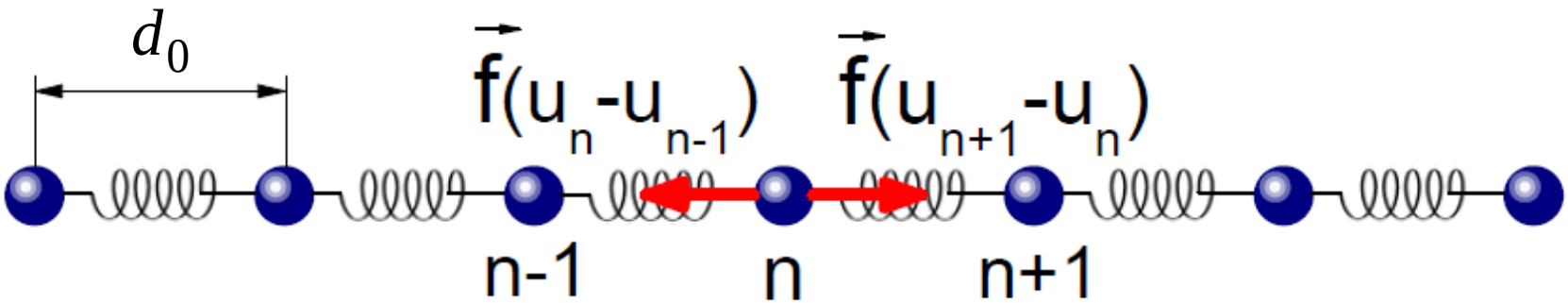

Equation of motion of Hirota lattice

$$\frac{m\ddot{u}_n}{1+\frac{\pi^2}{4}\frac{\dot{u}_n^2}{s^2}} = \frac{2}{\pi}\gamma d_0 \left\{ \mathrm{tg}\left[\frac{\pi}{2}\left(\frac{u_{n\text{-}1}-u_n}{d_0}\right)\right] - \mathrm{tg}\left[\frac{\pi}{2}\left(\frac{u_n-u_{n+1}}{d_0}\right)\right]\right\}$$

$$H = \left(\frac{2}{\pi}\right)^2 ms^2 \sum_{n=-\infty}^{+\infty}\left\{\frac{1}{2}\ln\left[1+\mathrm{tg}^2\left(\frac{\pi}{2}\frac{p_n}{ms}\right)\right] + \frac{1}{2}\ln\left[1+\mathrm{tg}^2\left(\frac{\pi}{2d_0}(u_{n-1}-u_n)\right)\right]\right\}$$

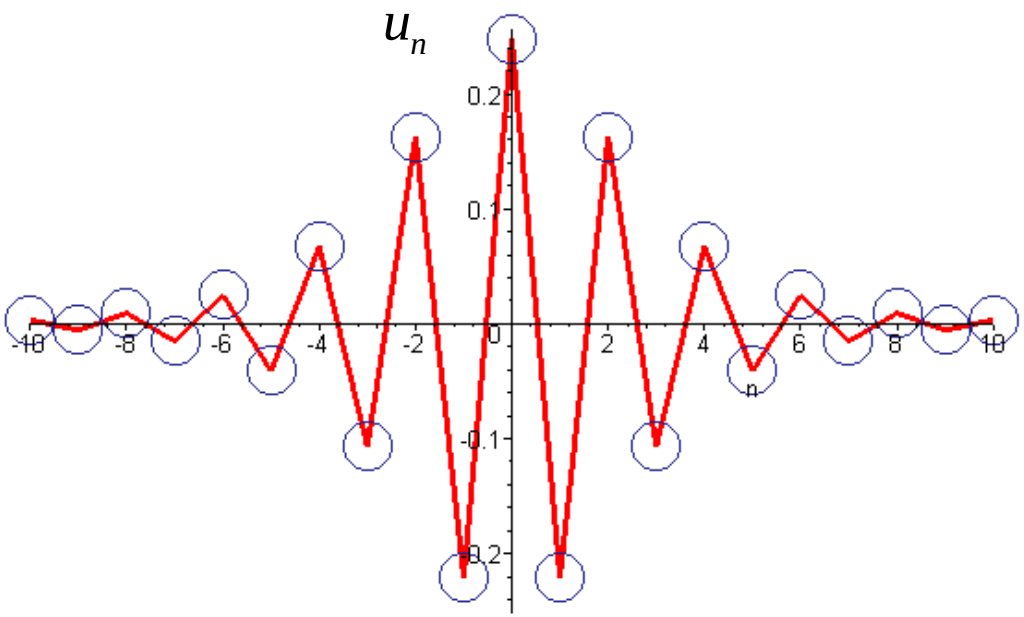

Standing **weakly localized** DB

Bogdan, 2002

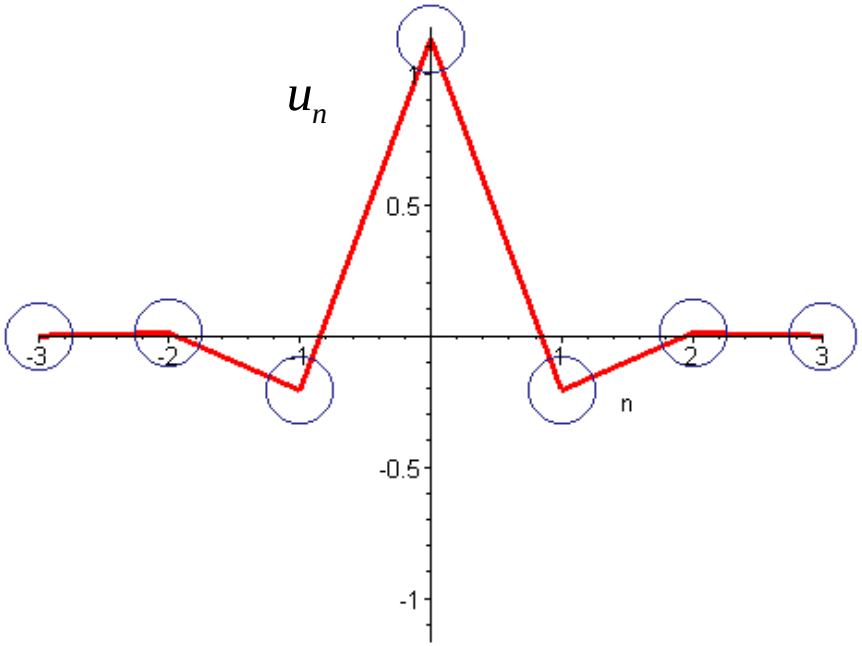

Standing **strongly localized** DB

$$u_n^{(b)} = \frac{2d_0}{\pi}\,\mathrm{arctg}\left[\frac{\mathrm{sh}\left(\kappa d_0/2\right)}{\sin\left(kd_0/2\right)}\frac{\cos\left(knd_0-\omega t\right)}{\mathrm{ch}\,\kappa\left(nd_0-Vt\right)}\right],$$

Bogdan, 2002

$$\omega = \frac{s}{d_0}\,2\,\mathrm{ch}\left(\frac{\kappa d_0}{2}\right)\sin\left(\frac{kd_0}{2}\right), \qquad V = s\,\frac{\mathrm{sh}\left(\kappa d_0/2\right)}{\kappa d_0/2}\cos\left(\frac{kd_0}{2}\right).$$

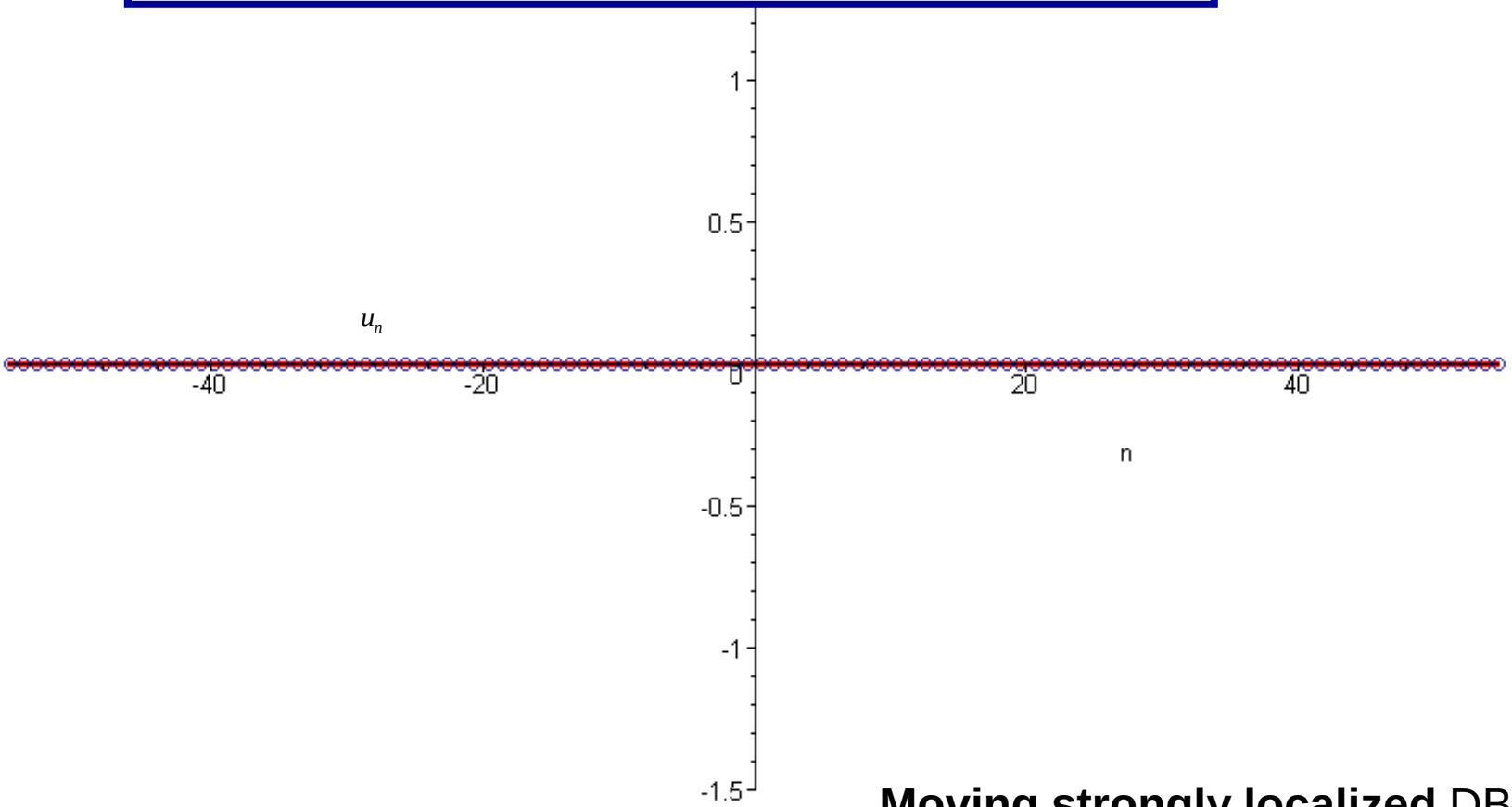

Moving strongly localized DB

Nonlinear coupled oscillators

$$V=\sum V(X_n)+C\,W(X_n,X_{n+1})$$

- Exact, periodic and localized solution

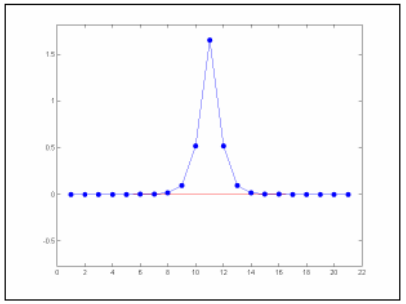

Phonons

- Frequency band $\omega^2_{ph}=w^2_0+4\,C\sin^2 q/2$
- Non localized states

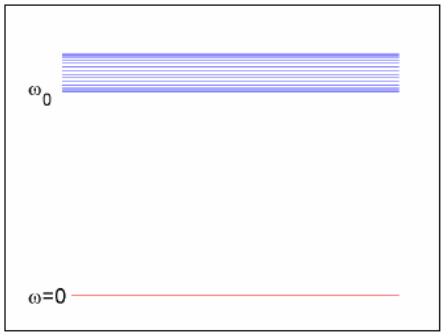

The concept of **LAV** in regular lattices is based on *large anharmonic* atomic oscillations in **Discrete Breathers** excited outside the phonon bands.

Existence of breathers (1994)

Soft Hard

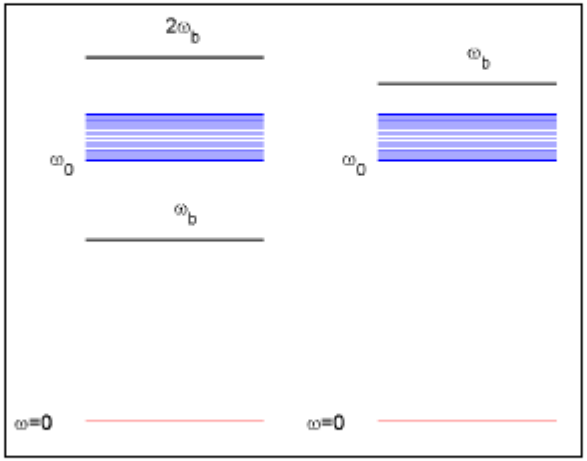

$$n\,\omega_b \notin [\omega_0, \omega_{f,máx}], \quad \omega_b'(E) \neq 0$$

LAV examples:

- Discrete Breathers in periodic crystals
- Phasons in quasicrystals
- Calthrate guest-host systems
- Dynamics of the central tetrahedron in Tsai QCs
- Vibrations of magic clusters
- etc

DBs in metals Hizhnyakov et al (2011)

PREDICTION OF HIGH-FREQUENCY INTRINSIC . . .

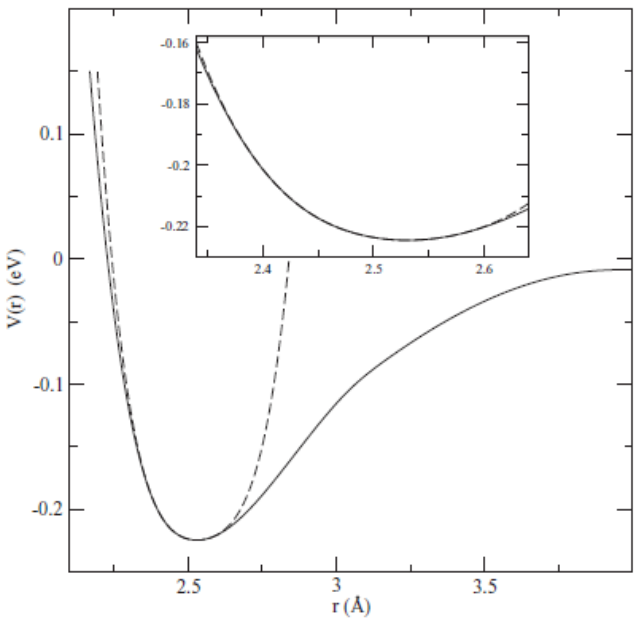

FIG. 1. The pair potential $V(r)$ of Ni (solid line) and its approximation by the fourth-order polynomial (dashed line). The inset shows an expanded view.

The distance between the nearest atoms in Ni at room temperature is $r_0 = 2.49$ Å and longitudinal sound velocity is $v_l = 5266$ m/s. These values give $\tilde{K}_2 = 2.75$ eV/Å^2 (as expected, $\tilde{K}_2 > K_2$) and $\tilde{\kappa} \approx 1.2$. The distance r_0 increases

HAAS, HIZHNYAKOV, SHELKAN, KLOPOV, AND SIEVERS

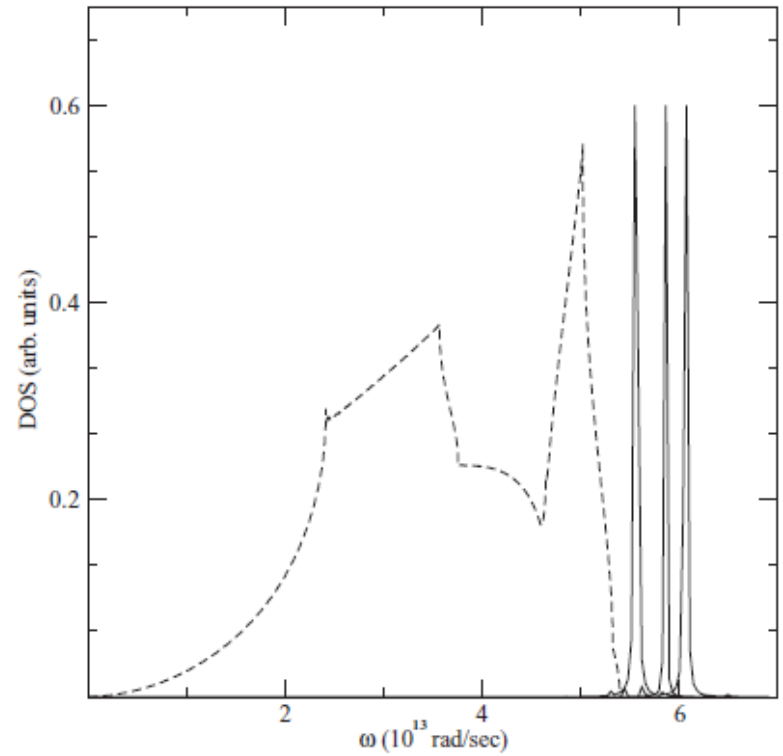

FIG. 2. Phonon density of states and three ILM spectral signatures for Ni. Phonon spectrum (dashed line) and spectrographs (solid line) of the different ILM's: The frequencies are 5.58, 5.86, and 6.07 (10^{13} rad/s) and the amplitudes of vibrations of the central bond are 0.18, 0.31, and 0.42 Å.

Standing DB in bcc Fe: d_0=0.3 Å

D.Terentyev, V. Dubinko, A. Dubinko (2013)

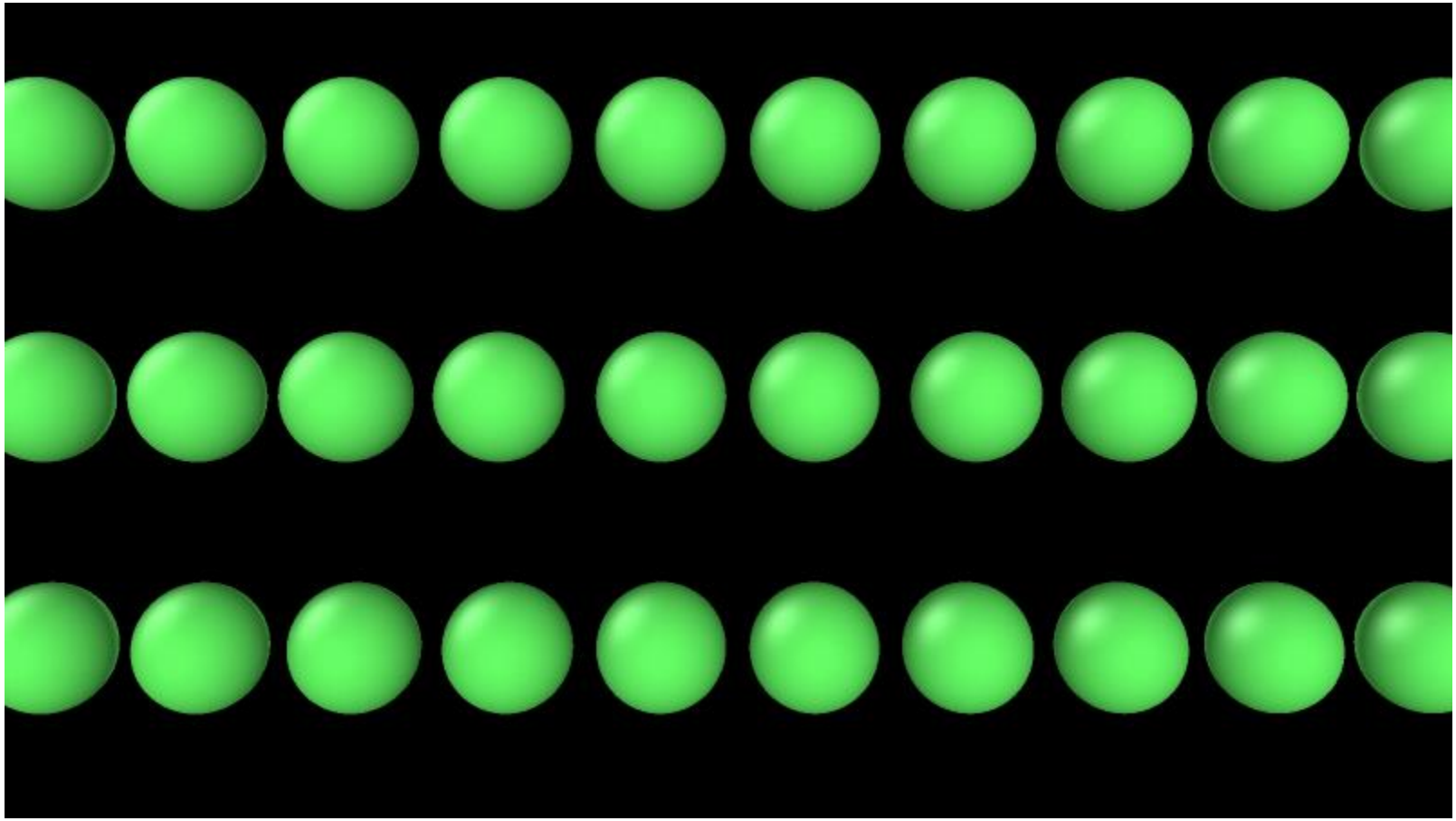

DB along [111] direction in bcc Fe at T=0K

Modelling Simul. Mater. Sci. Eng. **23** (2015) 085007 D A Terentyev *et al*

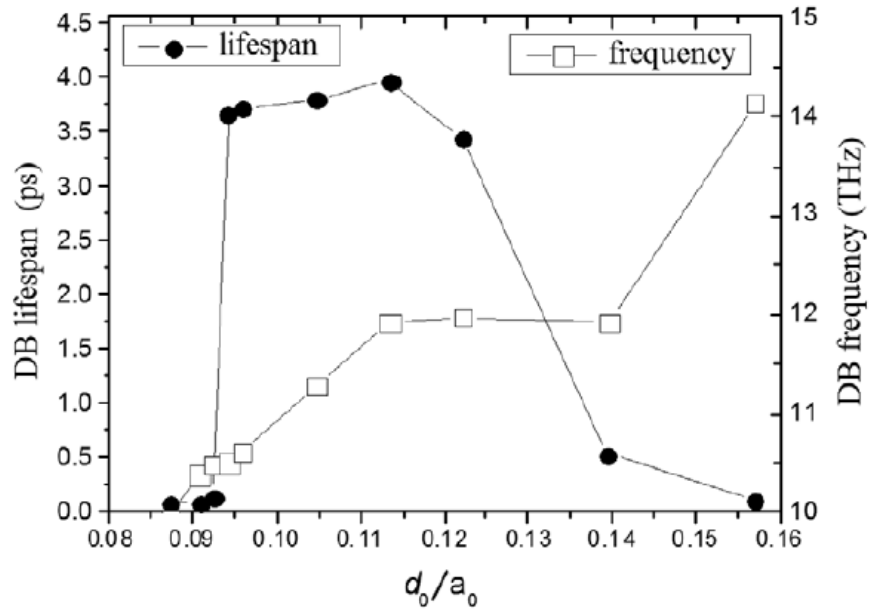

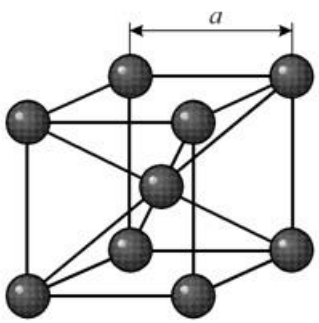

Figure 1. Lifespan and frequency of standing DB as the function of the relative initial displacement d_0/a_0 for the IAP derived in [28].

Initial conditions:

$$x_{n-2} = +0.2 \quad x_{n-1} = -0.2 \quad x_n = +0.4 \quad x_{n+1} = -0.4 \quad x_{n+2} = +0.2 \quad x_{n+3} = -0.2$$

Boundary conditions: periodic

It is seen from the visualization, that the DB has been generated from the initial anti-phase displacements of 6 atoms.

Moving DB in bcc Fe: d_0=0.4 Å, E= 0.3 eV

D.Terentyev, V. Dubinko, A. Dubinko (2013)

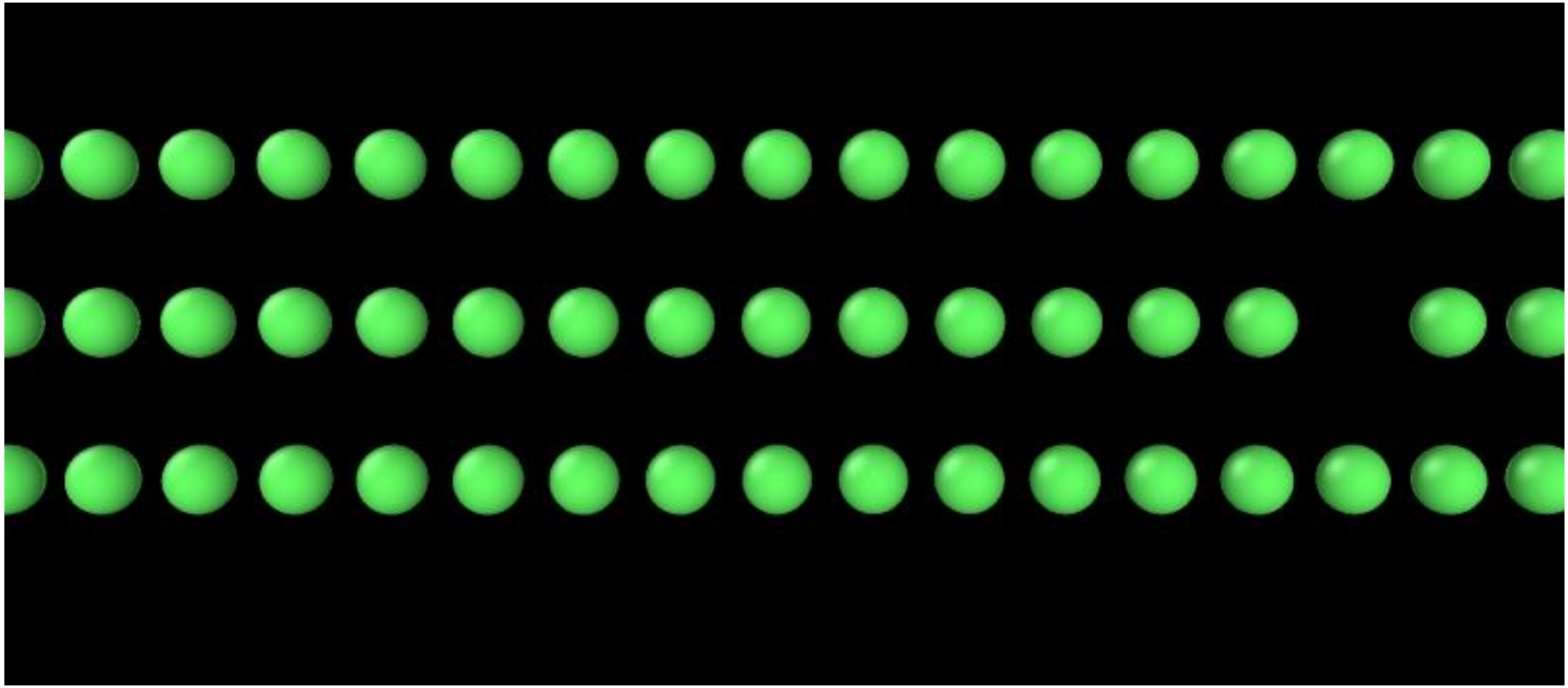

DB in bulk Pd 3D lattice (2017)

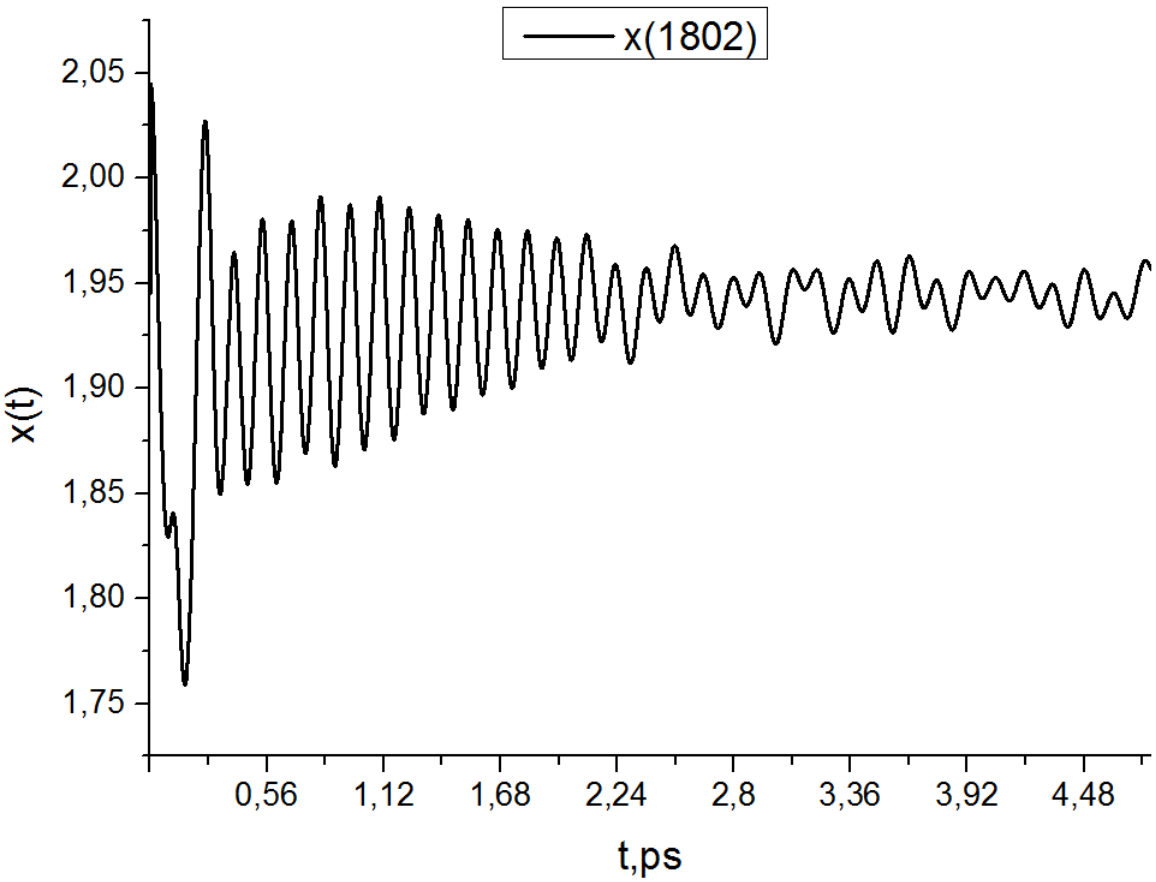

LAV Time Period= 0.1292 ps
LAV frequency = 7.7399 THz

The DB frequency lies above the phonon vibration spectrum

Effective ‘temperature’ of DB (#1100) and lattice (#1095) atom in fcc Pd lattice

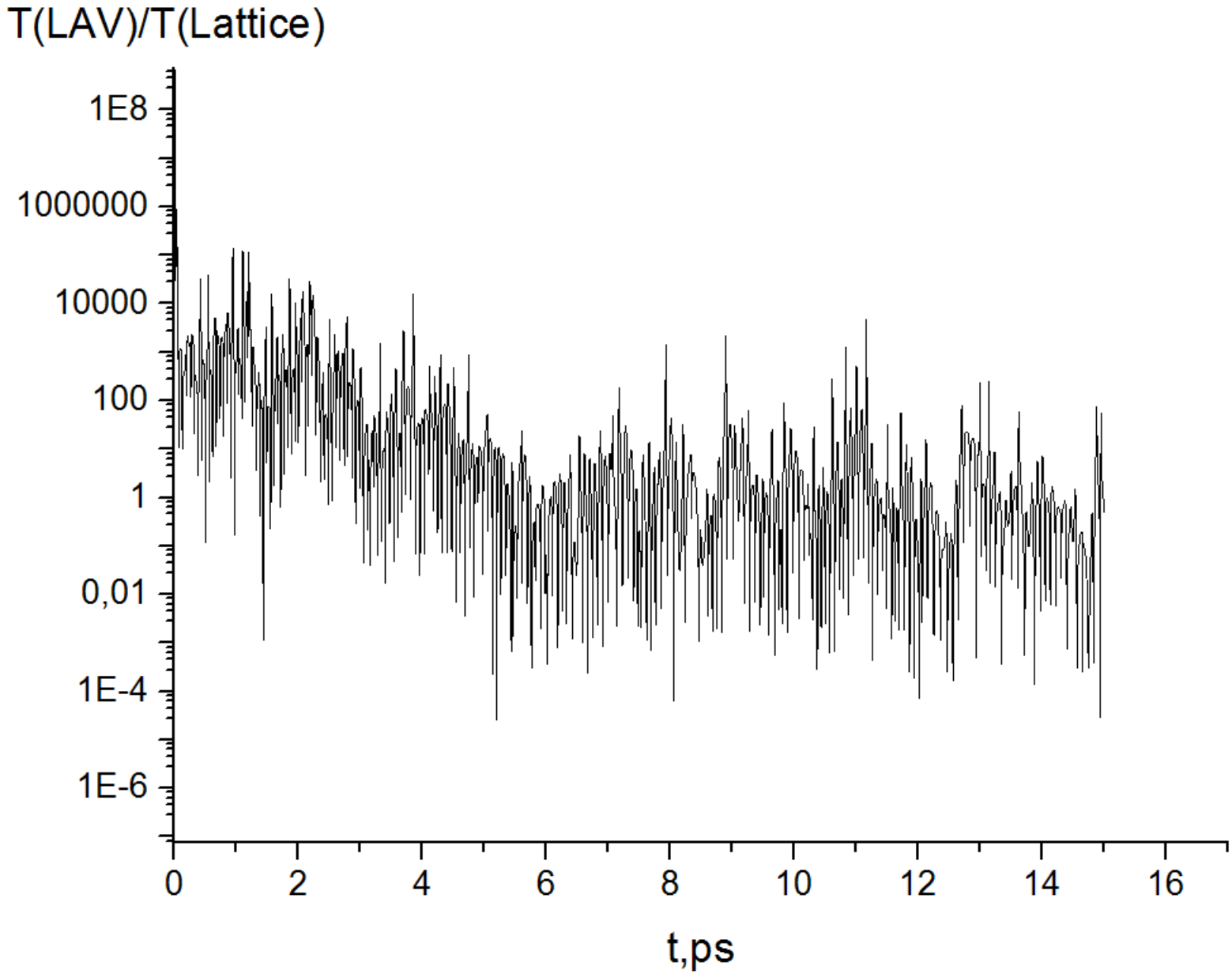

DB effect (1): peiodic in time modulation of the potential barrier height

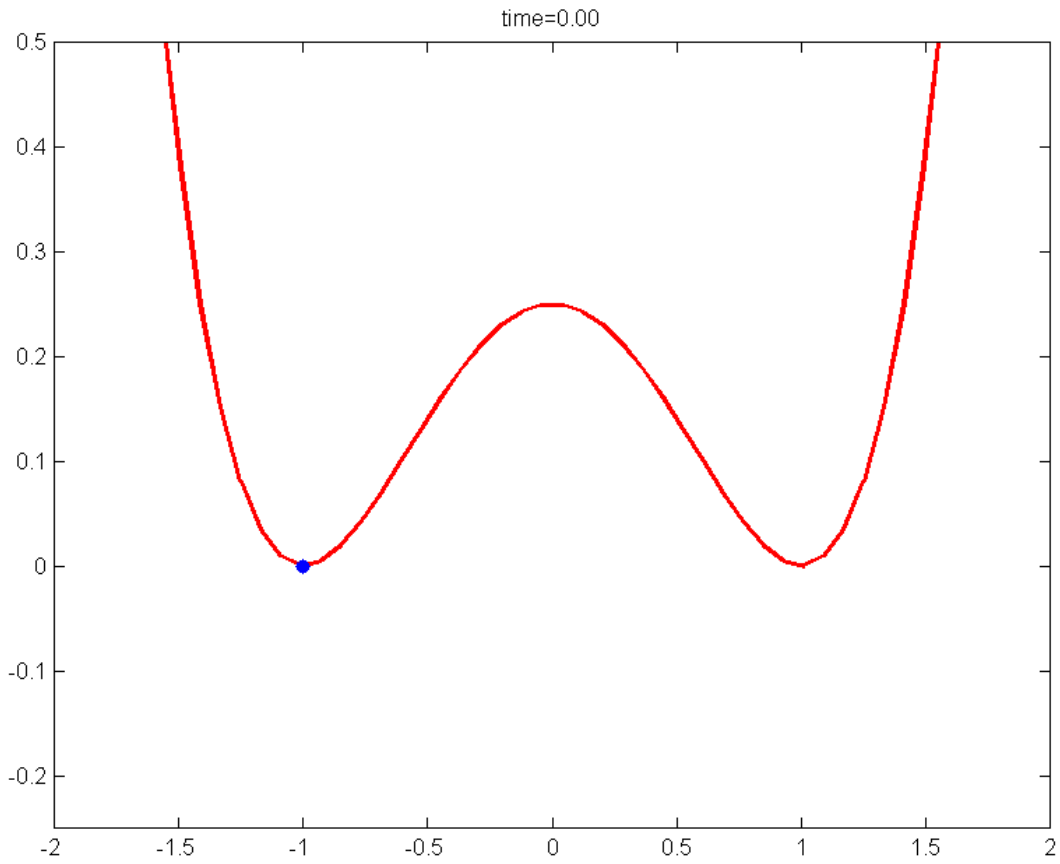

Reaction-rate theory with account of the crystal anharmonicity

Dubinko, Selyshchev, Archilla, Phys. Rev. E. (2011)

$$R_K = \frac{\omega_0}{2\pi}\exp\left[-E_0/k_B T\right]$$ <= Kramers rate

$$U(x,t) = U(x) - (V \cdot x/x_m)\cos(\Omega t)$$

Kramers rate is amplified by:

$I_0\left(V_m/k_B T\right)$ - Bessel function

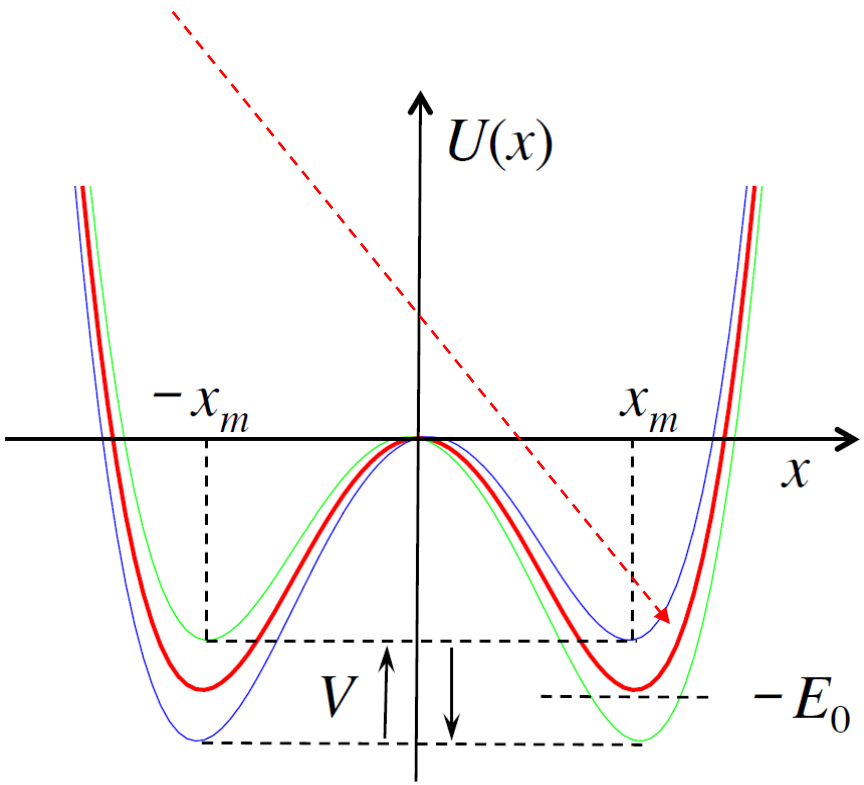

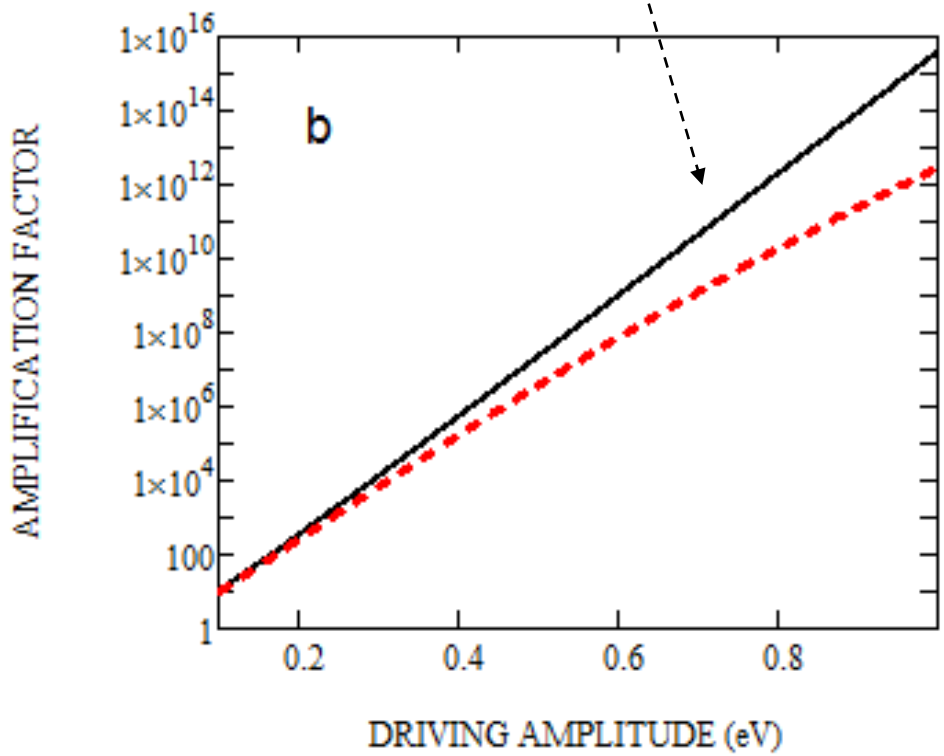

Low temperature reconstructive transformation of muscovite

$K_2[Si_6Al_2]^{IV}[Al_4]^{VI}O_{20}(OH)_4$

Disilicate of Lutetium
$Lu_2Si_2O_7$

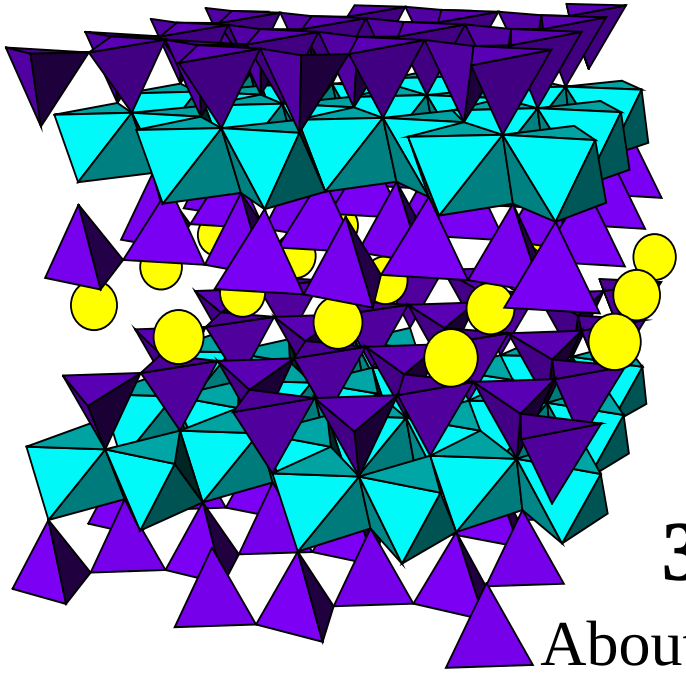

E_a >1 eV

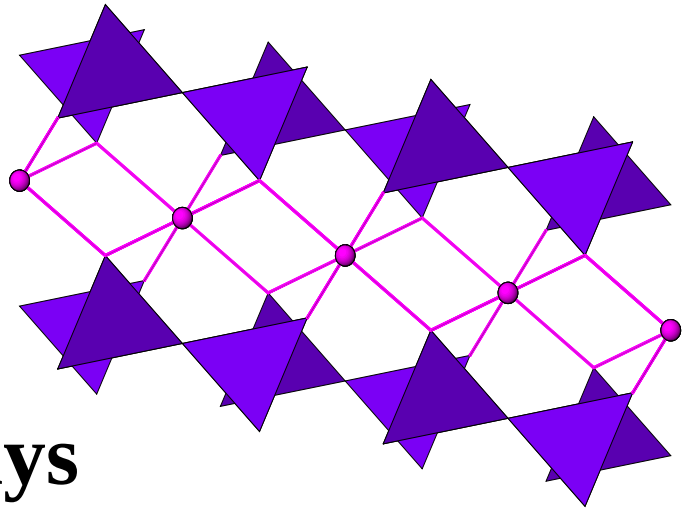

300° C, 3 days

About 36% of muscovite is transformed, which is **10^4 - 10^5** times faster than by **Arrhenius law:**

K$^+$

At T= 1000° C, 3 days

At T = 300° C, 10^3 years

$$\dot{R}_K = \nu \exp(-E_a/k_b T)$$

Transformation rate of muscovite with account of DB statistics Dubinko et al (2011)

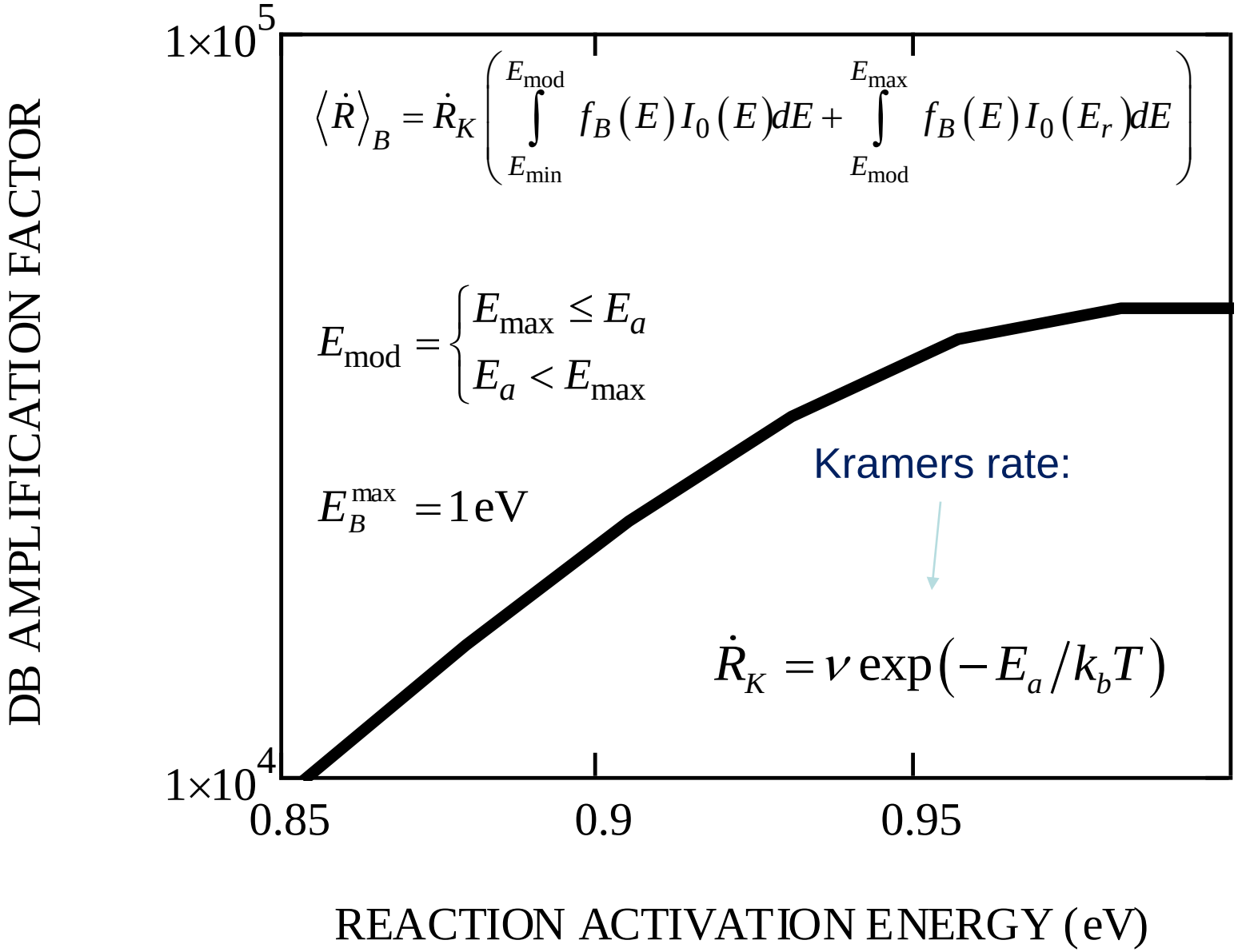

How extend this concept to include

Quantum effects, Tunneling

?

Tunneling: Numerical solution of **Schrödinger equation**

Stationary: $t_{Kramers}$~10^5 cycles at $\mathbf{V_{barrier}=12E_0}$

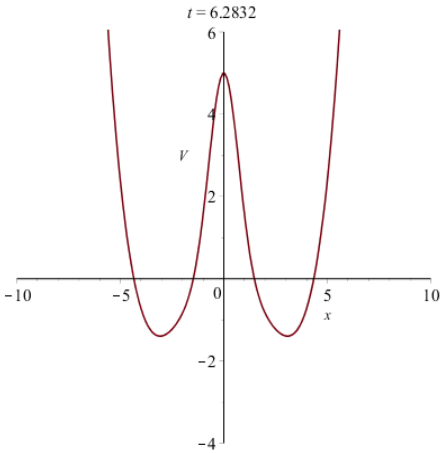

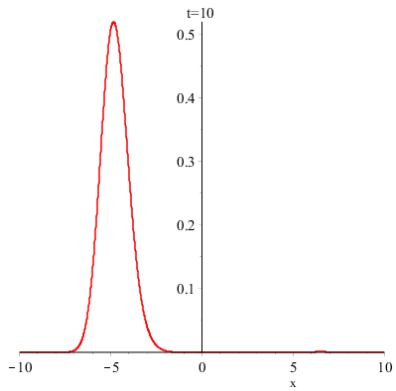

10 cycles

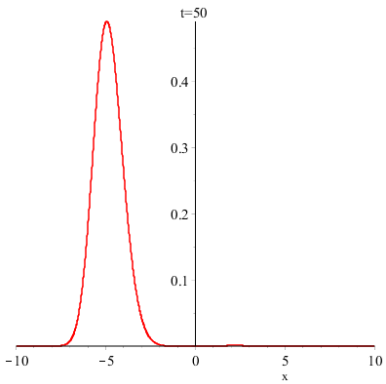

50 cycles

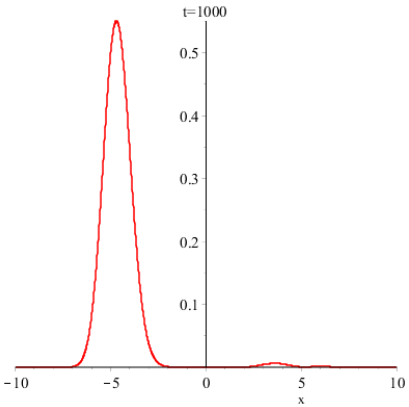

1000 cycles

Time-periodically driven: **$\Omega = 1.5\ \omega_0$, $g = 0.2$**

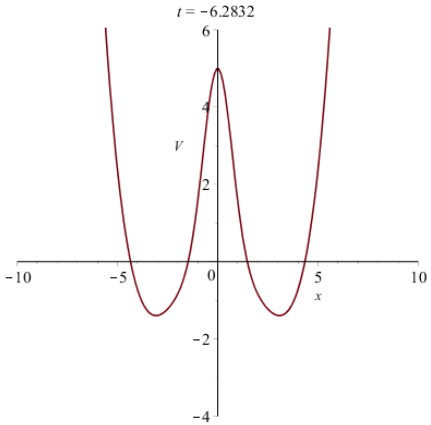

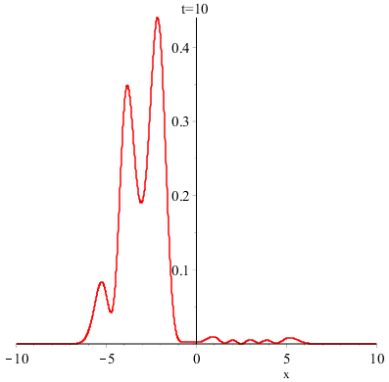

10 cycles

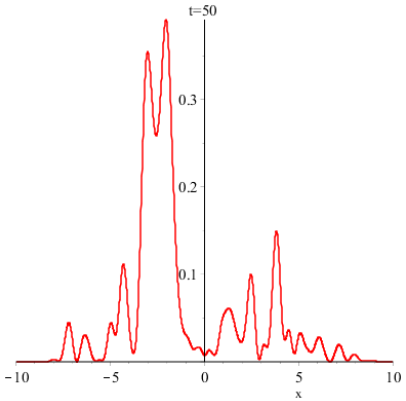

50 cycles

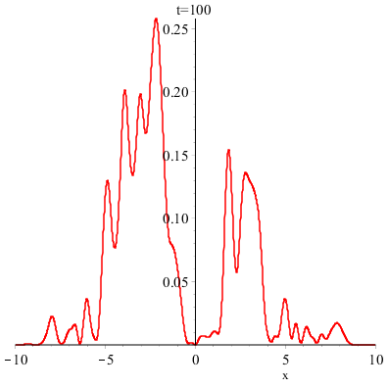

100 cycles

Tunneling as a classical escape rate induced by the vacuum zero-point radiation, A.J. Faria, H.M. Franca, R.C. Sponchiado Foundations of Physics (2006)

The Kramers theory is extended in order to take into account both the action of the thermal and zero-point oscillation (ZPO) energy.

$$R_K = \frac{\omega_0}{2\pi} \exp\left[-E_0 / D(T)\right]$$

$$D(T) = E_{ZPO} \coth\left(E_{ZPO}/k_B T\right) \approx \begin{cases} E_{ZPO}, \ T \to 0 \\ k_B T, \ T >> E_{ZPO}/k_B \end{cases}$$

T – temperature is a measure of *thermal* noise strength

$$E_{ZPO} = \frac{\hbar \omega_0}{2}$$ - ZPO energy is a measure of *quantum* noise strength

When we heat the system we increase temperature, i.e. we increase the *thermal* noise strength

Can we increase
the *quantum* noise strength,
i.e. ZPO energy?

Stationary harmonic potential

$$\langle E \rangle_n = \hbar\omega_0 \left(n + \frac{1}{2} \right)$$

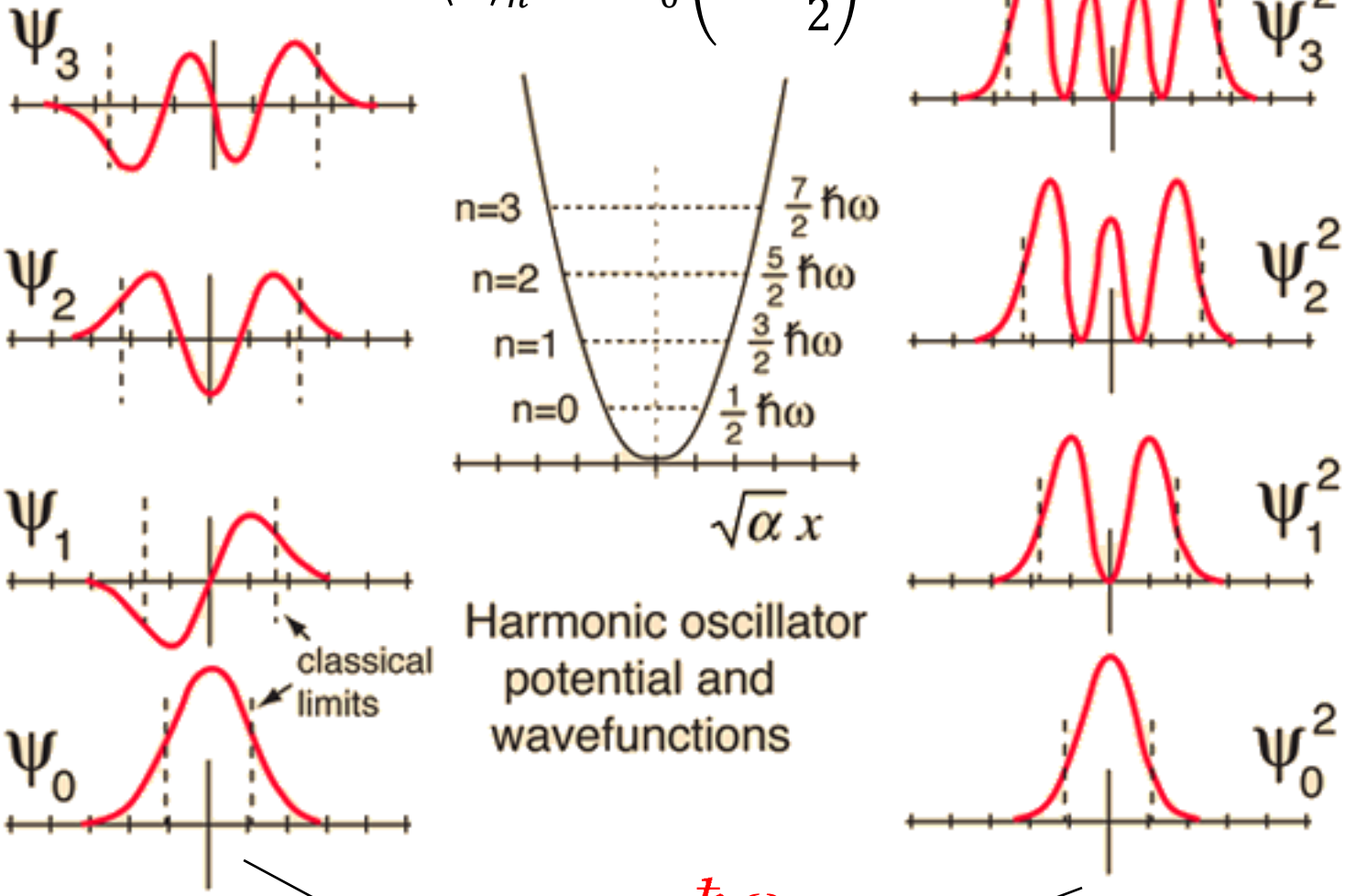

$$E_{ZPO} = \frac{\hbar\omega_0}{2}$$

Time-periodic modulation of the double-well shape changes (i) eigenfrequency and (ii) position of the wells

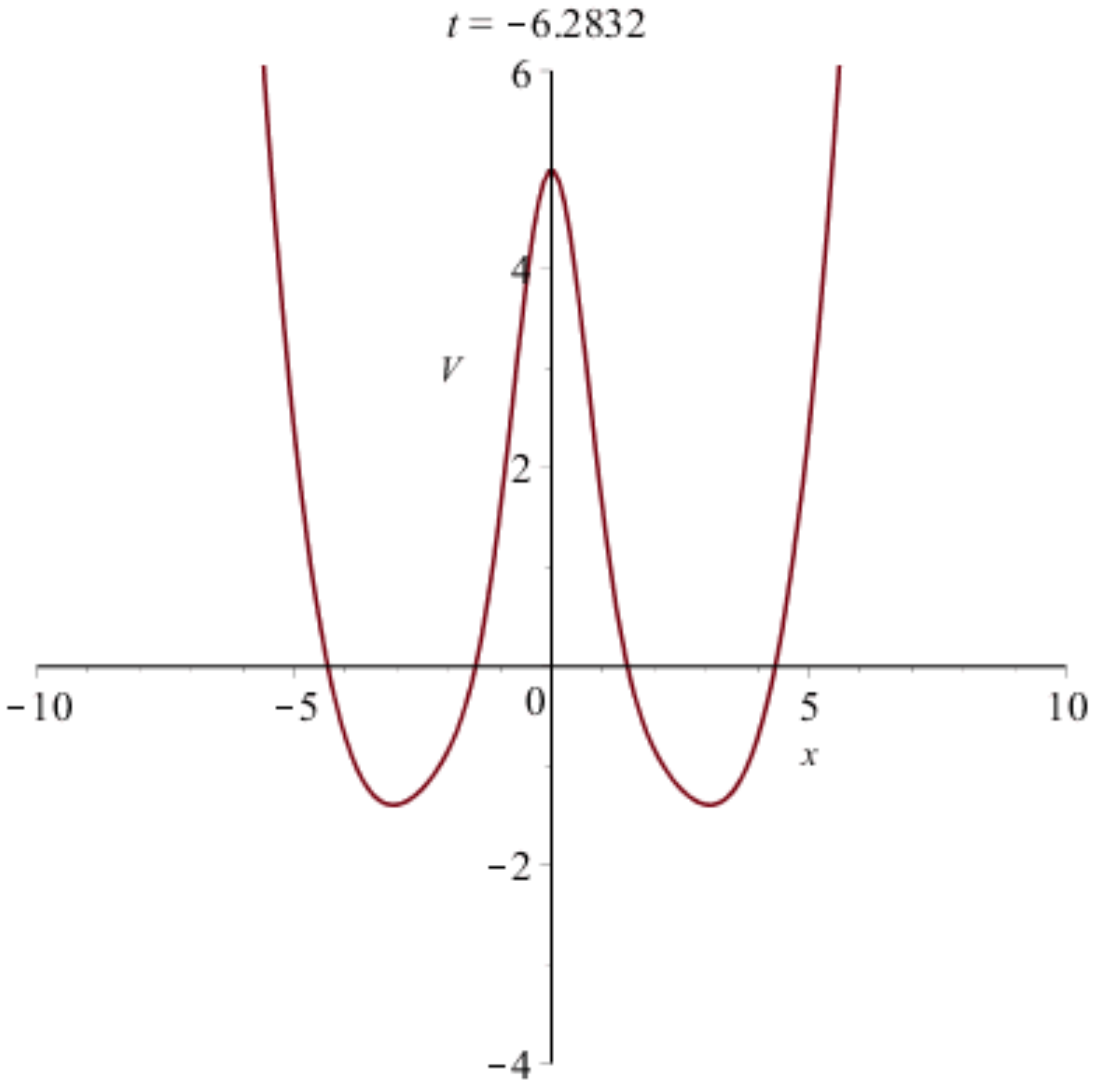

Parametric resonance with **time-periodic eigenfrequency $\Omega = 2\omega_0$**

$$i\hbar\frac{\partial\psi}{\partial t} = -\frac{\hbar^2}{2m}\frac{\partial^2\psi}{\partial x^2} + \frac{m\omega^2(t)}{2}x^2\psi$$

Schrödinger equation

$$\psi(x_0, t_0 = 0) = \frac{1}{\sqrt[4]{2\pi\sigma_0}}\exp\left(-\frac{x_0^2}{4\sigma_0}\right)$$

Initial Gaussian packet $\sigma_0 = \dfrac{\hbar}{2m\omega_0}$

Parametric regime $\Omega = 2\omega_0$:

$$\ddot{x} + \omega_0^2\left[1 - g\cos(2\omega_0 t)\right]x = 0$$

g << 1 – modulation amplitude

$$\sigma_x(t) = \sigma_0\cosh\left(\frac{g\omega_0 t}{2}\right)\left[1 + \tanh\left(\frac{g\omega_0 t}{2}\right)\sin(2\omega_0 t)\right]$$

dispersion

ZPO energy:

$$E_{ZPO}(t) = \frac{\hbar\omega_0}{2}\cosh\frac{g\omega_0 t}{2}$$

ZPO amplitude:

$$\Lambda_{ZPO}(t) = \sqrt{\frac{\hbar}{2m\omega_0}\cosh\frac{g\omega_0 t}{2}}$$

Non-stationary harmonic potential with **time-periodic eigenfrequency $\Omega = 2\omega_0$**

$$\Lambda_{ZPO}(t) = \sqrt{\frac{\hbar}{2m\omega_0}\cosh\frac{g\omega_0 t}{2}}$$

$$E_{ZPO}(t) = \frac{\hbar\omega_0}{2}\cosh\frac{g\omega_0 t}{2}$$

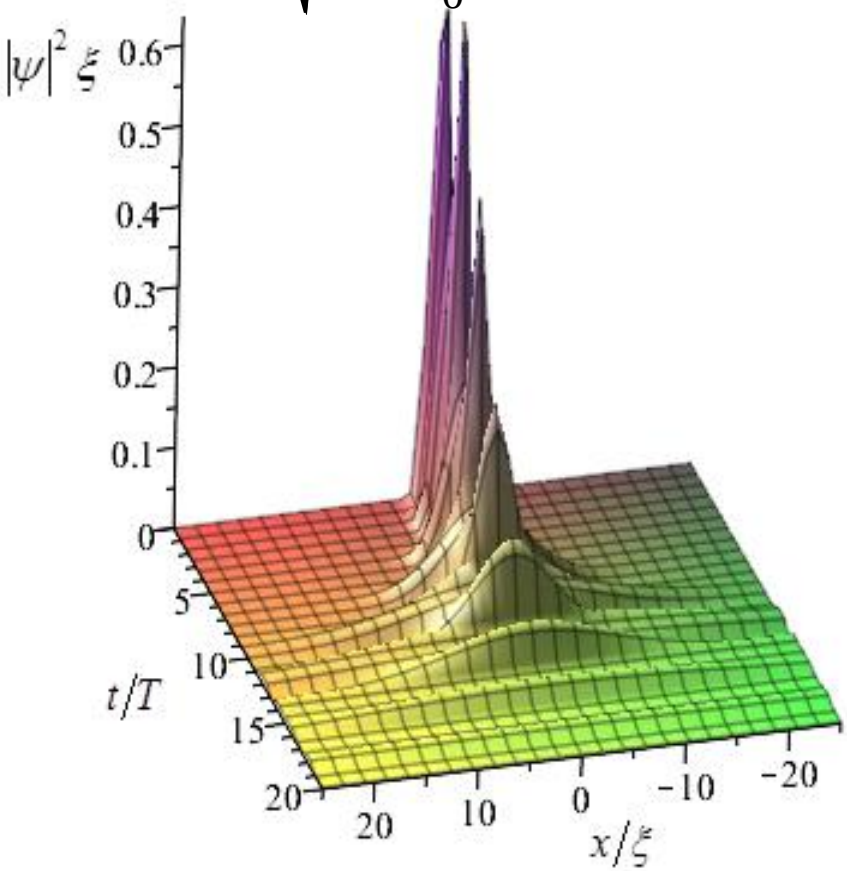

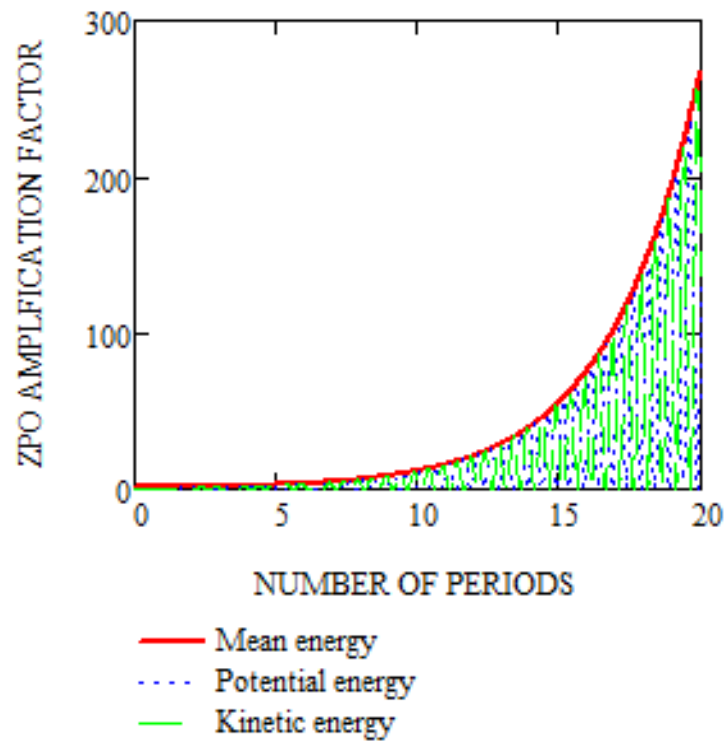

Escape rate in the modified Kramers theory with account of parametric driving of the **well eigenfrequency** $\Omega = 2\omega_0$

E_0 = 1 eV – the well depth; g=0.1 – the modulation amplitude

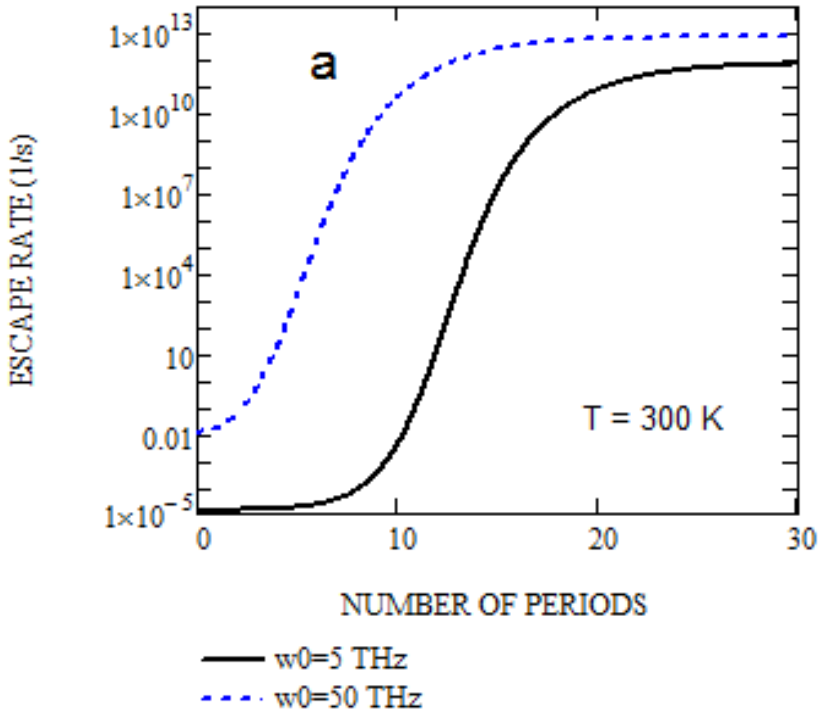

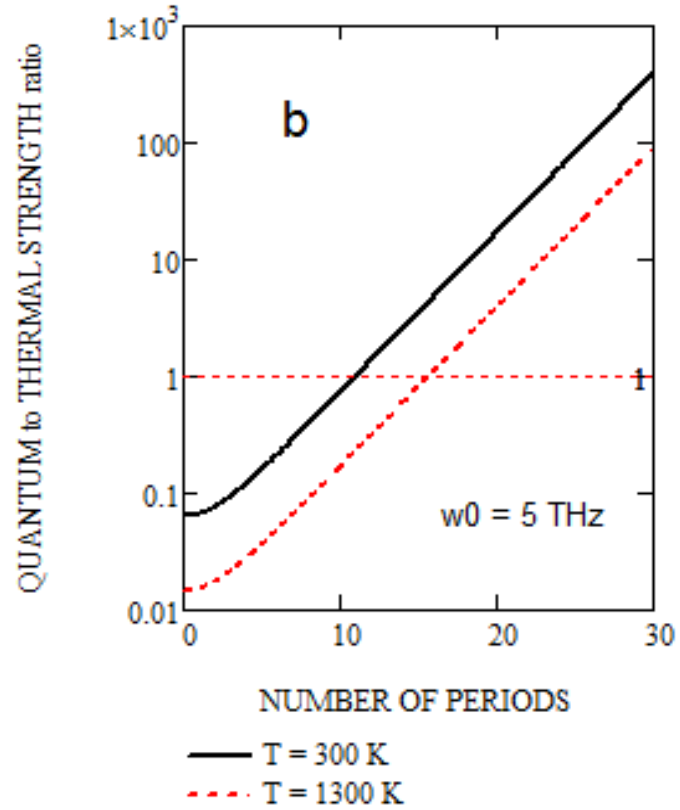

Non-stationary harmonic potential with **time-periodic** shifting of the **well position at $\Omega = \omega_0$**

$$\langle E \rangle = \frac{\hbar\omega_0}{2} + \frac{\left(g_A A_{ZPO}\right)^2 m\omega_0^2}{8}\left[\omega_0^2 t^2 + \omega_0 t \sin 2\omega_0 t + \sin^2 \omega_0 t\right]$$

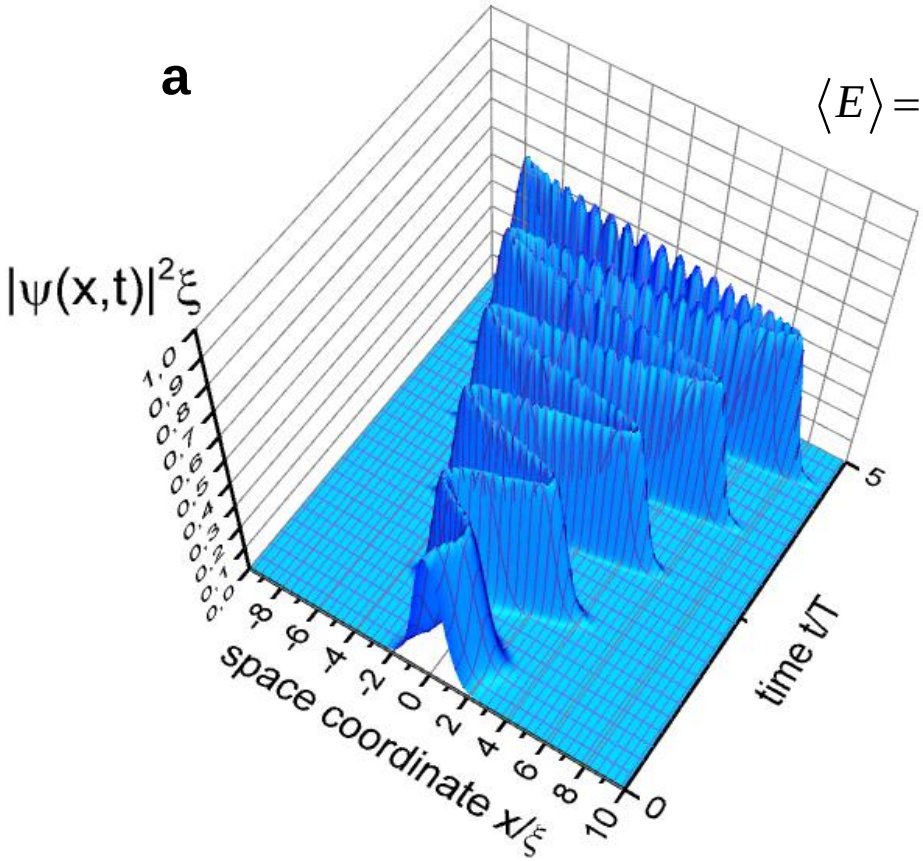

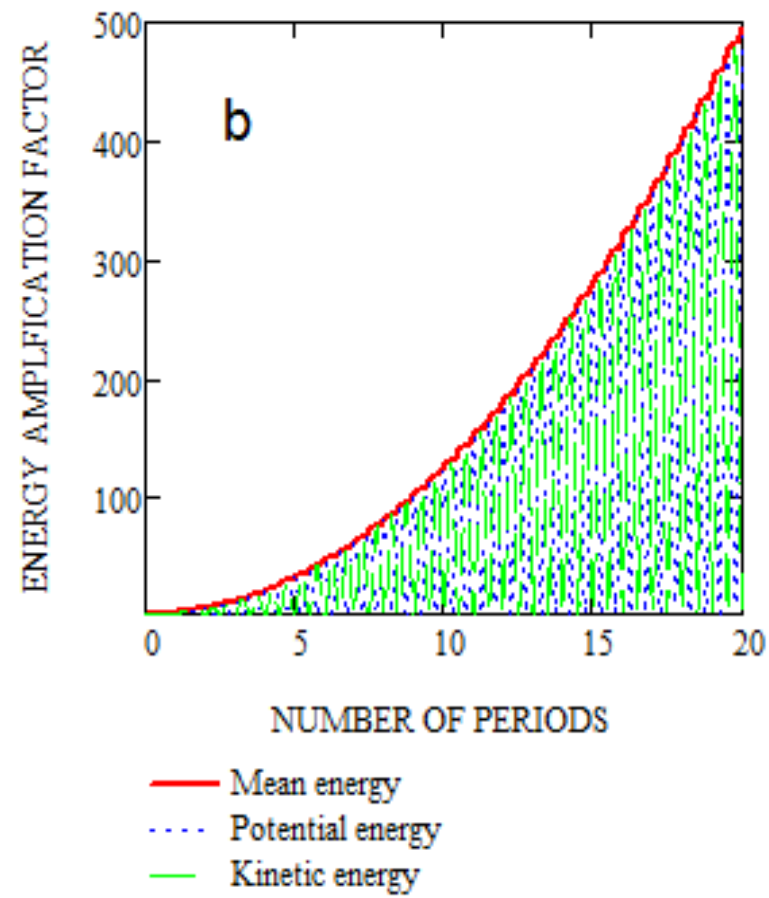

$$\lambda(t) = \frac{g_A A_{ZPO}}{2}\omega_0 t\left(\cos\omega_0 t - \frac{\sin\omega_0 t}{\omega_0 t}\right)$$

Escape rate in the modified Kramers theory with account of parametric driving of the well **position** at $\Omega = \omega_0$

$$R_K = \frac{\omega_0}{2\pi}\exp\left[-\left(E_0 - \langle E \rangle\right)/D(T)\right] \qquad D(T) = \frac{\hbar\omega_0}{2}\coth\left(\hbar\omega_0/2k_B T\right)$$

E_0 = 1 eV – well depth; g_A =0.5 – modulation amplitude

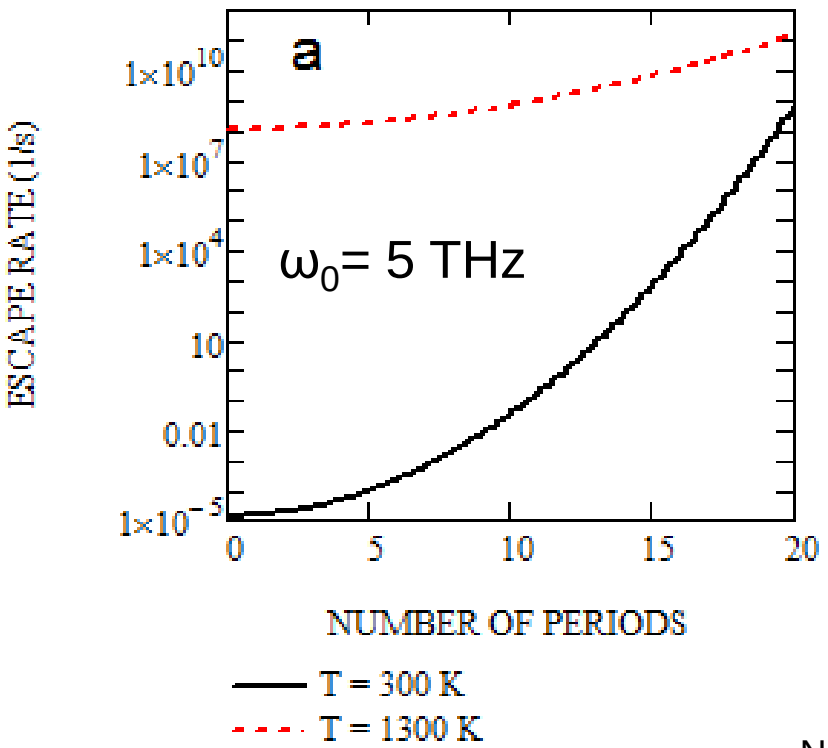

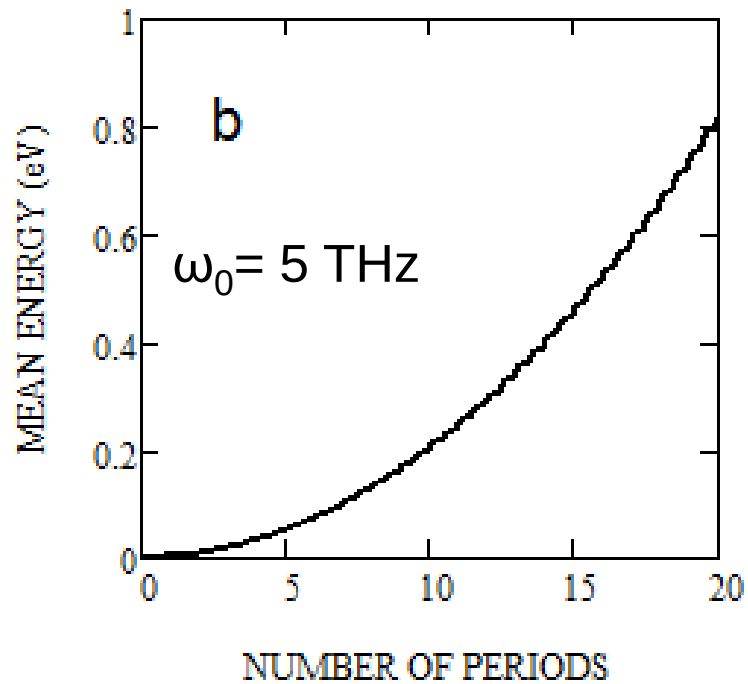

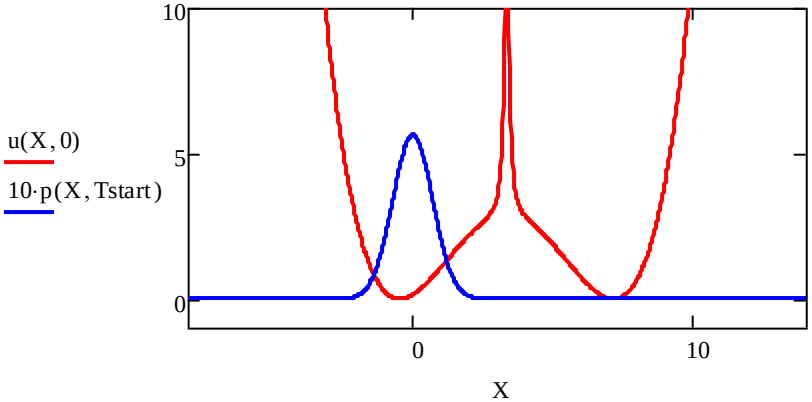
u(X, 0)
10·p(X, Tstart)
10
5
0
0
10
X

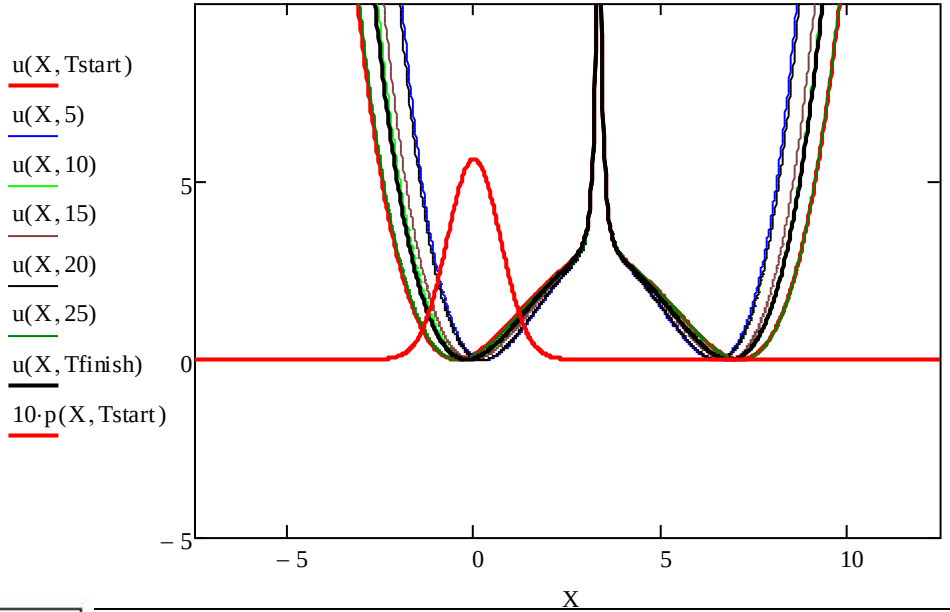
u(X, Tstart)
u(X, 5)
u(X, 10)
u(X, 15)
u(X, 20)
u(X, 25)
u(X, Tfinish)
10·p(X, Tstart)
5
0
− 5
− 5
0
5
10
X

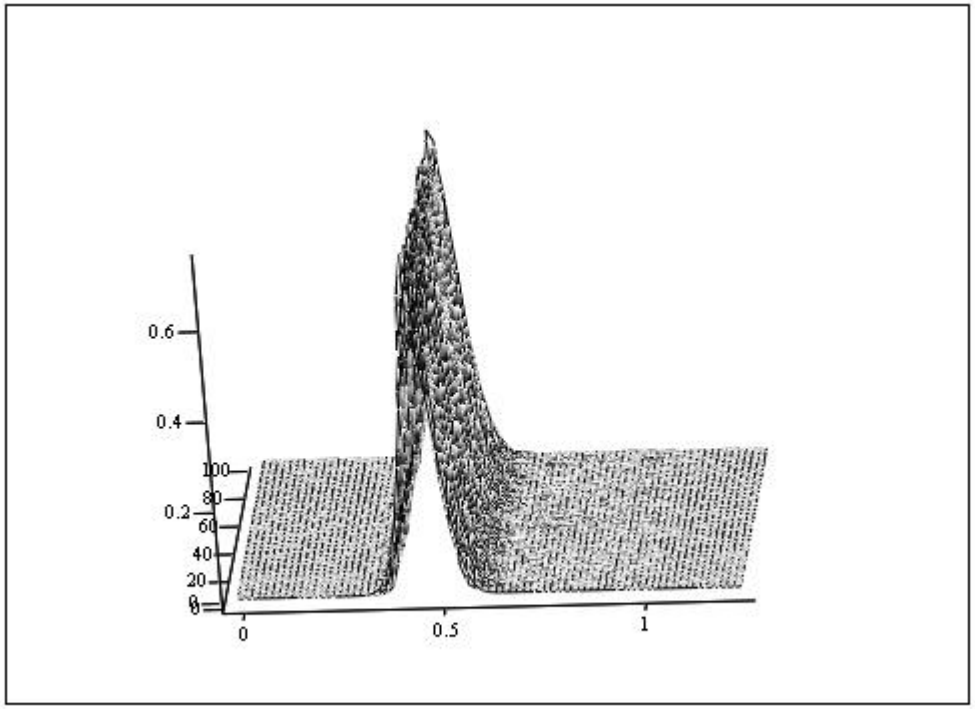
0.6
0.4
0.2
100
80
60
40
20
0
0
0.5
1

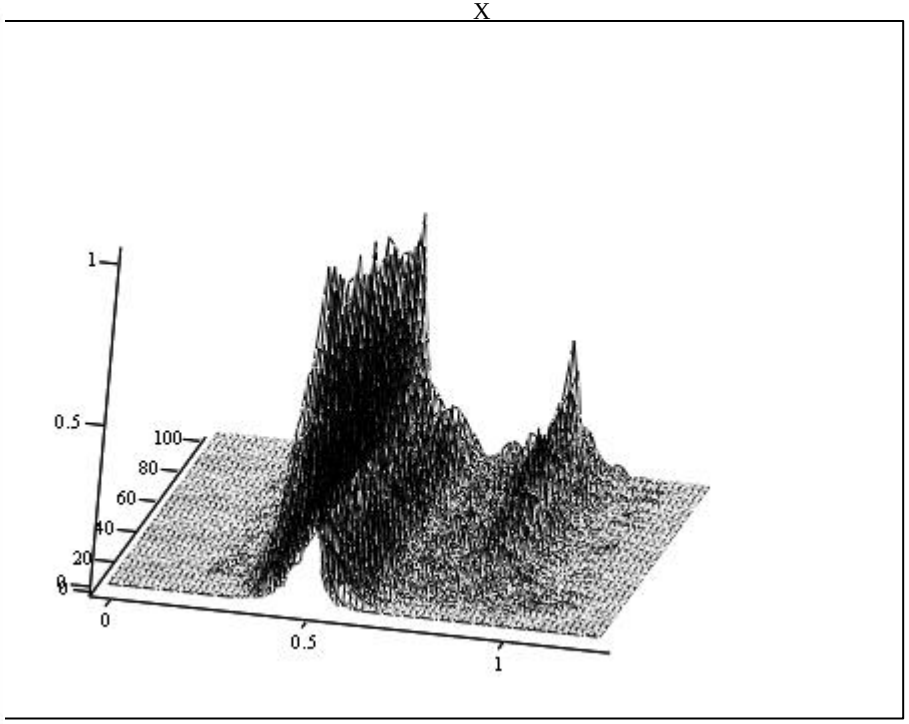
1
0.5
100
80
60
40
20
0
0
0.5
1

(xx, tt, Rez)

, Rez)

Extreme example – Low Energy Nuclear Reactions (LENR)

Why LENR is unbelievable?

G. Gamow, "Zur Quantentheorie des Atomkernes", *Z. Phys.*, **51**, 204–212 (1928).

$$G \approx \exp\left\{-\frac{2}{\hbar}\int_{r_0}^{R_c} dr\sqrt{2\mu\left(V(r)-E\right)}\right\}$$

Gamow factor

$$r_0 \sim 3\ \text{fm}$$

Nuclear radius deduced from **scattering experiments**

$$V(R_0) = \frac{e^2}{r_0} \approx 450\ \text{keV}$$

Coulomb barrier

At any crystal Temperature:

$$E << V(r_0) \Rightarrow G \approx 10^{-2760}$$

HOWEVER, is the Coulomb barrier that huge in the lattice **?**

Willis Eugene *Lamb*
Nobel Prize 1955

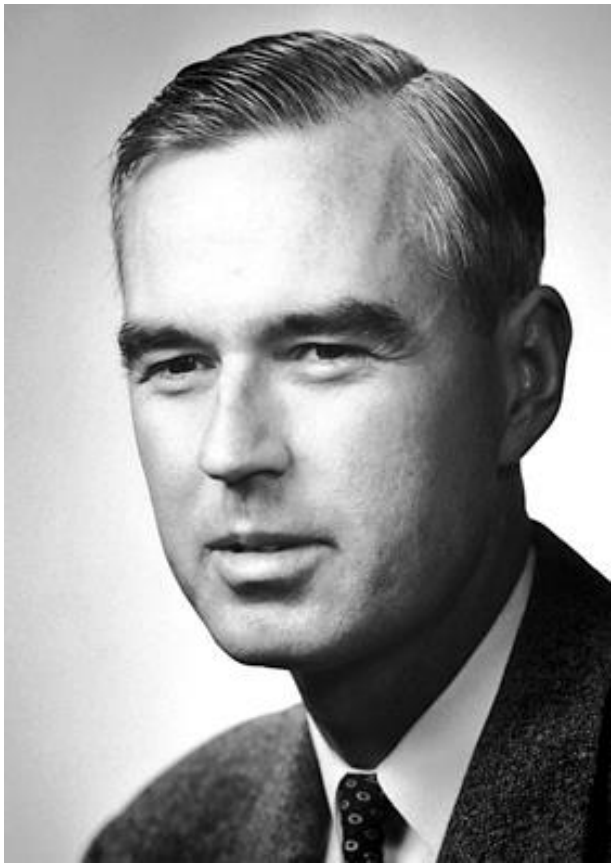

R.H. Parmenter, **W.E. Lamb**,
Cold fusion in Metals (1989)
Electron screening

Julian Schwinger
Nobel Prize 1965

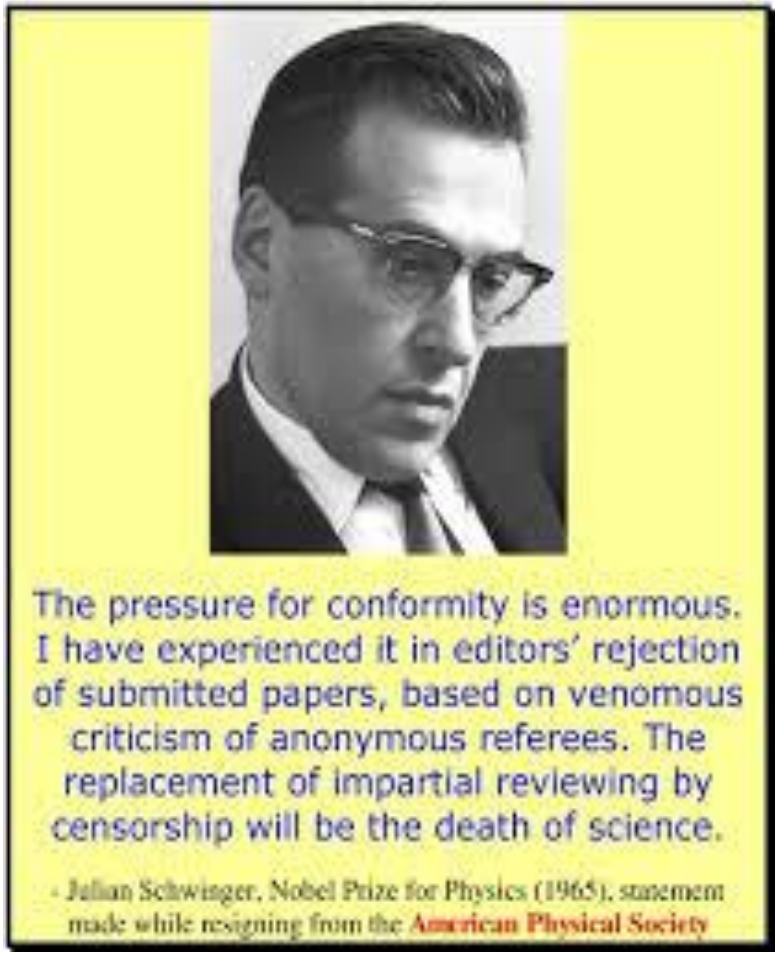

J. Schwinger, Nuclear Energy in an Atomic Lattice (1990)
Lattice screening

J. Schwinger, *Nuclear Energy in an Atomic Lattice* I, Z. Phys. D 15, 221 (**1990**)

Effective Coulomb repulsion with account of **zero-point oscillations**

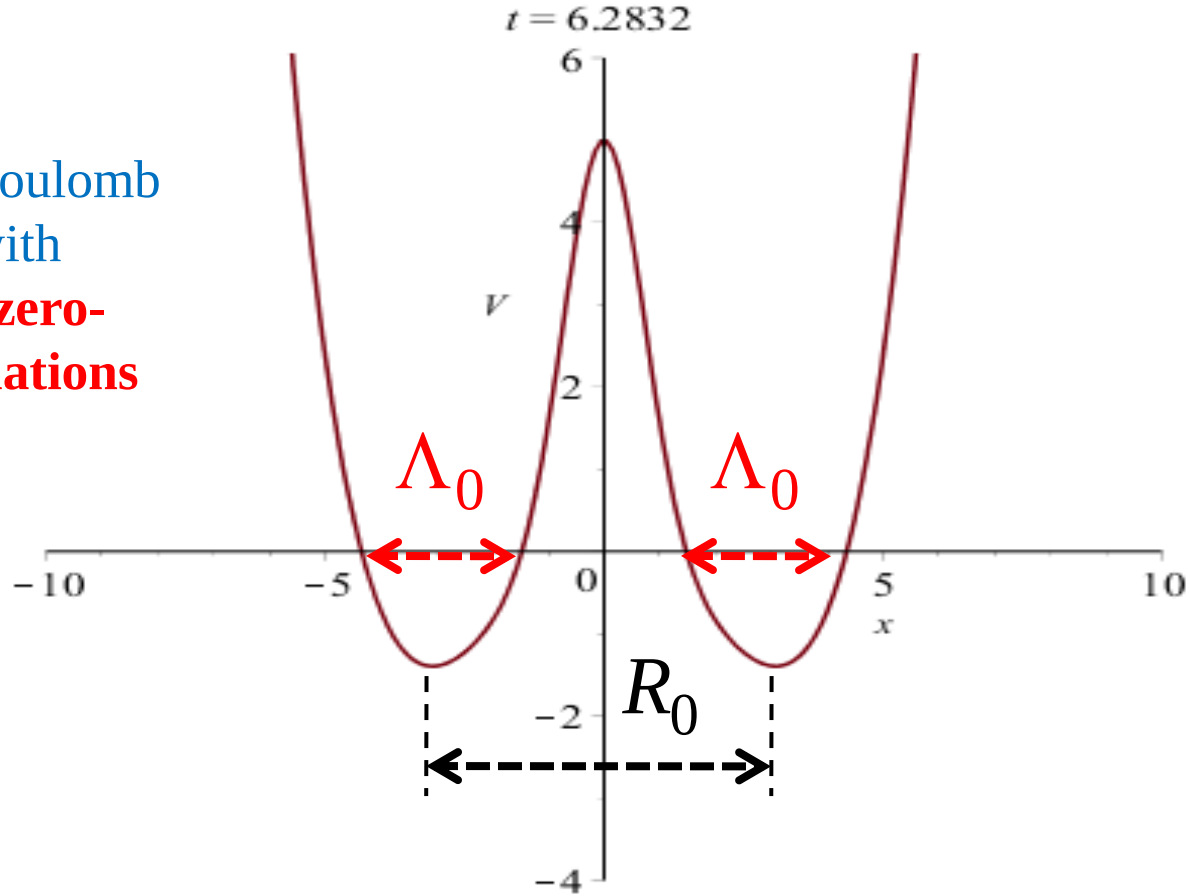

$$ {}_0\langle V_c(r)\rangle_0 = \frac{e^2}{r}\sqrt{\frac{2}{\pi}}\int_0^{r/\Lambda_0} dx \exp\left(-\tfrac{1}{2}x^2\right) \approx \begin{cases} r \gg \Lambda_0 : \dfrac{e^2}{r} \\ r \ll \Lambda_0 : \left(\dfrac{2}{\pi}\right)^{1/2} \dfrac{e^2}{\Lambda_0} \end{cases} $$

~ **100 eV** (!!!)

J. Schwinger, *Nuclear Energy in an Atomic Lattice* The First Annual Conference on Cold Fusion. University of Utah Research Park, Salt Lake City (**1990**)

D-D fusion rate in Pd-D lattice: $\upsilon_{D-D} = \frac{1}{T_0} = \left(2\pi/\hbar\right)_0 \left\langle V\delta\left(H-E\right)V\right\rangle_0$

T_0 is the mean lifetime of the *phonon vacuum* state before releasing the nuclear energy **directly** to the lattice **(no radiation!)**:

$$\frac{1}{T_0} \approx 2\pi\omega_0 \left(\frac{2\pi\hbar\omega_0}{E_{nucl}}\right)^{\frac{1}{2}} \left(\frac{r_{nucl}}{\Lambda_0}\right)^3 \exp\left[-\frac{1}{2}\left(\frac{R_0}{\Lambda_0}\right)^2\right] \sim 10^{-19}\, s^{-1} \div 10^{-30}\, s^{-1}$$

$$\Lambda_0 = 0.1\text{A} \qquad R_0 = 0.94\text{A} \div 2.9\text{A}$$

Schwinger, ***Nuclear Energy in an Atomic Lattice*** I, Z. Phys. D 15, 221 (**1990**).

Parmenter, **Lamb**, Cold fusion in Metals, Proc. Natl. Acad. Sci. USA, v. 86**,** 8614-8617 (**1989**).

$$V_{eff}(r) \approx \frac{m\omega_0^2}{2} r^2 + \frac{e^2}{R_0 - r} \exp\left(-\frac{R_0 - r}{\lambda_D}\right) \sqrt{\frac{2}{\pi}} \int_0^{(R_0 - r)/\Lambda_0} dx \exp\left(-\tfrac{1}{2} x^2\right)$$

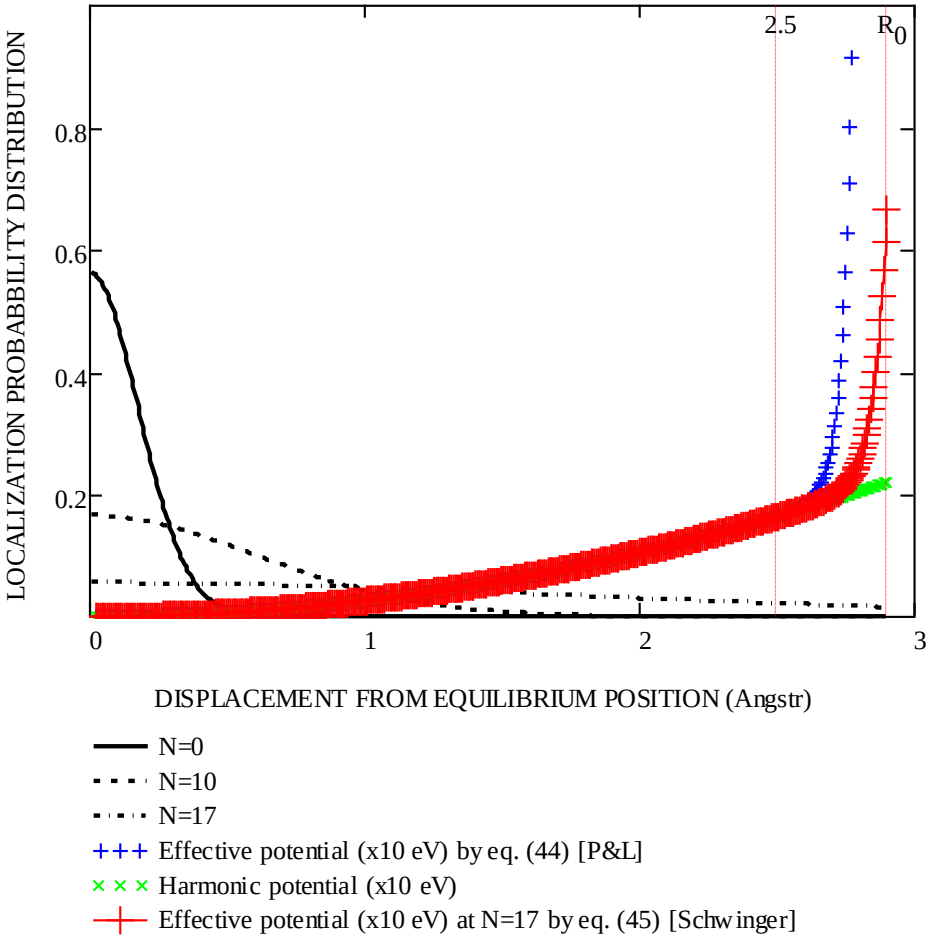

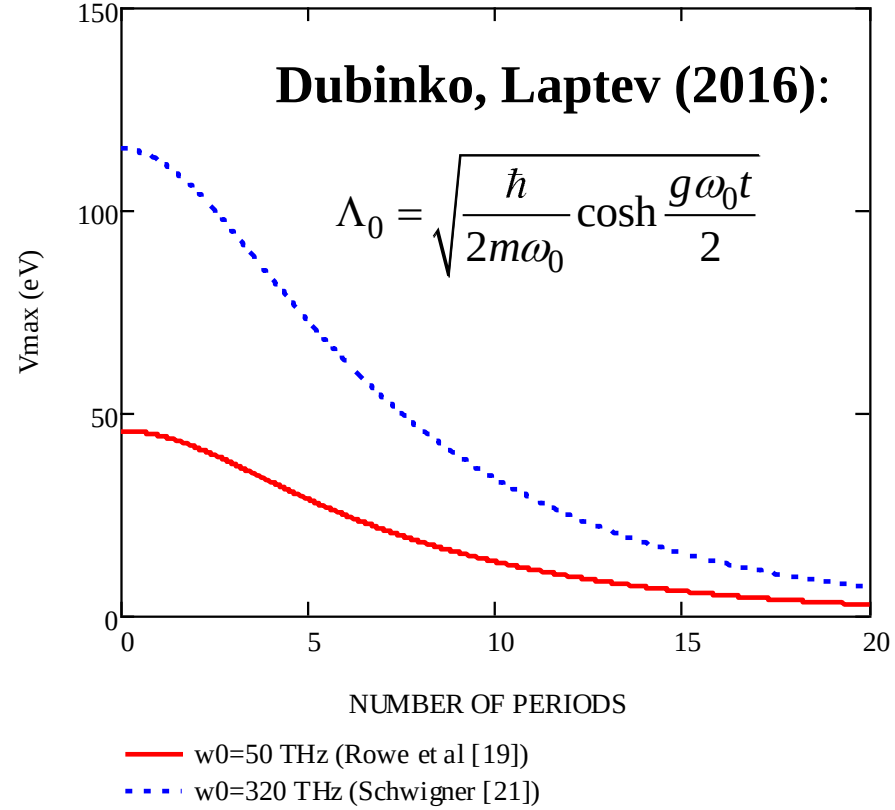

Schwinger, *Nuclear energy in an atomic lattice*. Proc. Cold Fusion Conf. (1990)
Dubinko, Laptev, *Chemical and nuclear catalysis driven by LAVs*, LetMat (2016)

$$\frac{1}{T} \approx 2\pi\omega_0 \left(\frac{2\pi\hbar\omega_0}{E_{nucl}}\right)^{\frac{1}{2}} \left(\frac{r_{nucl}}{\Lambda}\right)^3 \exp\left[-\frac{1}{2}\left(\frac{R_0}{\Lambda_0}\right)^2\right]$$

$$\Lambda_0 = \begin{cases} \sqrt{\dfrac{\hbar}{2m\omega_0}} = const \\ \sqrt{\dfrac{\hbar}{2m\omega_0}\cosh\dfrac{g\omega_0 t}{2}} \end{cases}$$

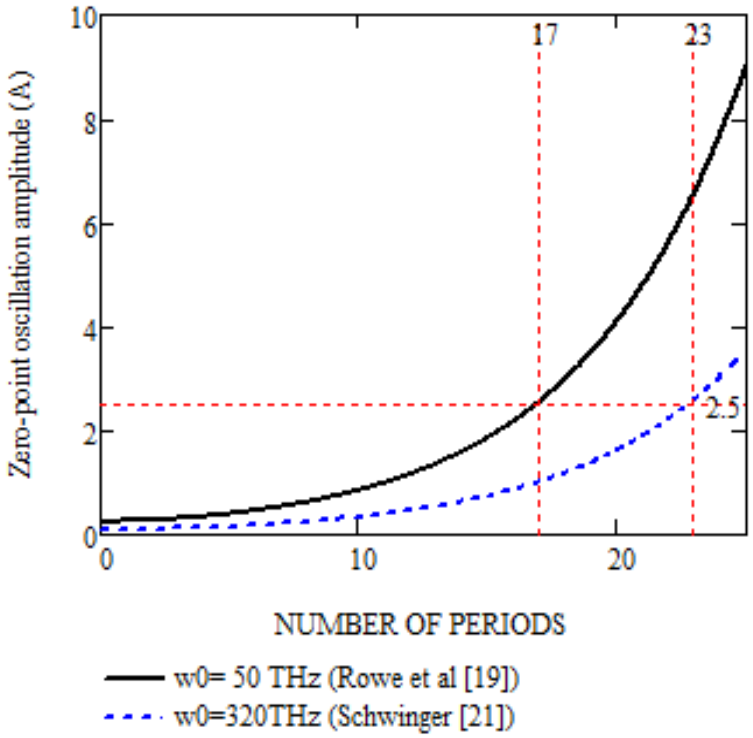

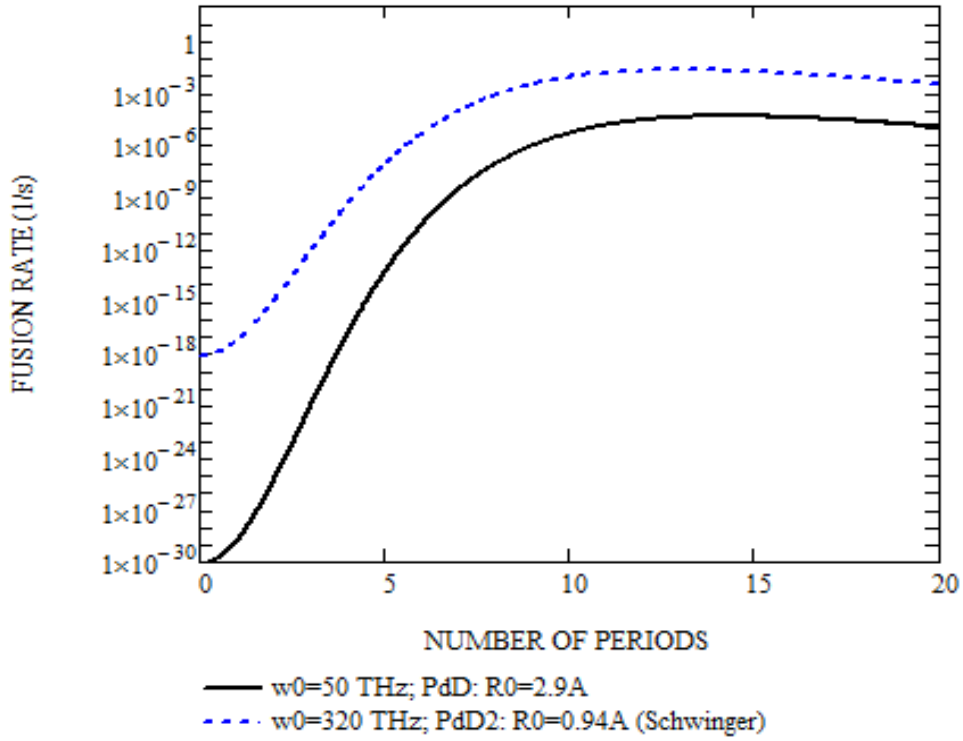

LENR power density under D_2O electrolysis

$$P_{D-D}(T,J) = K_{DB}^{J}\left(E_{DB}^{*},T,J\right)E_{D-D}$$

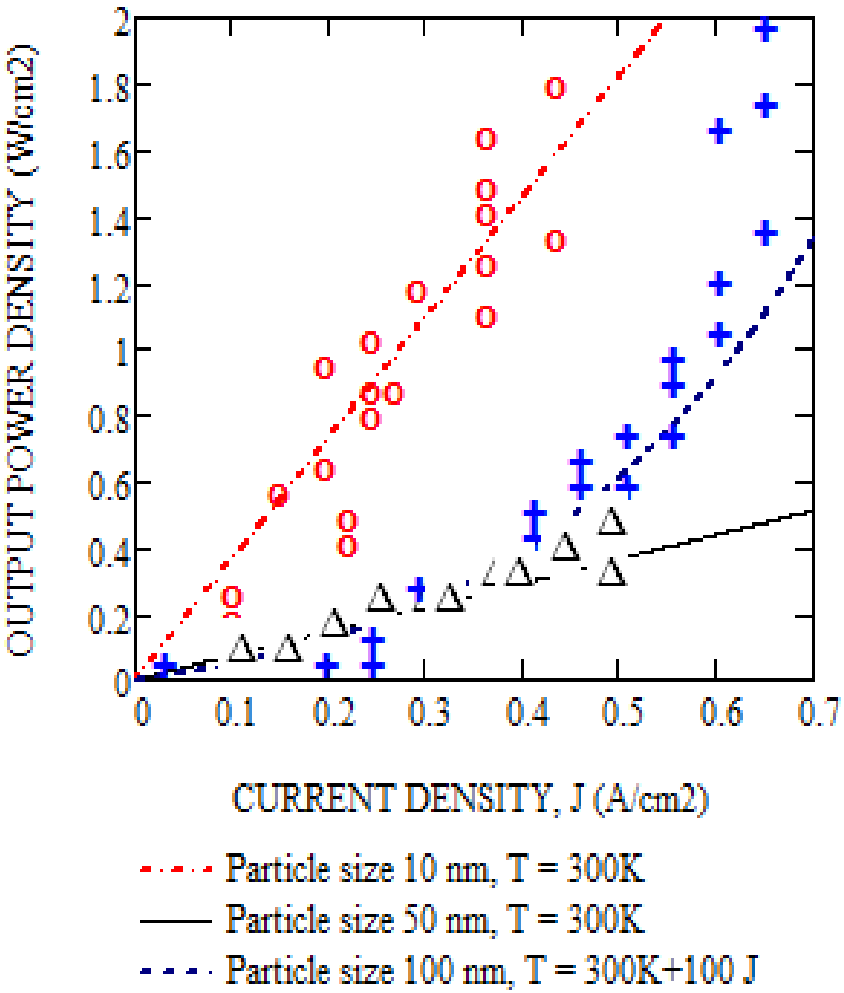

Table 1

Parameter	Value
D-D equilibrium spacing in PdD, b (Å)	2.9
DB excitation efficiency, k_{eff}	10^{-10}
Fusion energy, (MeV)	23.8
Mean DB energy, (eV)	1
DB oscillation frequency, ω_{DB} (THz)	20
Critical DB lifetime, τ_{DB} (ps/cycles)	10/100
Quodon excitation energy (eV)	0.8
Quodon excitation time, τ_{ex} (ps/cycles)	1/10
Quodon propagation range, l_q (nm)	2.9
Cathod size/thickness (mm)	5

BNC can provide up to 10^{14} "collisions" per cm^3 per second

Where to look for
Nuclear Active Environment?

Small Energy Gap
is required for

LAV formation

Nuclear Active Environment

MD modeling of LAVs in NiH and PdH crystals

Visualization of the Pd(Ni)H fcc Lattice (NaCl type)

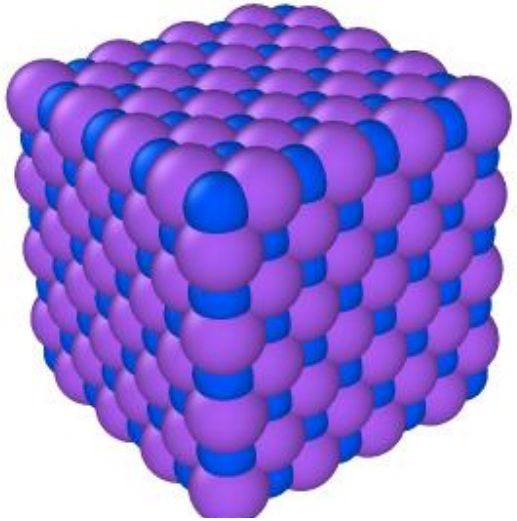

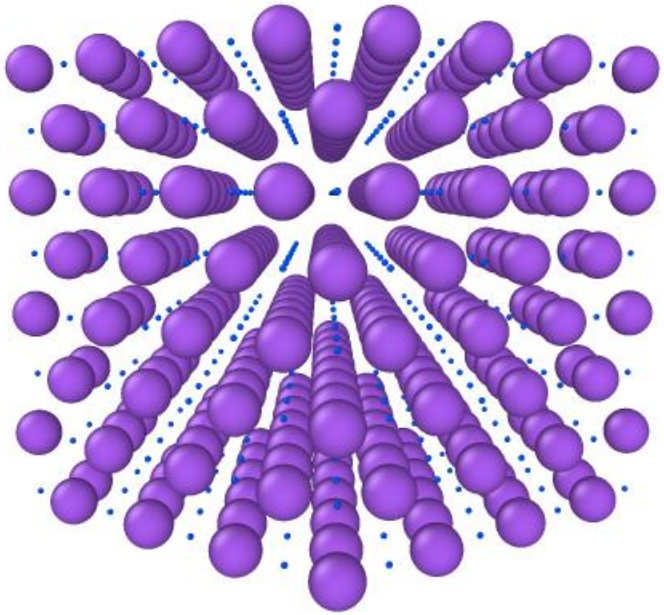

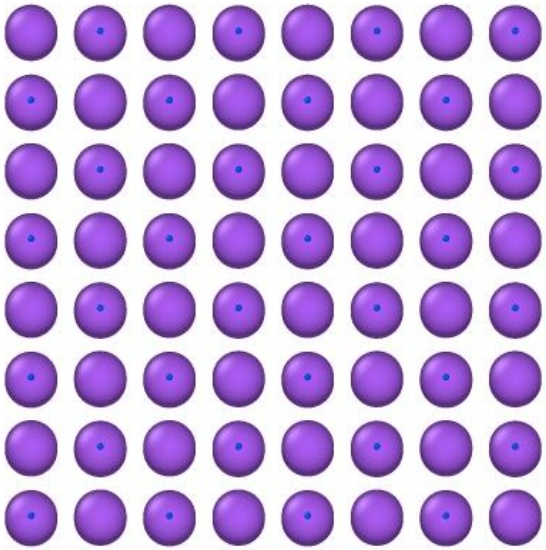

NiH lattice

The following potential was used for Ni lattice modeling in **LAMMPS** package:

Material	File with potential used	The link to the corresponding publication in the literature
NiH	NiAlH_jea.eam.alloy	see James E Angelo, Neville R Moody, Michael I Baskes"Trapping of hydrogen to lattice defects in nickel", Modelling andSimulation in Materials Science & Engineering, vol. 3, pp. 289-307 (1995)

Density Of States of NiH at 0 K

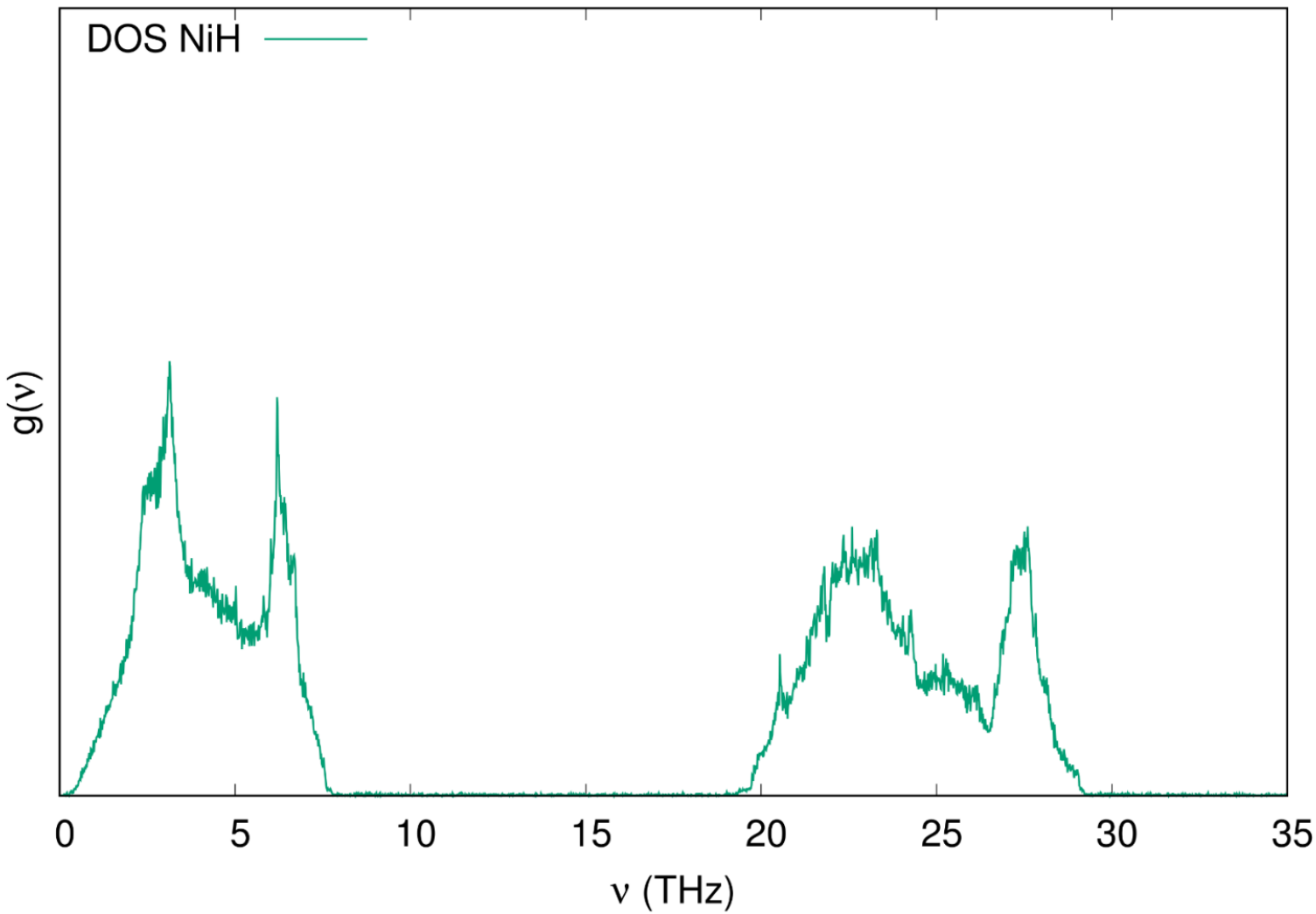

H-H atoms displaced along[110] in NiH at T=0K

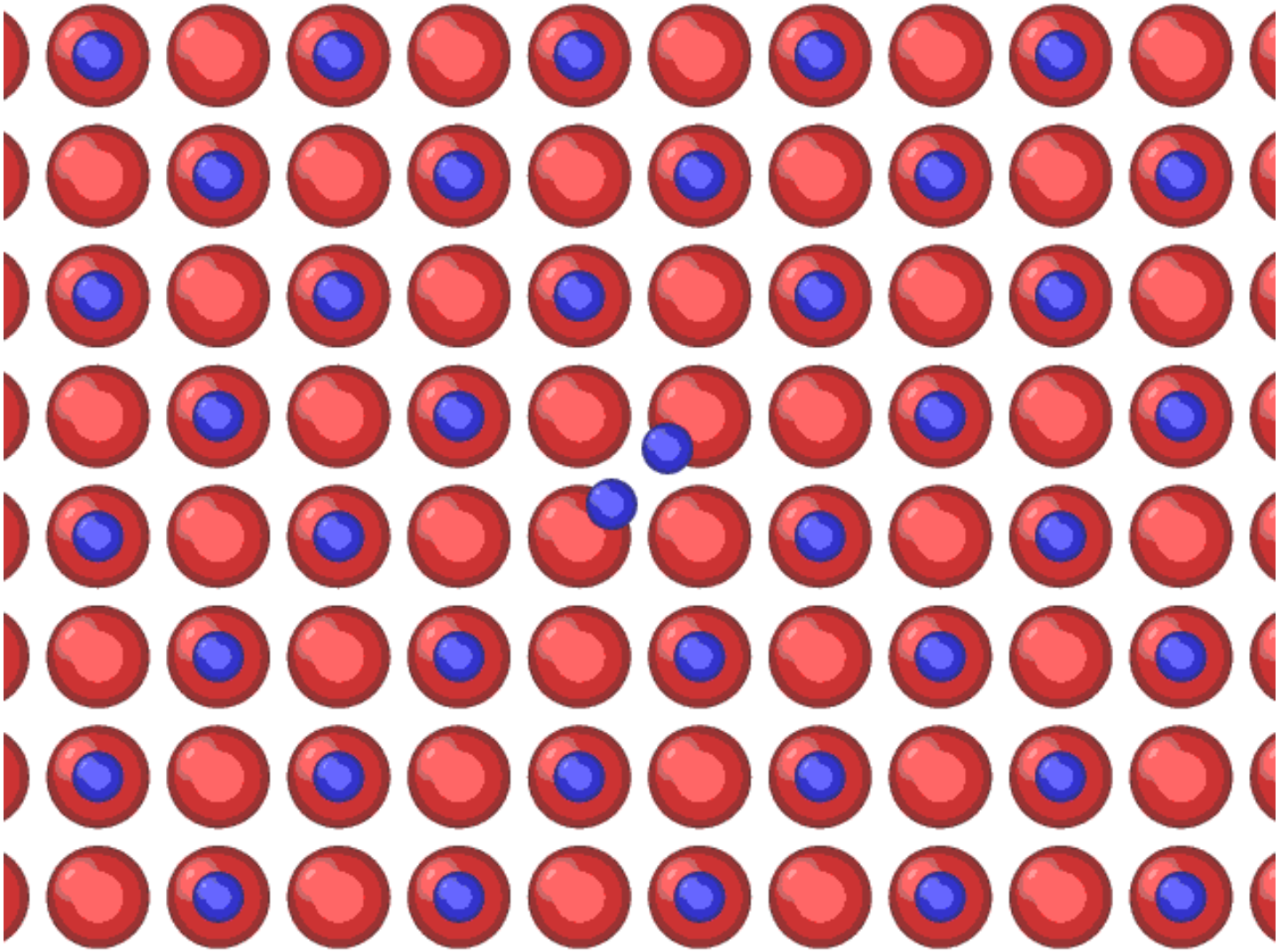

1 H atom displaced along <110> in NiH at T=0K

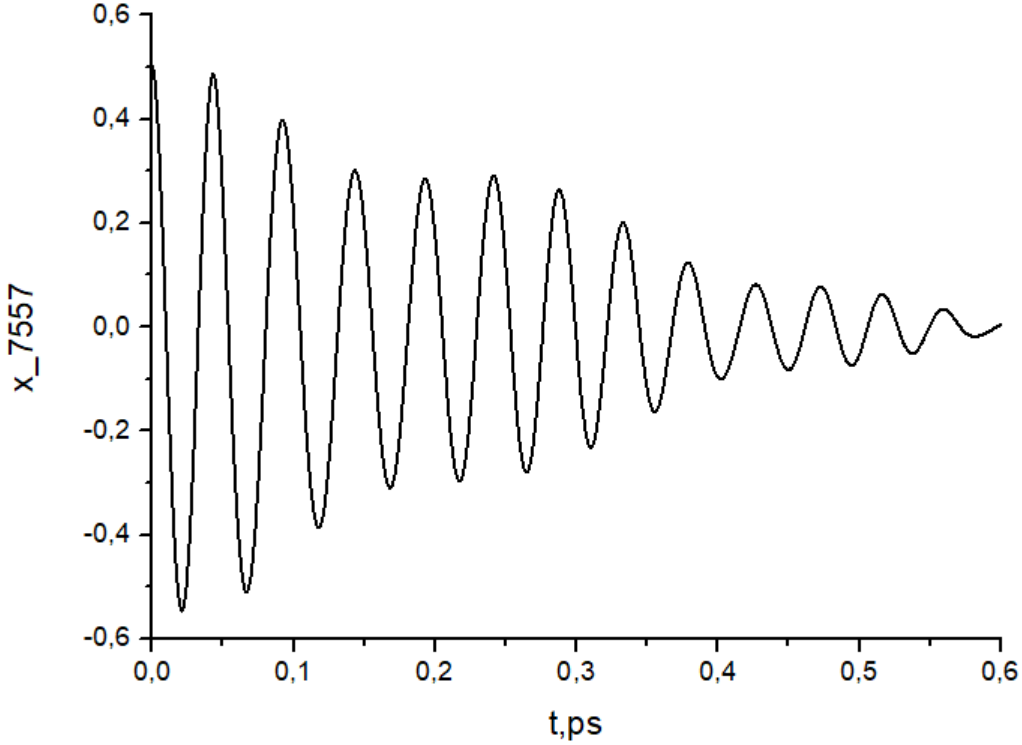

T=0.5 ps, Frequency = 20THz (**inside** the optical band)

Discrete Breather in the 3d NiH Lattice at 0 K

Ni-H-Ni: 1 atom H is displaced along <100> at 0.8 A. Initial velocity = 0.

DB frequency= 29 THz
DB amplitude= 0.9A
Lattice constant= 3.5A

$$\rho_i = \sum_j f_j(r_{ij})$$

$$E = \sum_{i<j} V_{ij}(r_{ij}) + \sum_i F_i(\rho)_i$$

The Embedded Atom Method has been used

DB frequency lies near the upper edge of the phonon band

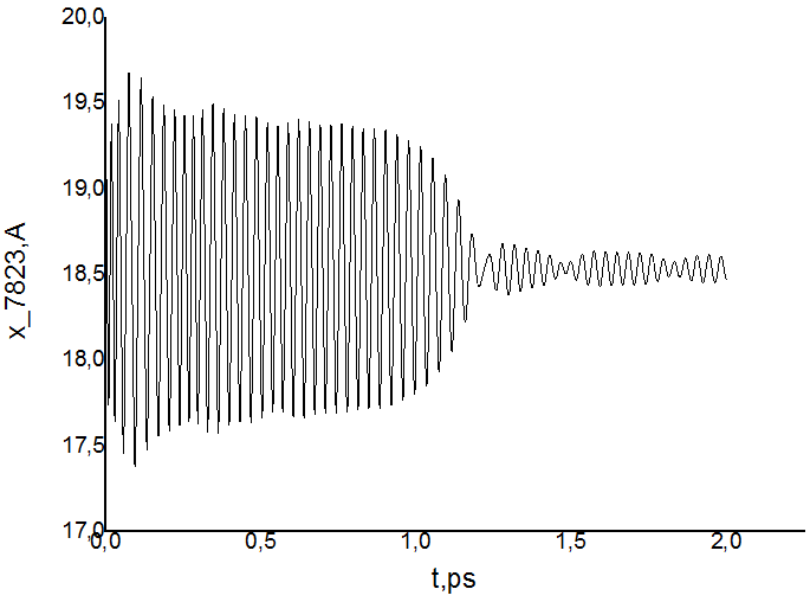

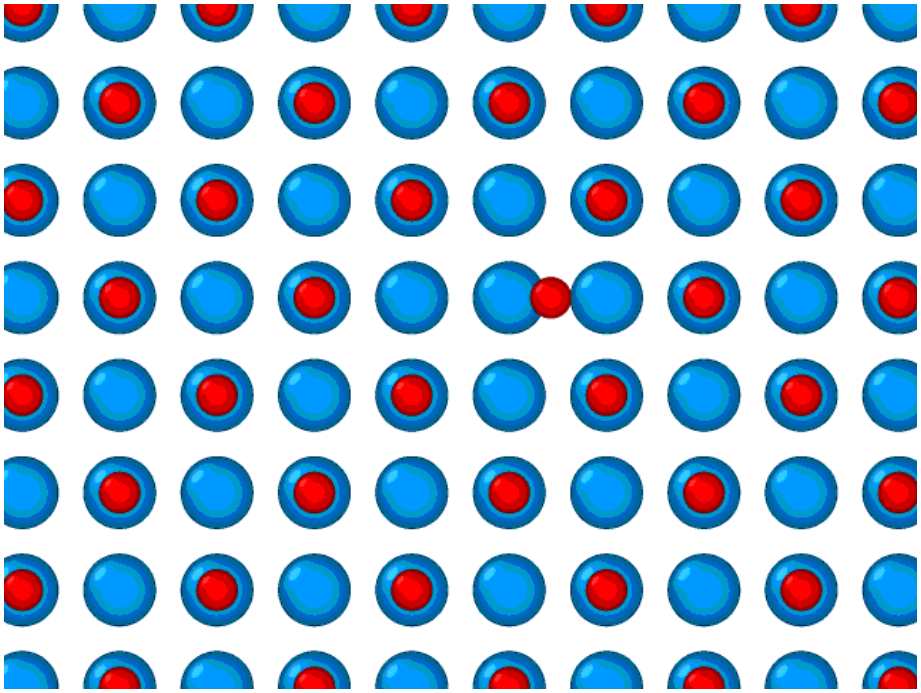

H-Ni-H atoms [100] and [-100] in NiH at T=0K

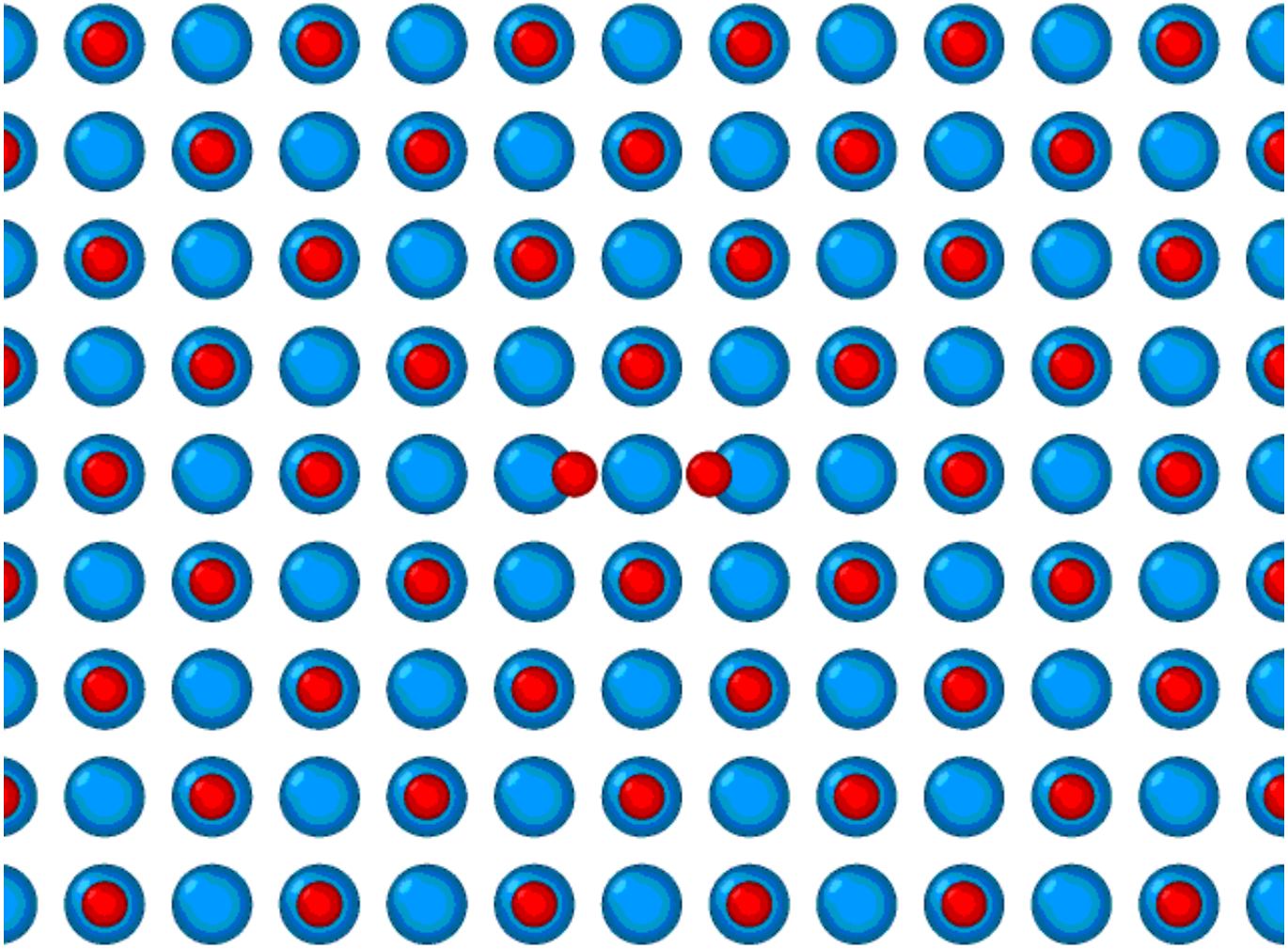

H-Ni-H atoms [100] and [-100] in NiH at T=0K

DB frequency = 33 THz **(above the optic band)**
DB amplitude = 0.8A
Lattice constant = 3.5A

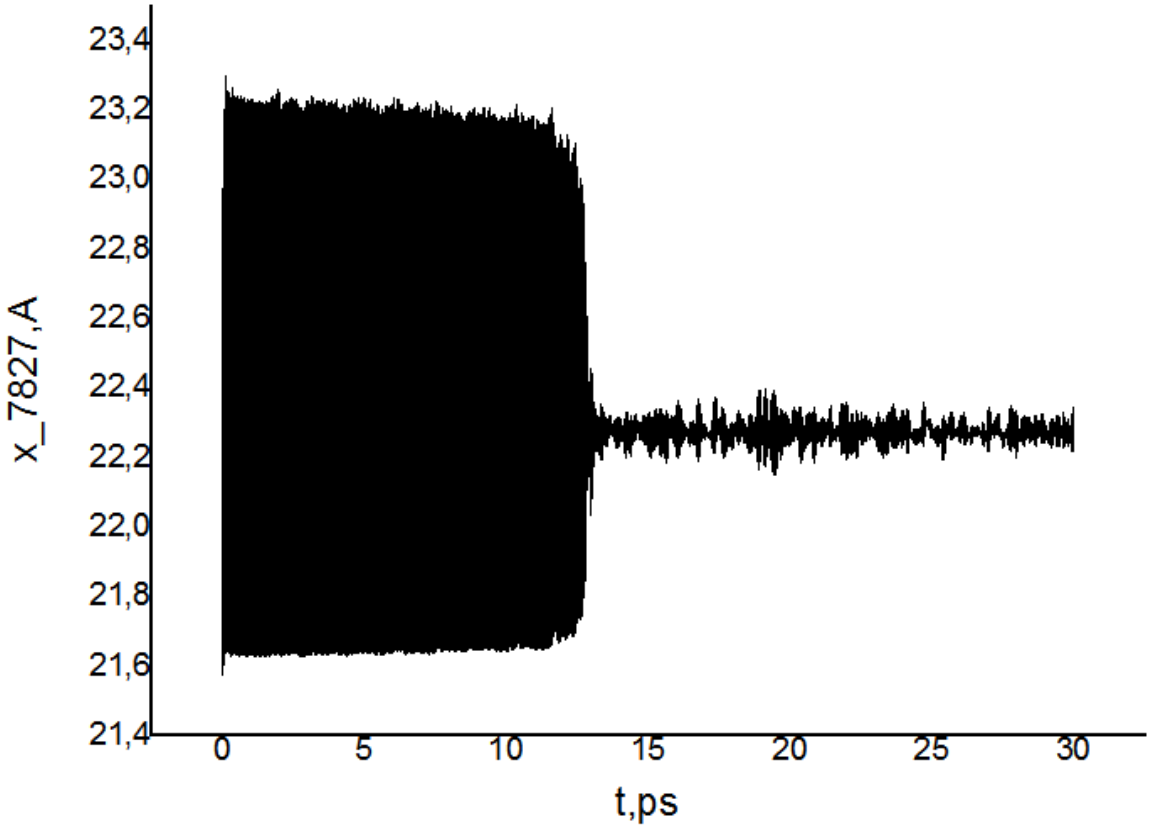

Ni-H-Ni atom <111> at T=0K

Oscillation of a hydrogen atom forming the M-H-M <111> breather in NiH lattice with d0=0.85A. The resulting oscillation amplitude is 0.79 A, oscillation frequency is 16.39 THz, oscillation period 0.061 ps and lifetime is higher than 100 ps (the simulation run was stopped before the breather oscillation decayed).

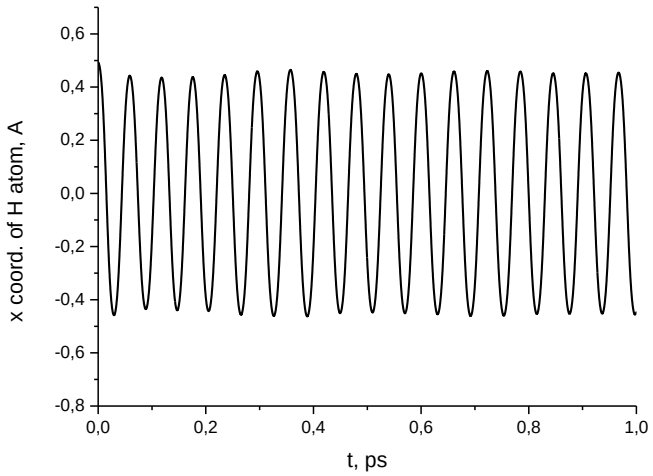

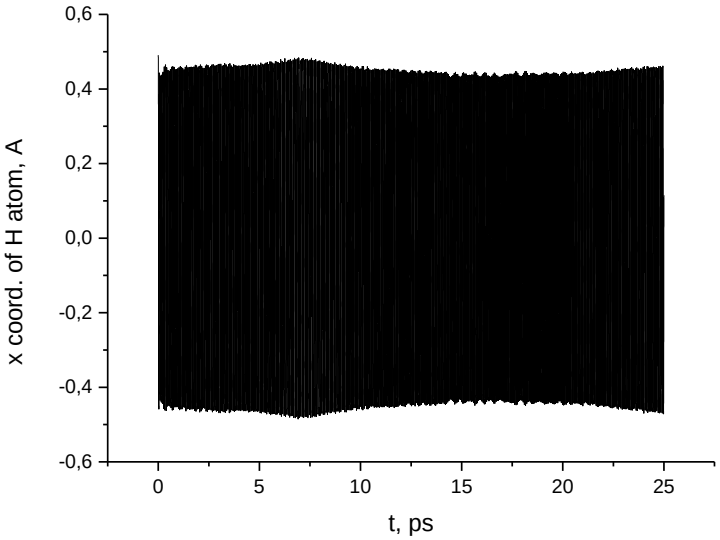

Do DBs exist at finite T ?

Gap DBs in diatomic crystals at elevated temperatures

Hizhnyakov et al (2002), Dmitriev et al (2010)

$$K^*_{B,n}/\bar{K} \approx 5.1$$

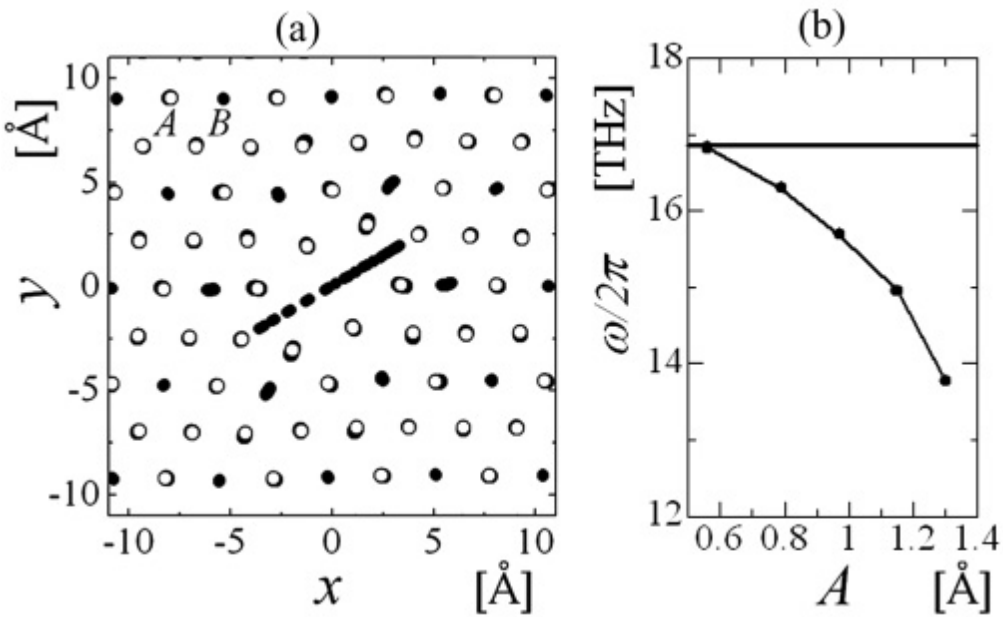

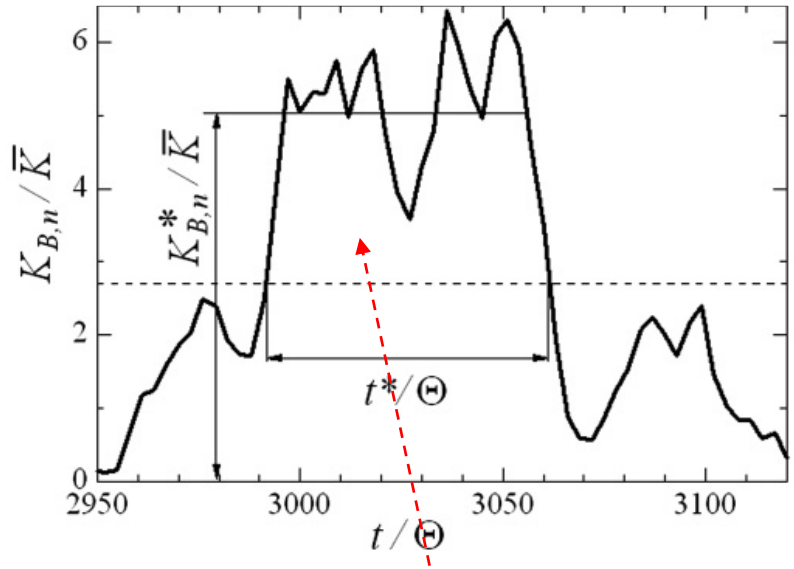

A_3B type crystals $M_H/M_L = 10$

$$t^*/\Theta \approx 70 \quad \bar{K} = 0.1eV \geq 1000K$$

In NaI and KI crystals Hizhnyakov et al has shown that DB amplitudes along <111> directions can be as high as 1 Å, and $t^*/\Theta \sim 10^4$

Lifetime and concentration of ***high-energy light atoms*** increase exponentially with increasing T

Visualization of the PdH fcc Lattice Oscillations at T=100 K

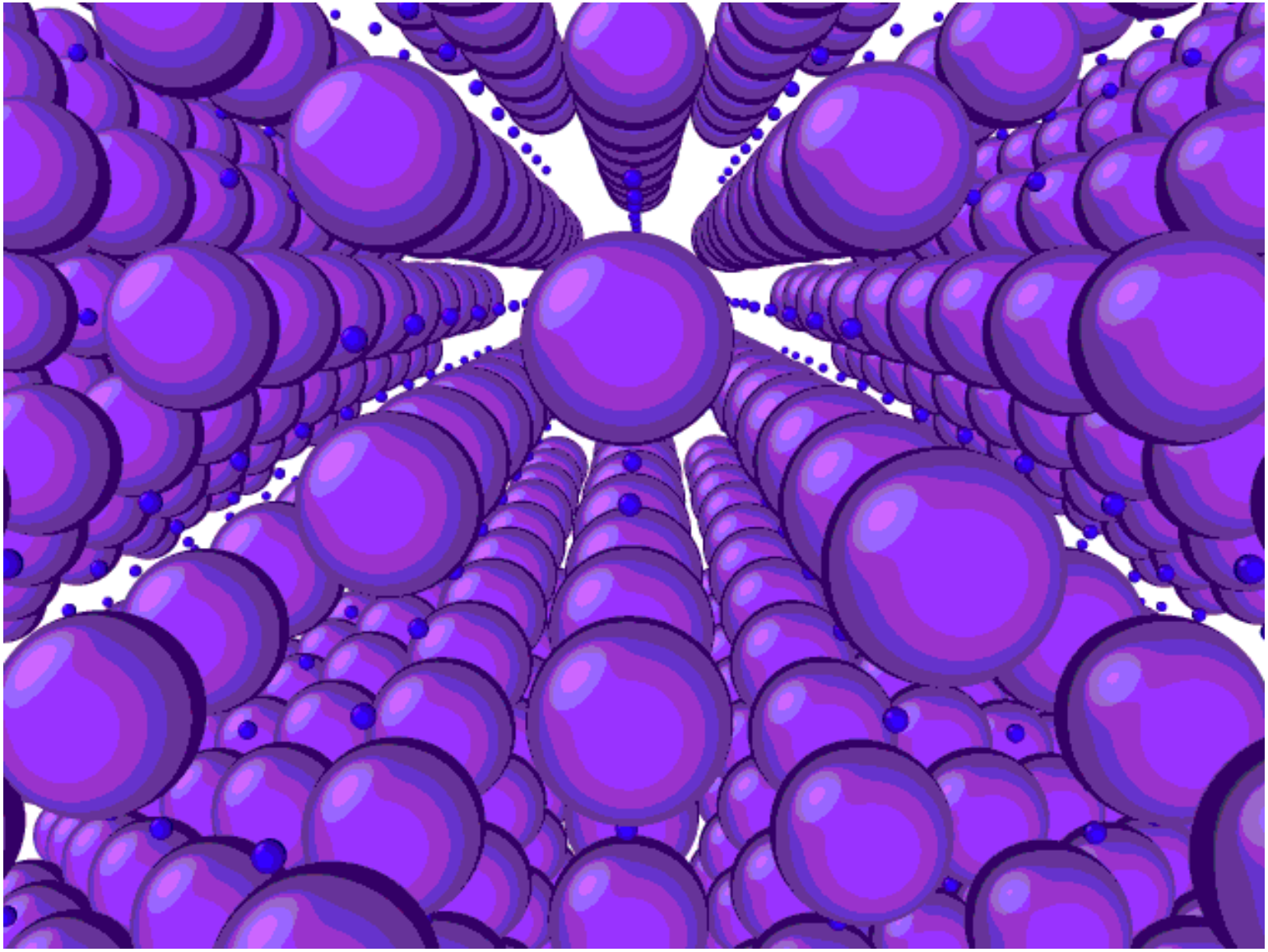

Visualization of the PdH fcc Lattice Oscillations at T=1000K

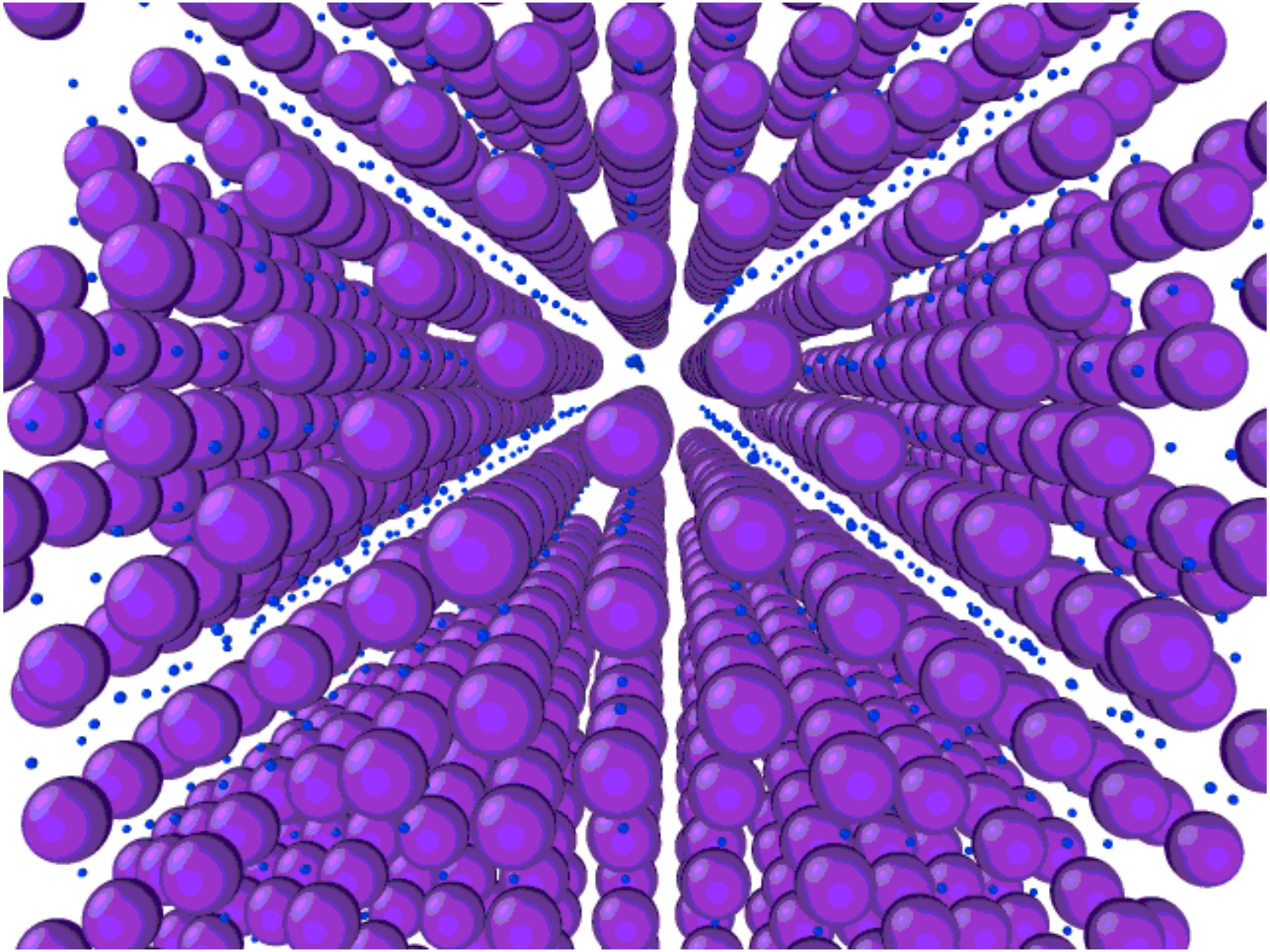

NiH lattice (not deformed) at different T

При повышении температуры начинают преобладать низкие частоты, что, по видимому, связано с разрушением решётки гидрида и увеличением длины свободного пробега атомов водорода, которые начинают «сободное» движение внутри решётки.

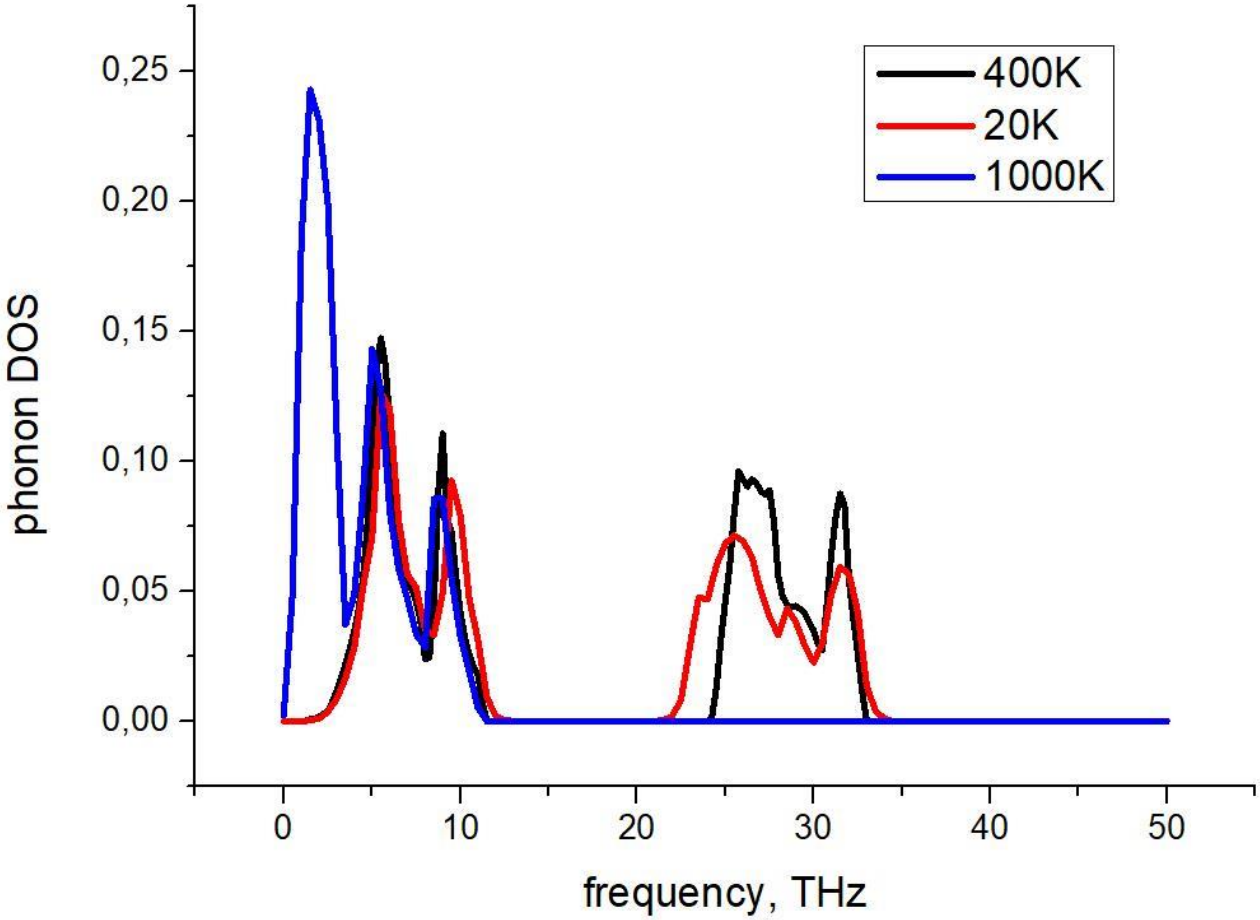

Compressed (on 10%) PdH lattice at T=620K and T=1000K

При повышении температуры график плотности фононных состояний несколько сдвигается в область высоких частот.

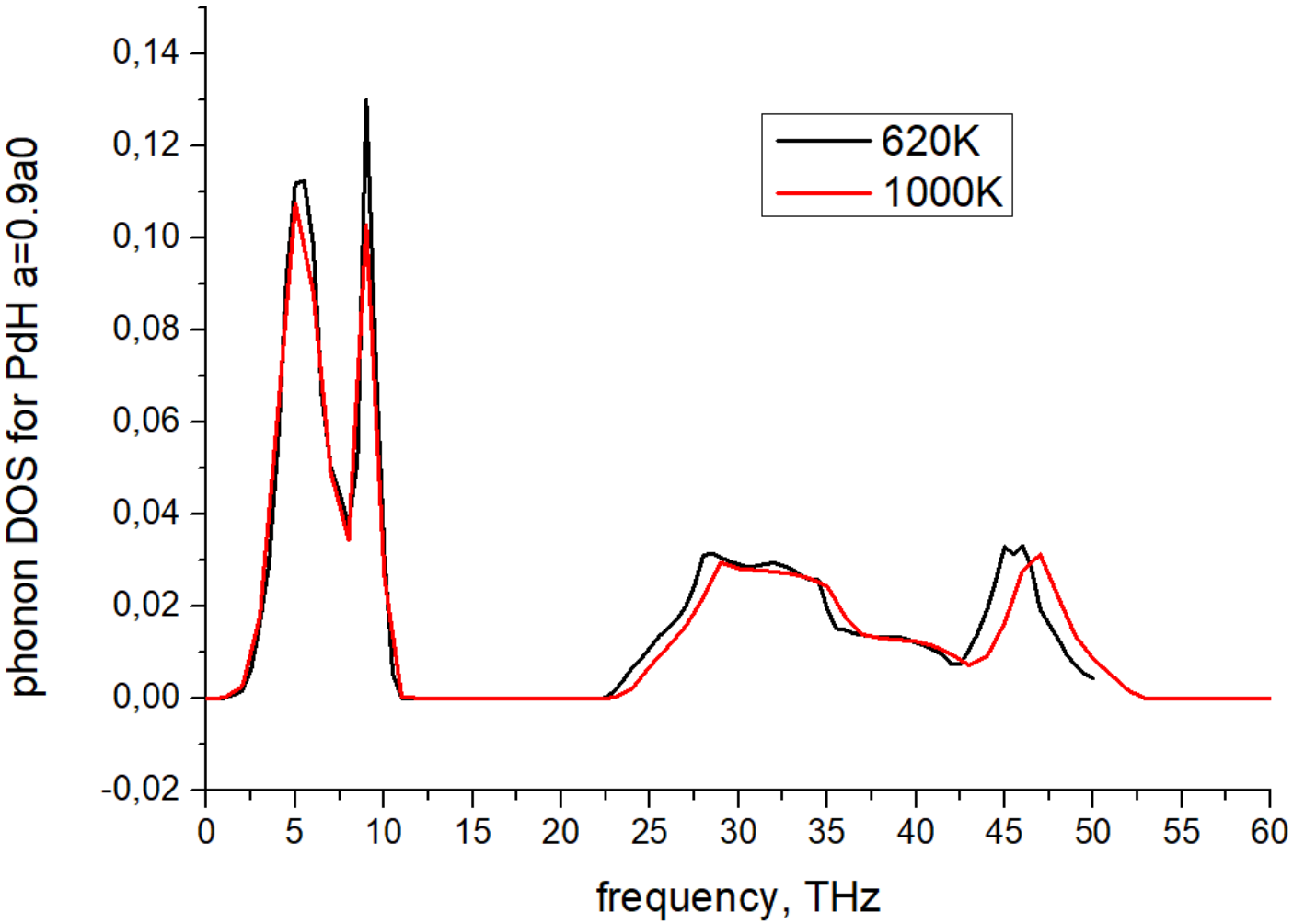

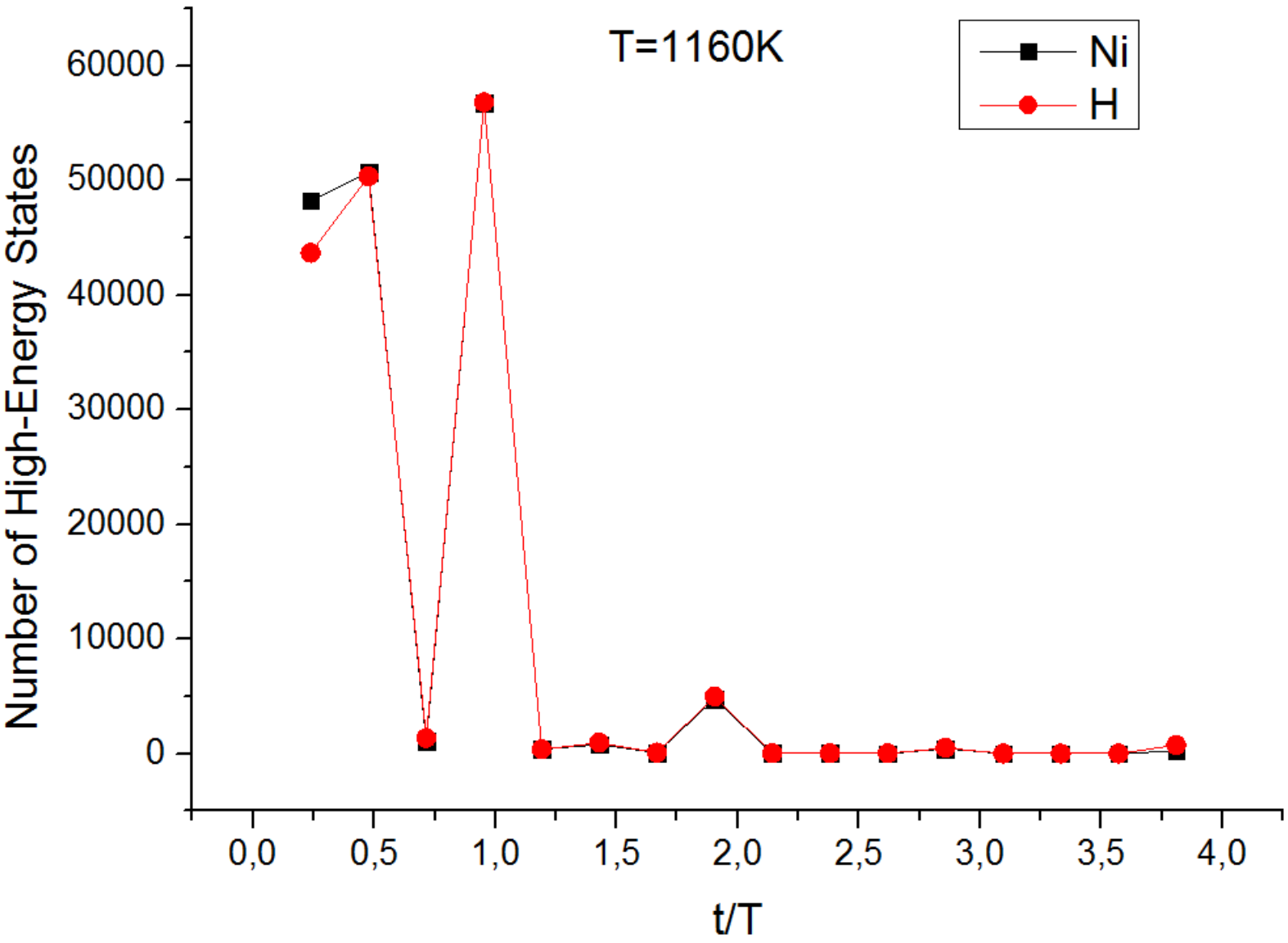

NiH MD modeling in LAMMPS package

NiH lattice at T=1160K. High energy oscillations

Data for some arbitrary H atom in the Lattice

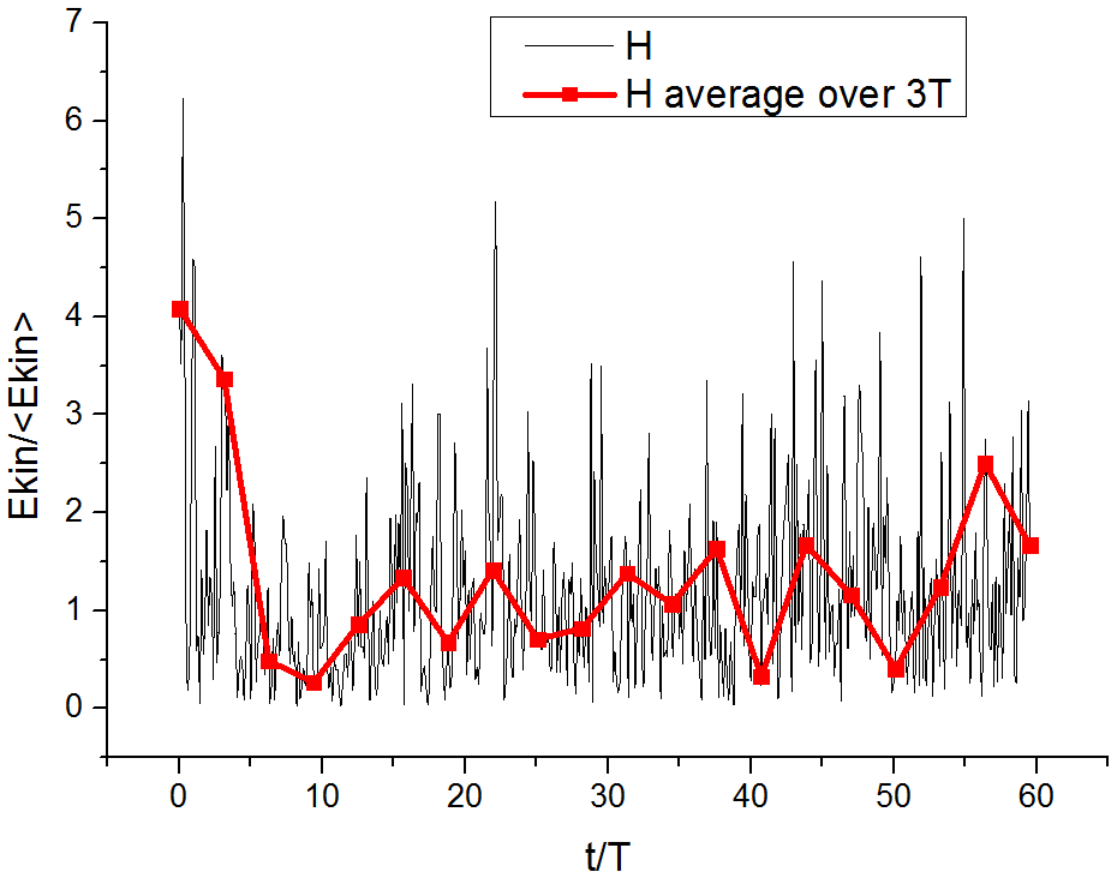

NiH MD modeling in **LAMMPS** package

Wavelet imaging of LAV in NiH MD (Francesco Piazza, 2018)

The technique is based on continuous wavelet transform of velocity time series coupled to a threshold dependent filtering procedure to isolate excitation events from background noise in a given spectral region.

By following in time the center of mass of the reference frequency interval, the data can be easily exploited to investigate the statistics of the burst excitation dynamics, by computing, for instance, the distribution of the burst lifetimes, excitation times, amplitudes and energies.

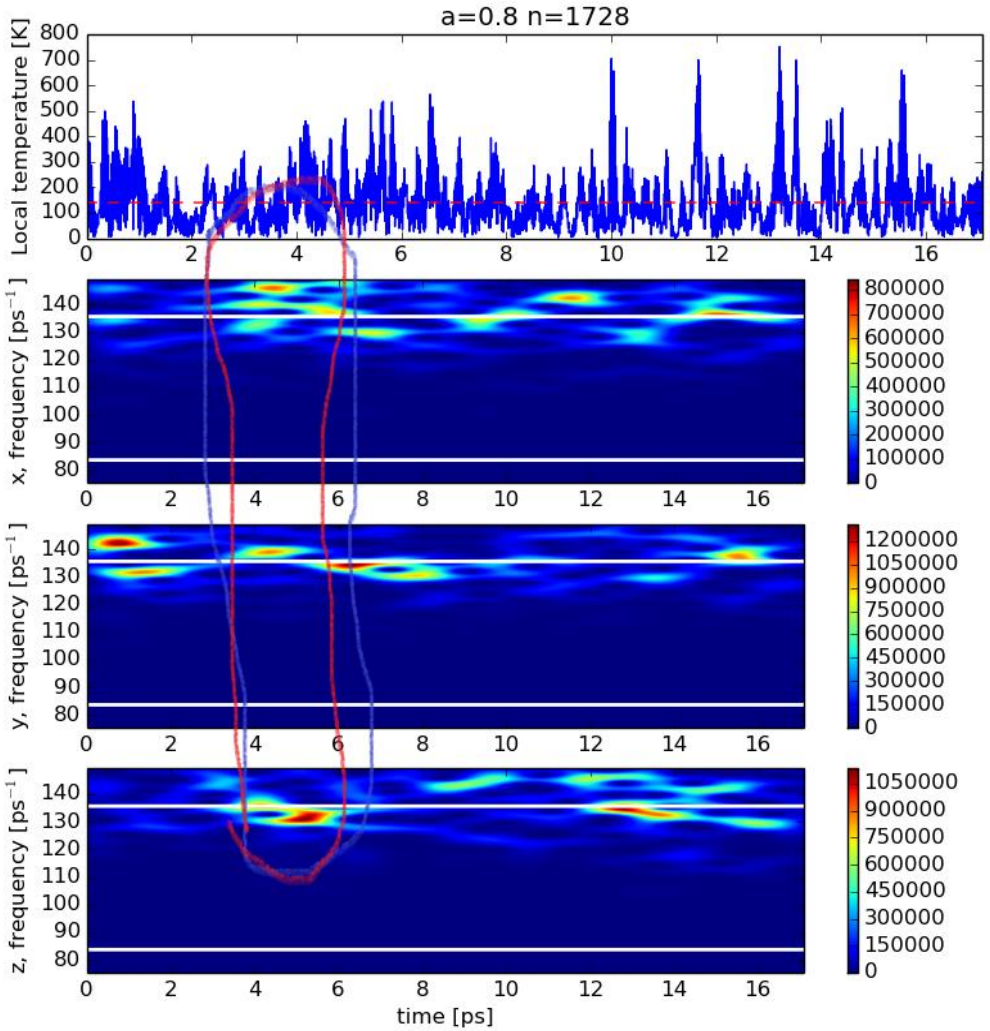

Wavelet imaging of LAV in NiH MD (Francesco Piazza, 2018)

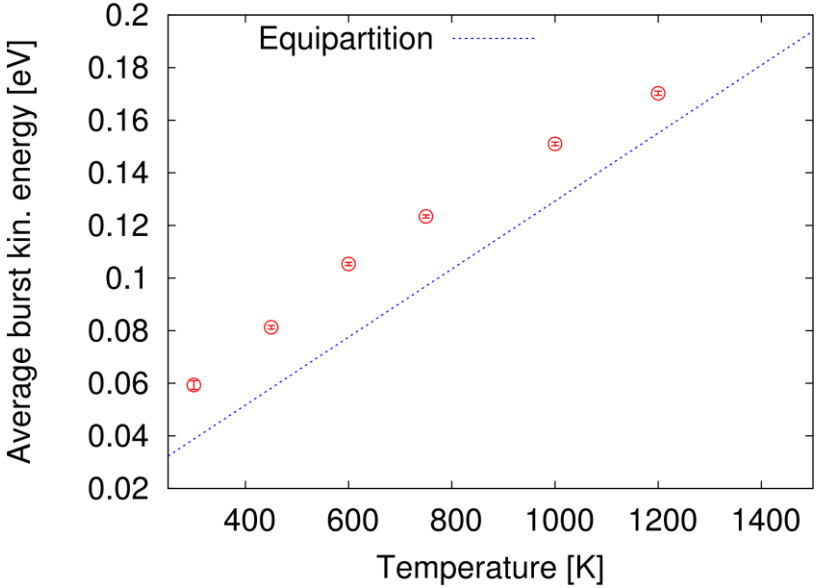

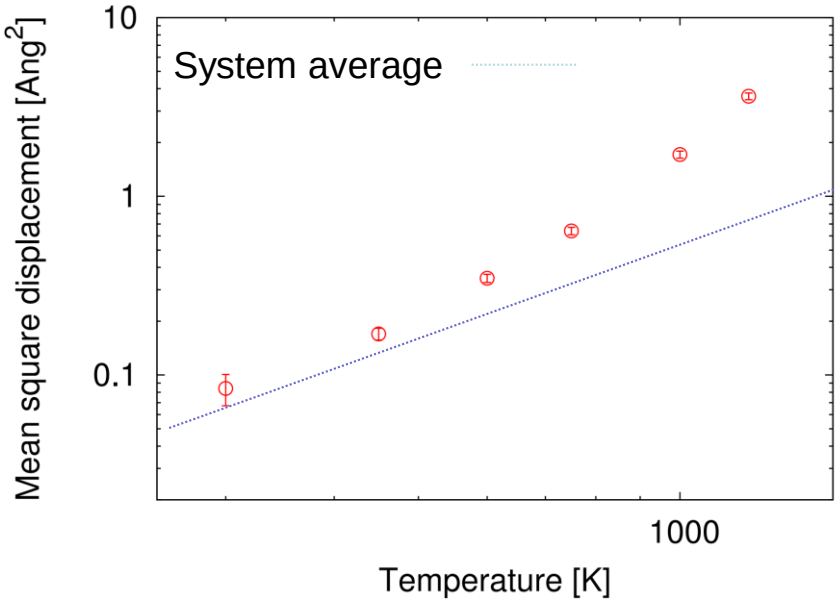

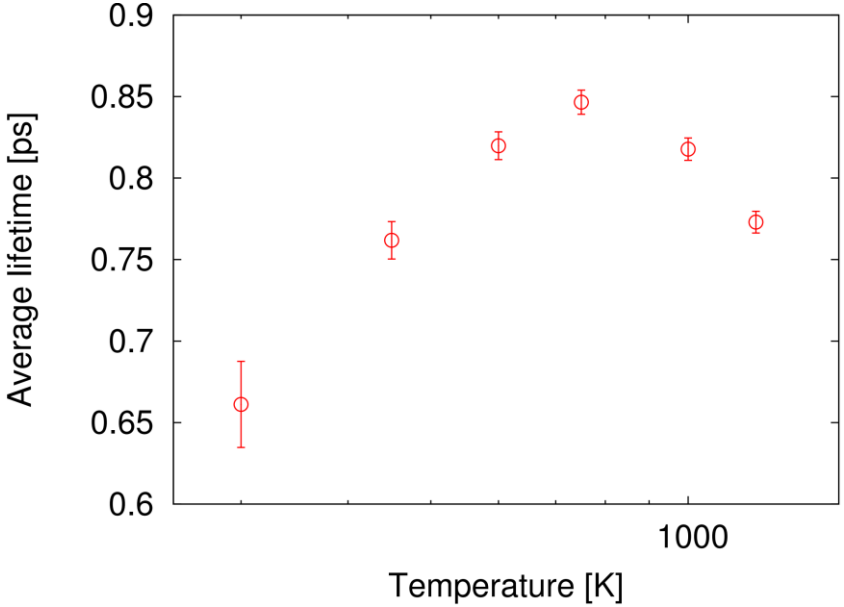

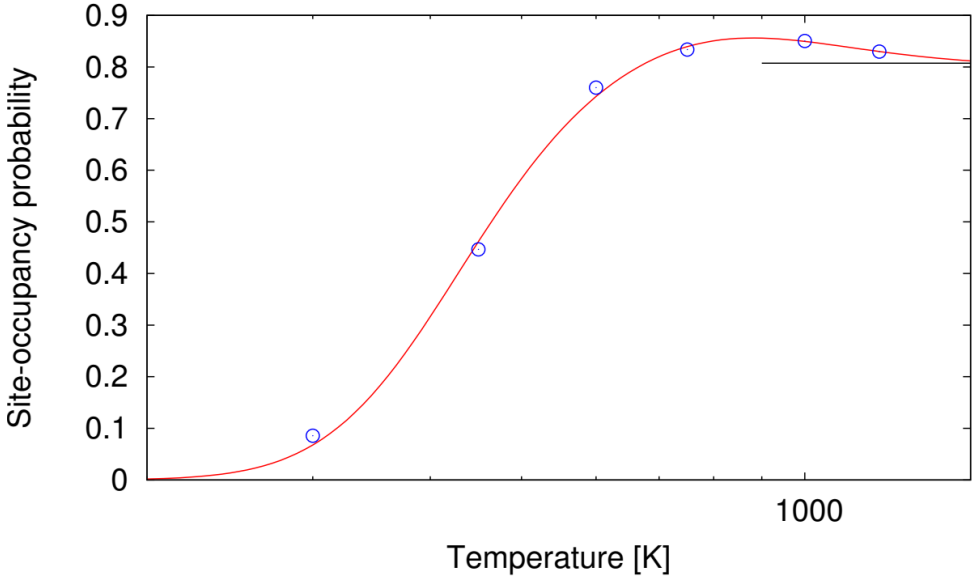

Nucleus	$\mathrm{Ni}^{A} + \mathrm{p}^{1} \longrightarrow \mathrm{Cu}^{A+1}$
Ni^{58}	$3,41$
Ni^{59}	$4,48$
Ni^{60}	$4,80$
Ni^{61}	$5,86$
Ni^{62}	$6,12$
Ni^{63}	$7,2$
Ni^{64}	$7,45$

$$\frac{1}{T} \approx 2\pi\omega_0 \left(\frac{2\pi\hbar\omega_0}{E_{nucl}}\right)^{\frac{1}{2}} \left(\frac{r_{nucl}}{\Lambda}\right)^3 \exp\left[-\frac{1}{2}\left(\frac{R_0}{\Lambda_0}\right)^2\right]$$

Mean MSD at 300K

LAV MSD at 300K

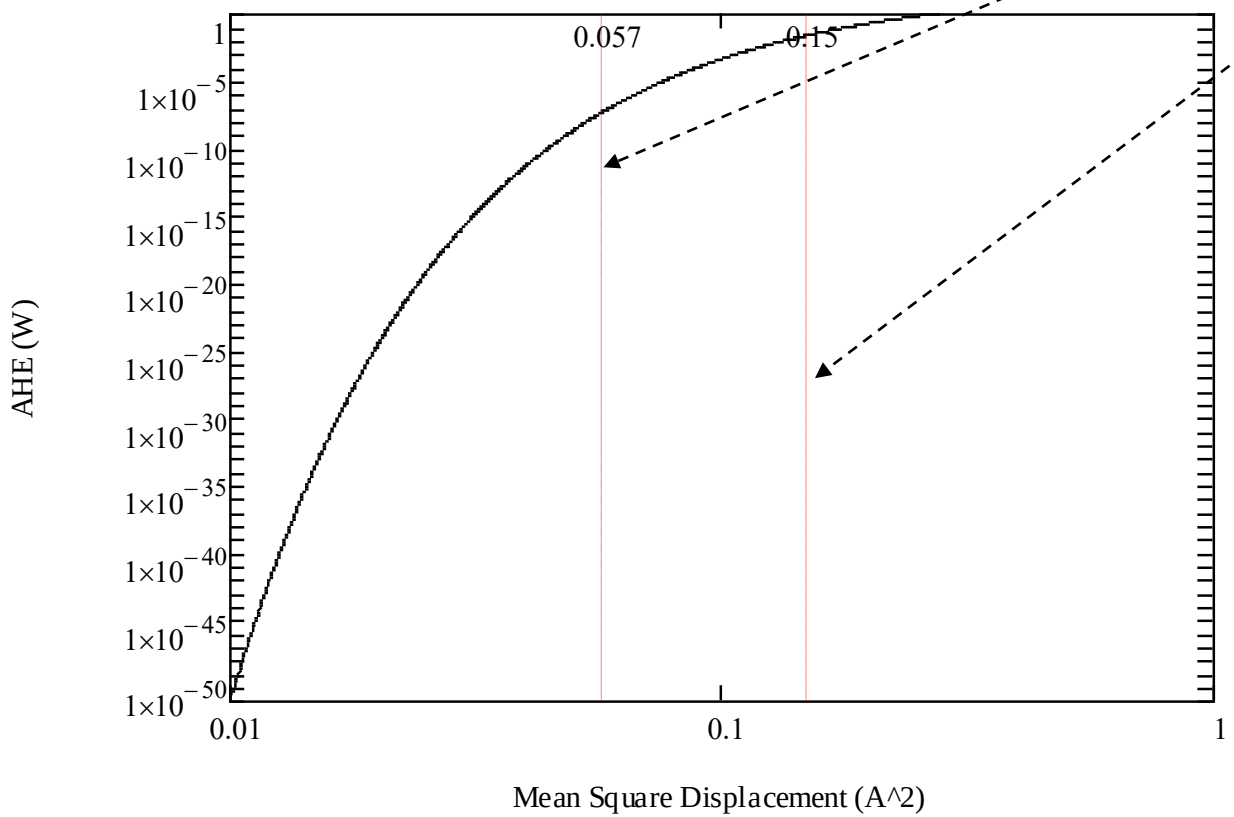

Magic Clusters

magic clusters (rus. кластеры, магические) — clusters of certain ("magic") sizes, which, due to their specific structure, have higher stability as compared to clusters of other sizes.

Number of atoms in the icosahedral cluster

$$n = (2N+1) + 10\sum_{k=1}^{N} k^2$$

$$n = 13, 55, 147, 309, 561$$

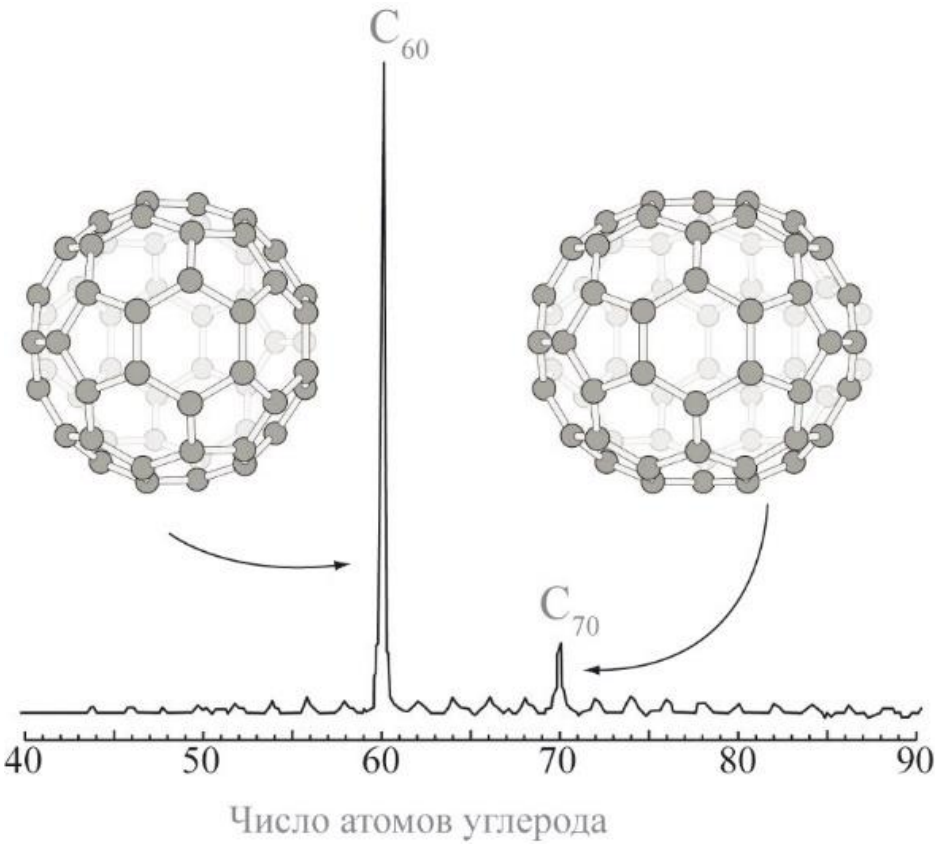

Mass spectrum of carbon clusters produced by laser evaporation of graphite. The highest peak corresponds to C_{60} fullerene molecules, and the less intensive peak represents C_{70} molecules

Quasi-crystaline Pd cluster

E0=0.1eV

Cluster of 13 Pd atoms with quasi-crystalline 5th order symmetry axis.

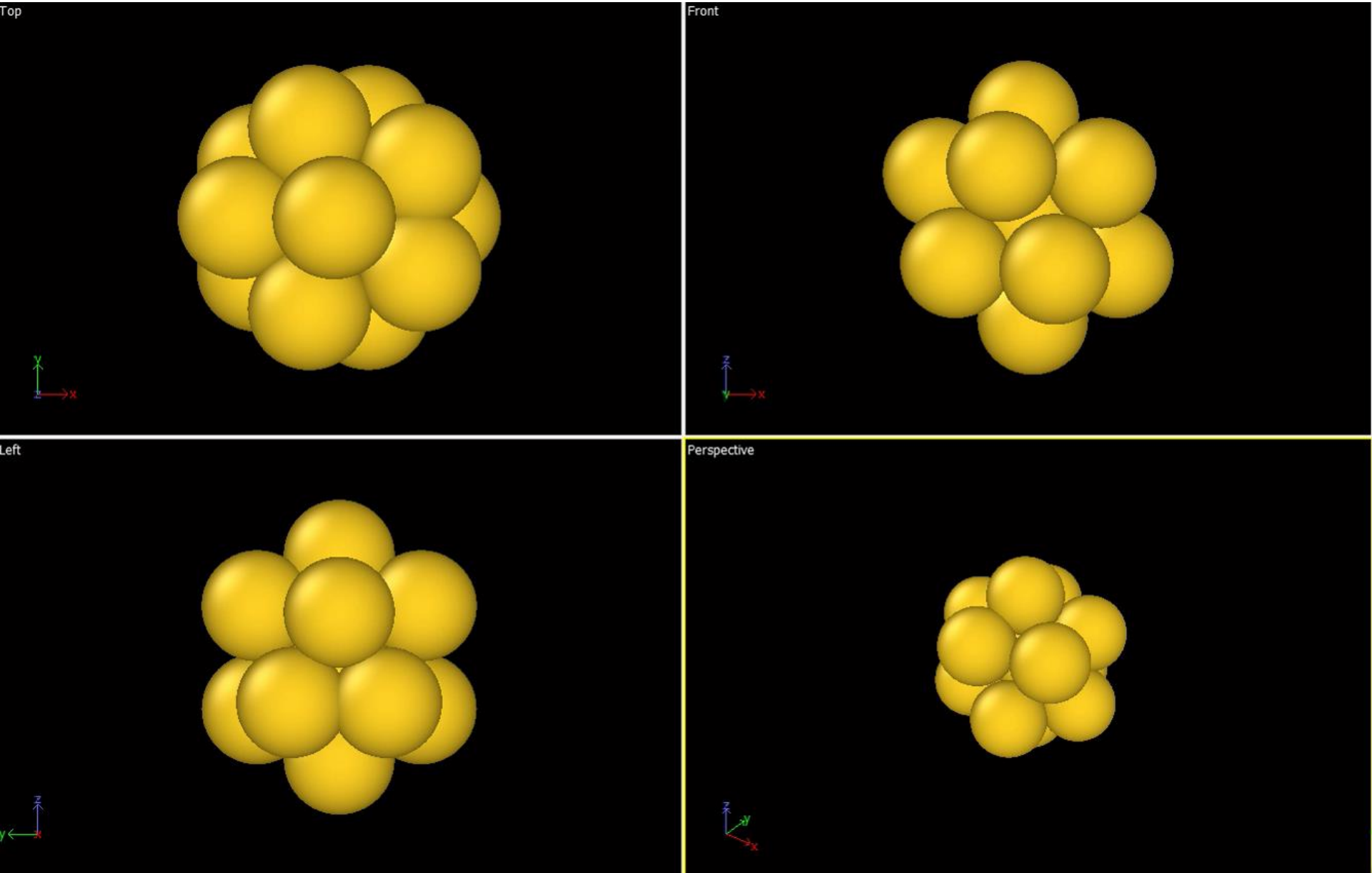

3d breather in a Magic cluster of 55 Pd atoms

with quasicrystalline 5th order symmetry axis.

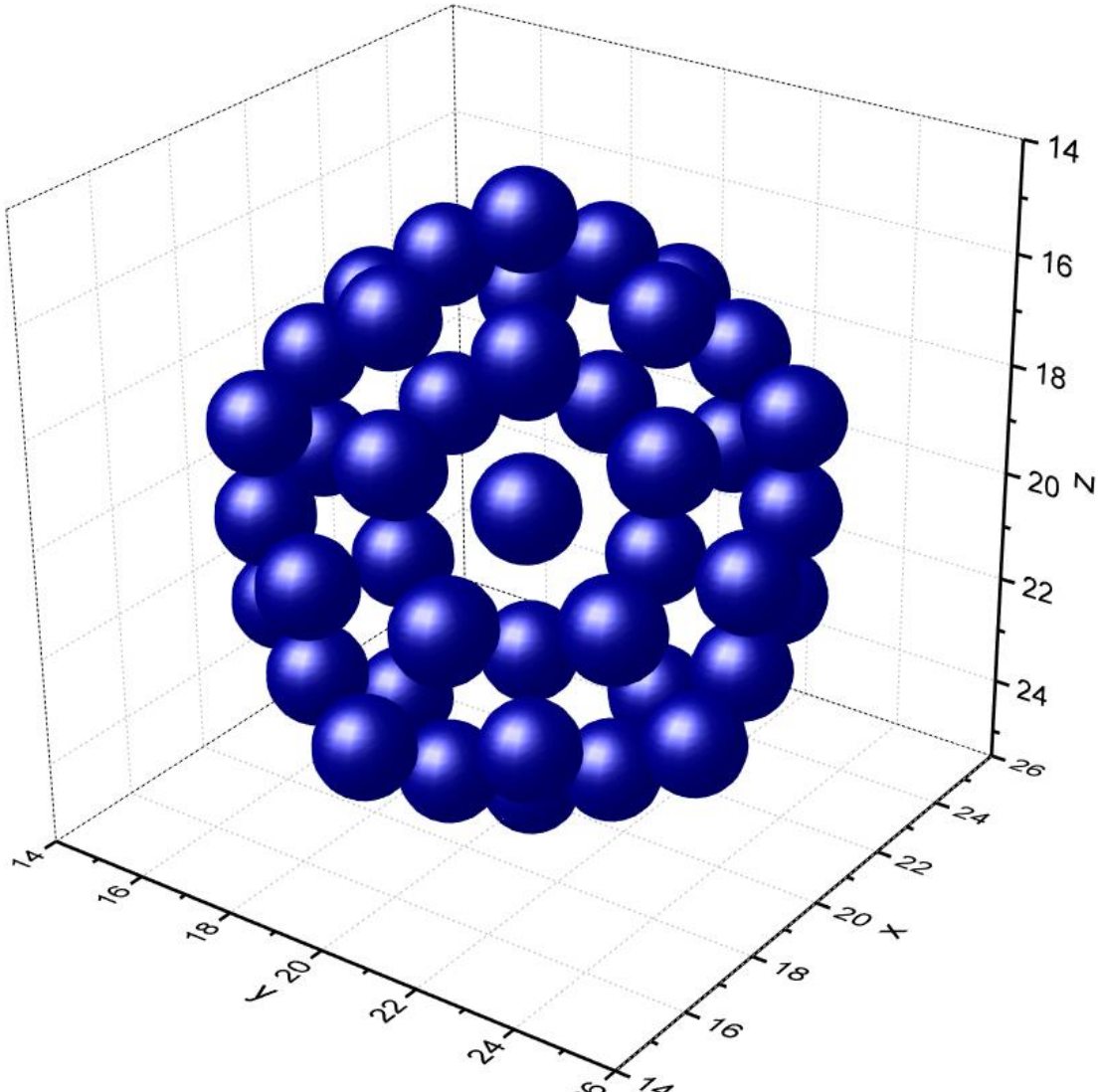

Icosahedral cluster of 55 Pd atoms

Initial conditions: at the initial time moment all particles have zero displacements from equilibrium positions.

Atom #1 has initial kinetic energy **1.5**eV in [00-1] direction.

Atom #12 has initial kinetic energy **1.5**eV in [001] direction

Boundary conditions: free surfaces of cluster

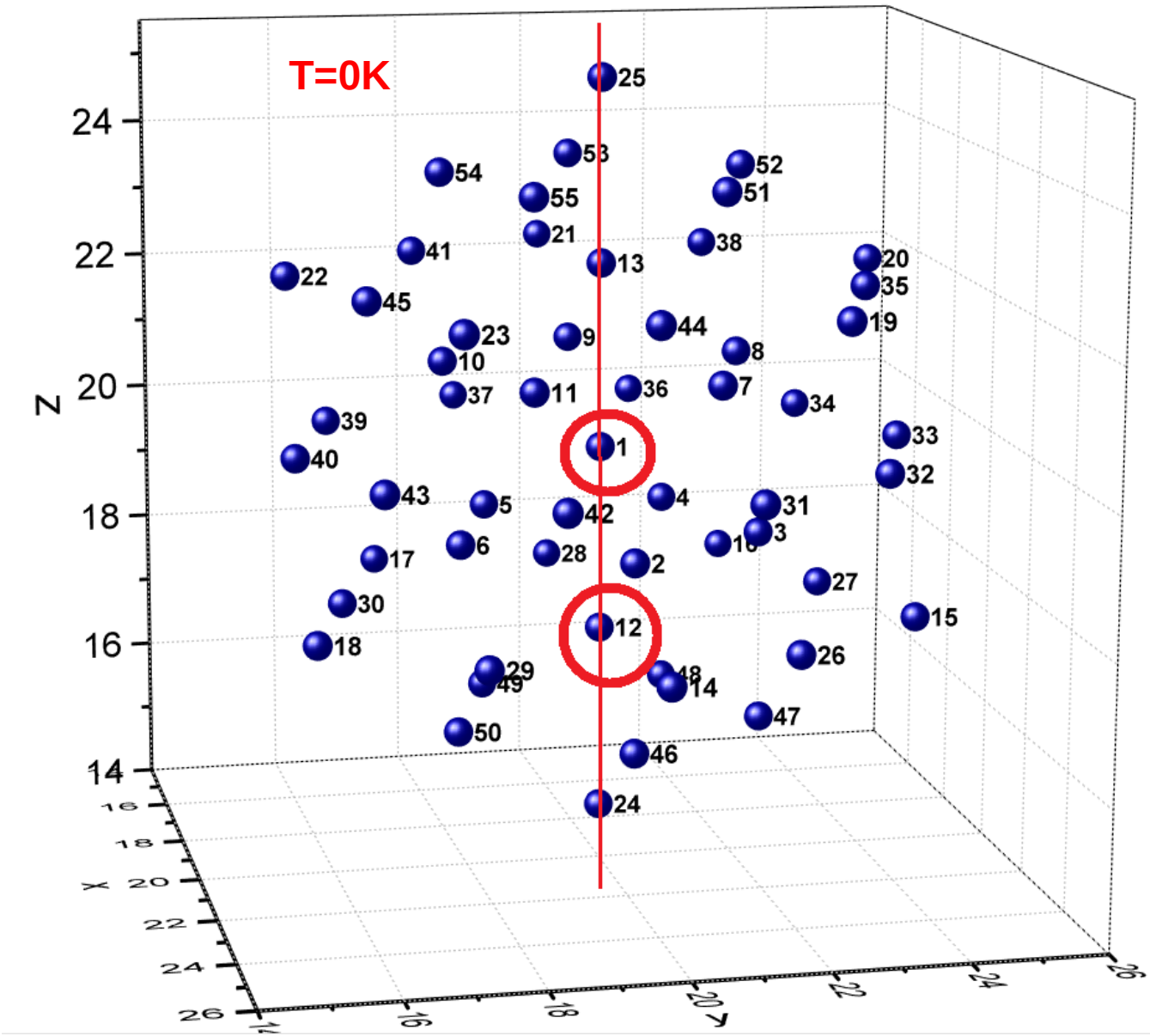

Dynamics of the icosahedral cluster of 55 Pd atoms

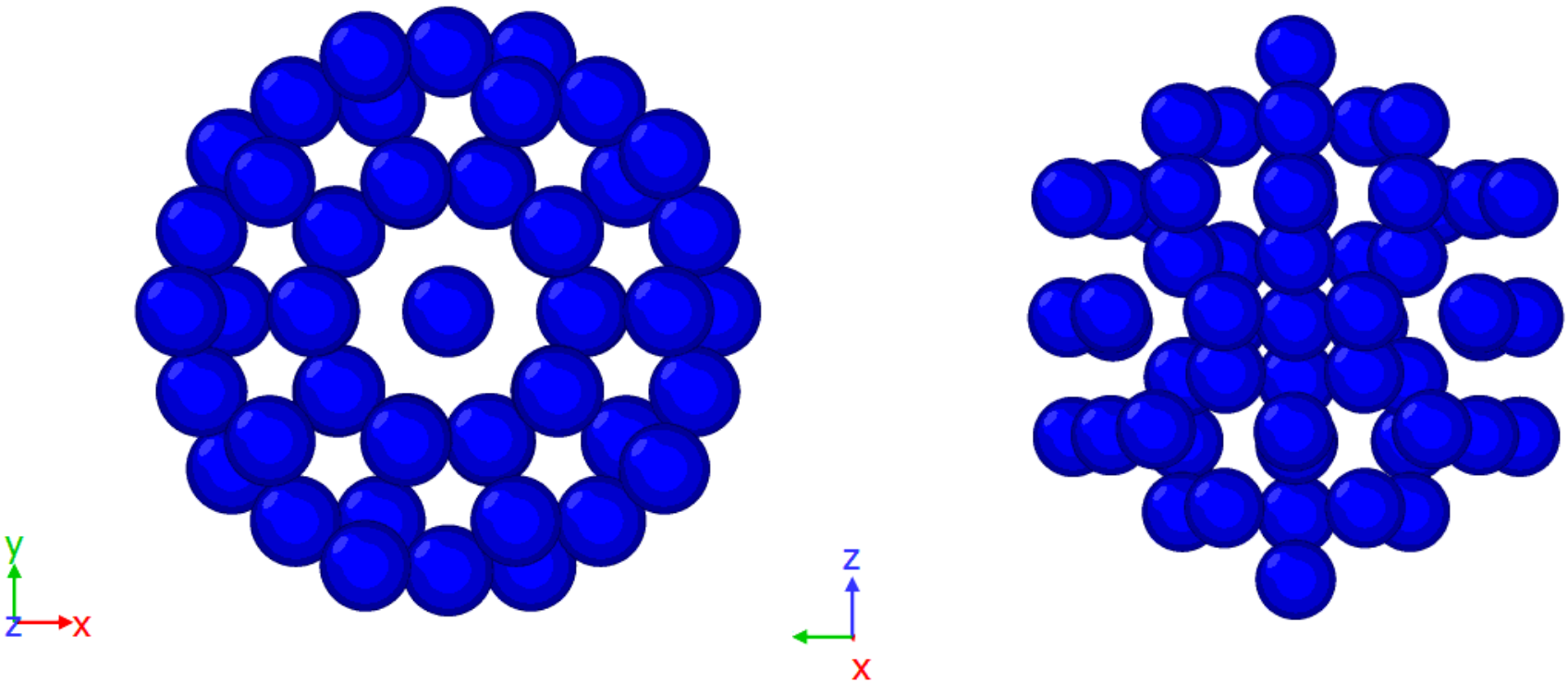

It is seen from the visualization, that Localized Anharmonic Vibration is generated. The observed LAV in the atomic cluster represents the coherent collective oscillations of Pd atoms along quasi-crystalline symmetry directions.

Computer Modeling of the Jitterbug Transformation of the Ni and Pd clusters

The aim of the research is the computer modeling of the Jitterbug transformation in the real physical objects – atomic clusters of palladium and nickel and investigation of the geometrical, mechanical, thermodynamical and quantum properties of these objects.

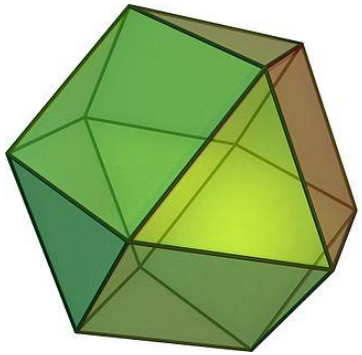

cuboctahedron

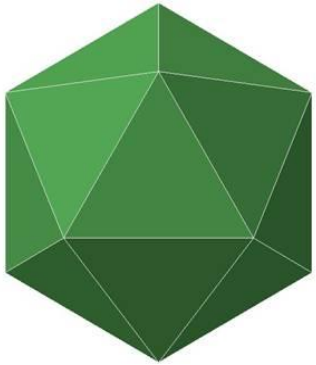

icosahedron

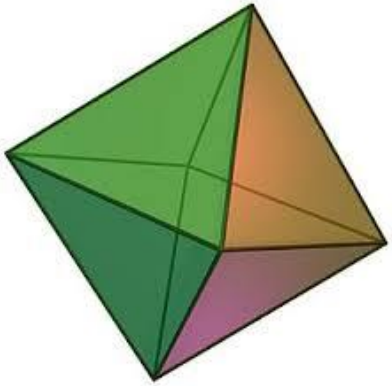

octahedron

Jitterbug Transformation Concept

"Jitterbug" is the name given by Fuller to a transformation of the "vector equilibrium" (VE) stick-model in which the 12 vertices move symmetrically. The jitterbug transforms smoothly a cuboctahedron into a regular octahedron with an intermediate icosahedral shape; thus it appears as a unifying motion between 4-fold (octahedral) and 5-fold (icosahedral) polyhedral symmetries.

“Vector equilibrium" (VE). R. Buckminster Fuller called "vector equilibrium" (VE) a set of 12 vectors in the space defined by the center and the 12 vertices of a cuboctahedron; the angles between each vector and its four "neighbours" are all 60° and the vectors are opposite by pairs. The VE is obviously related to the CCP (cubic close packing of spheres).

Cuboctahedron is the only spatial configuration in which the length the polyhedral edges is equal to that of the radial distance from its centre of gravity to any vertex.

Jitterbug Transformation Concept

"Jitterbug" is the name given by Fuller to a transformation of the "vector equilibrium" (VE) stick-model in which the 12 vertices move symmetrically. The jitterbug transforms smoothly a cuboctahedron into a regular octahedron with an intermediate icosahedral shape; thus it appears as a unifying motion between 4-fold (octahedral) and 5-fold (icosahedral) polyhedral symmetries.

“Vector equilibrium" (VE). R. Buckminster Fuller called "vector equilibrium" (VE) a set of 12 vectors in the space defined by the center and the 12 vertices of a cuboctahedron; the angles between each vector and its four "neighbours" are all 60° and the vectors are opposite by pairs. The VE is obviously related to the CCP (cubic close packing of spheres).

Cuboctahedron is the only spatial configuration in which the length the polyhedral edges is equal to that of the radial distance from its centre of gravity to any vertex.

For more information visit site:
http://maths.ac-noumea.nc/polyhedr/jitterbug_.htm

Ni13 CUBO-ICO Jitterbug Transition at T=0.1K

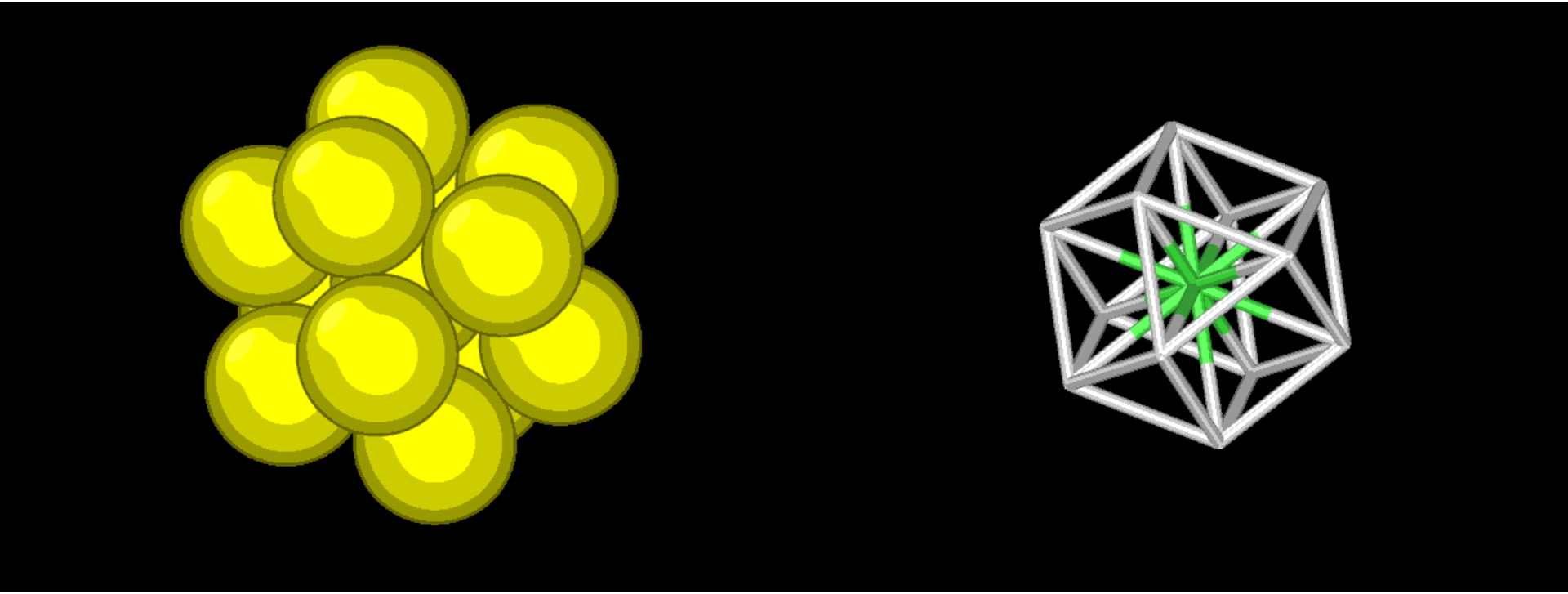

The modeling shows a Jitterbug transformation of the nickel cluster with 13 atoms from cuboctahedral to icosahedral symmetry at temperature T=0.1K

Difference of the Potential Energy of the Ni13_cubo and Ni13_ico cluster during Jitterbug Transition at T=0.1K

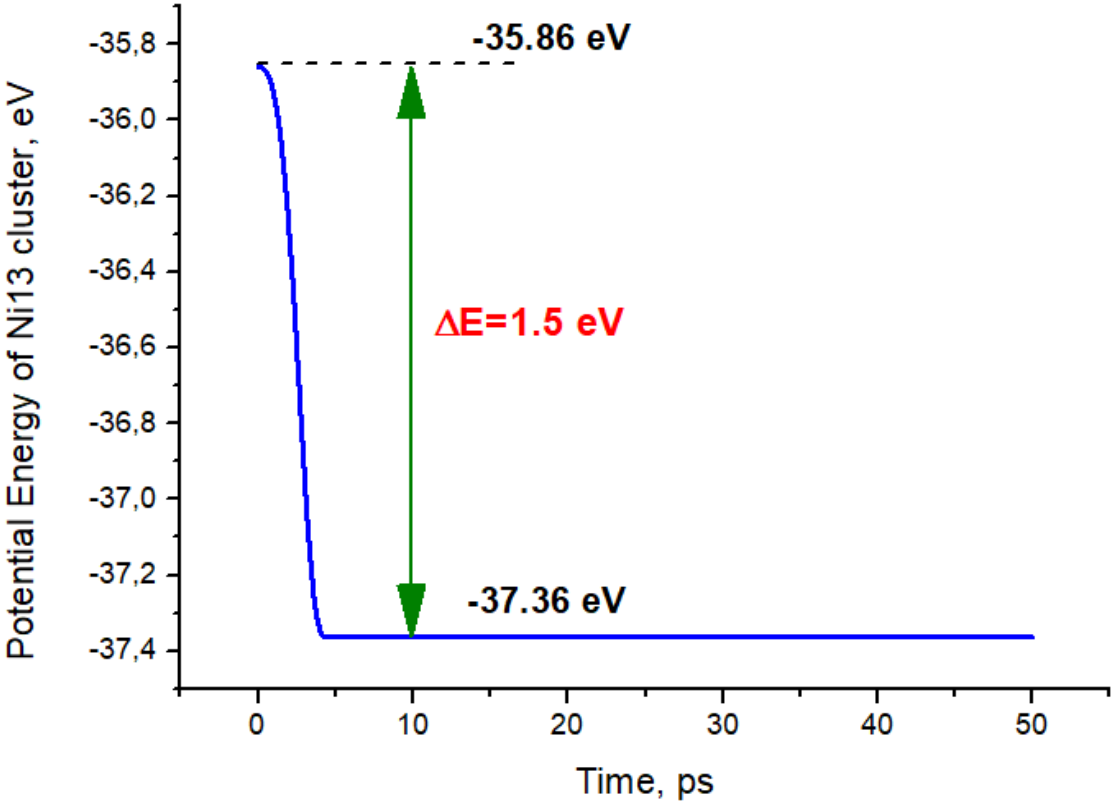

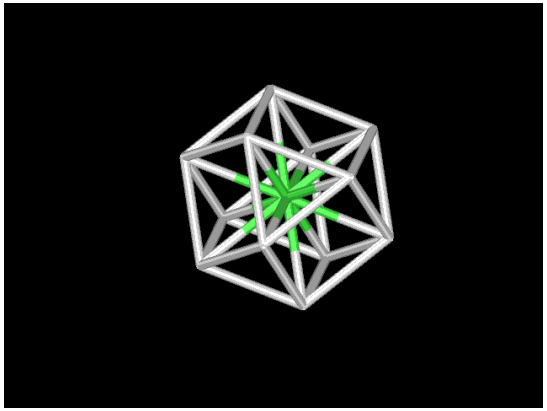

The potential energy of the cuboctahedral phase (-35.86 eV) is larger then for icosahedral phase (-37.36 eV).

Ni55 CUBO-ICO Jitterbug Transition at T=0.1K

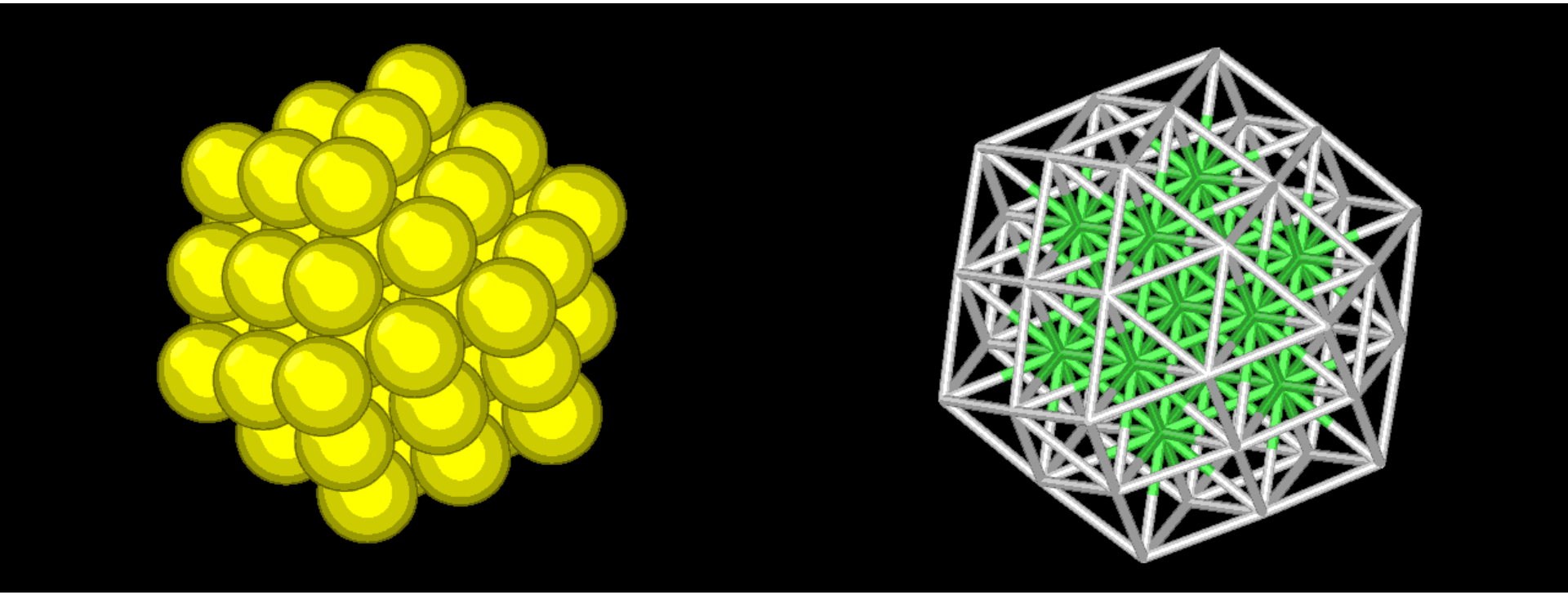

Difference of the Potential Energy of the Ni55_cubo and Ni55_ico cluster during Jitterbug Transition at T=0.1K

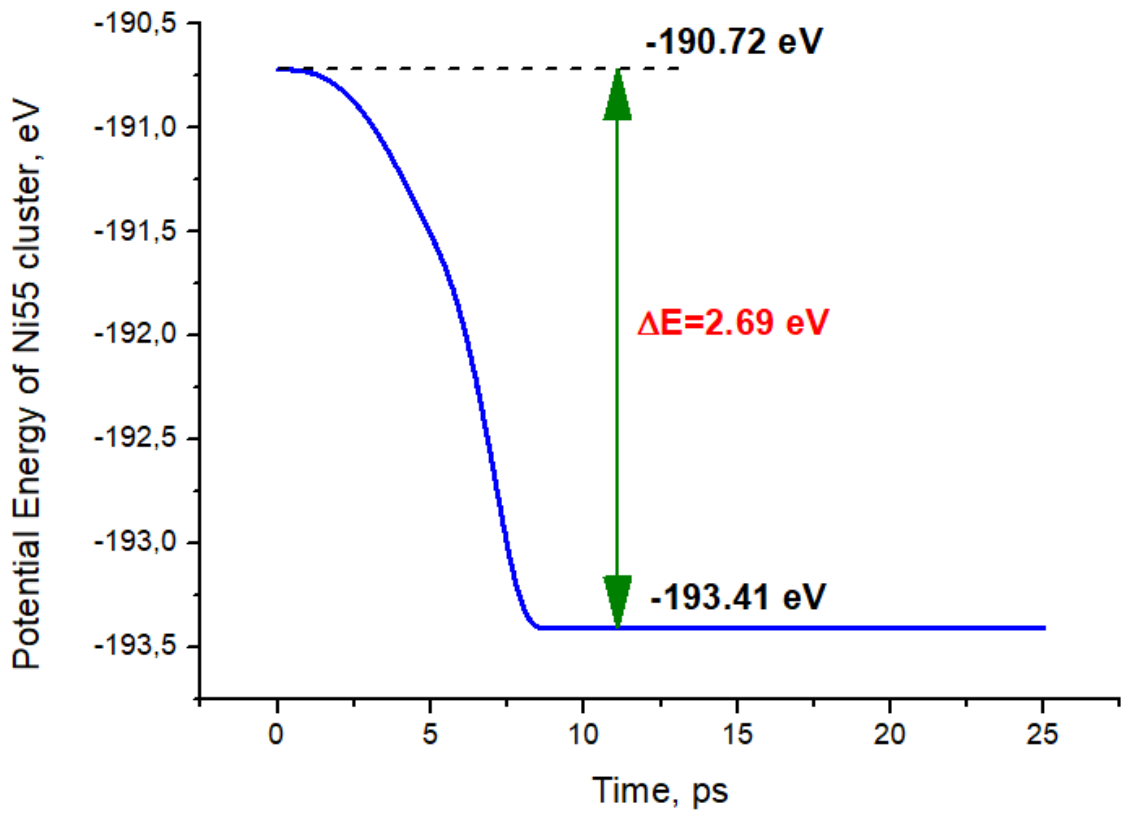

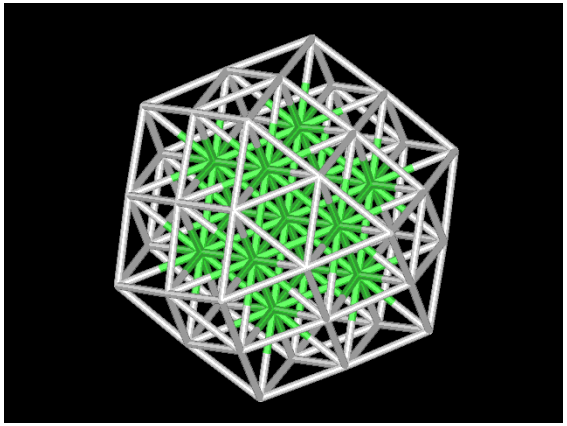

The potential energy of the cuboctahedral phase (-190.72 eV) is larger then for icosahedral phase (-193.41 eV).

Ni147 CUBO-ICO Jitterbug Transition at T=133K

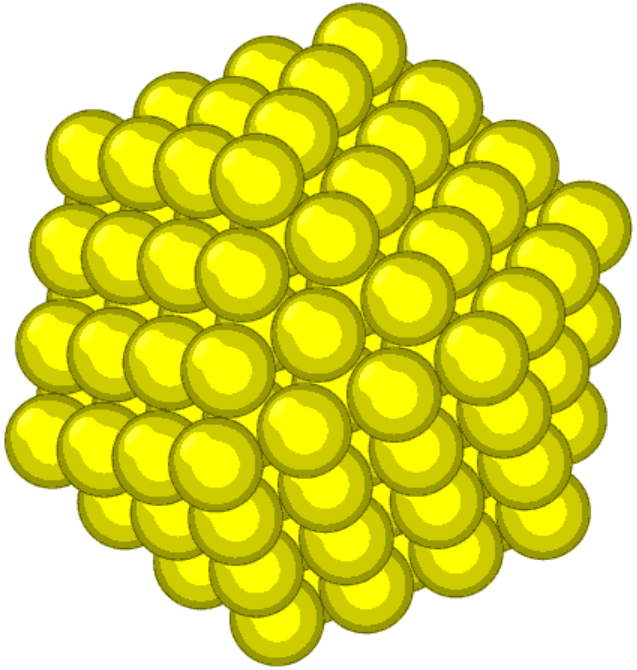

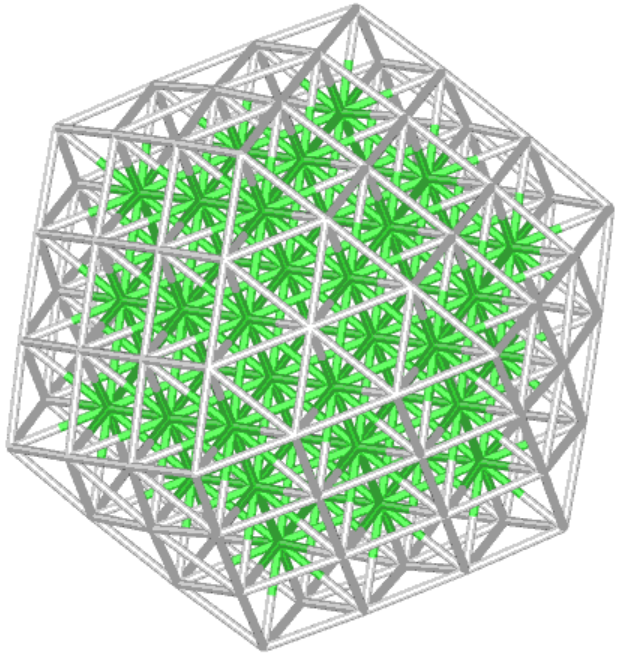

Difference of the Potential Energy of the Ni147_cubo and Ni147_ico cluster during Jitterbug Transition at T=133K

For Ni147 Jitterbug transition was observed at T=133K. For T<133K cuboctahedral cluster preserved it`s symmetry and didn`t transform to icosahedral cluster

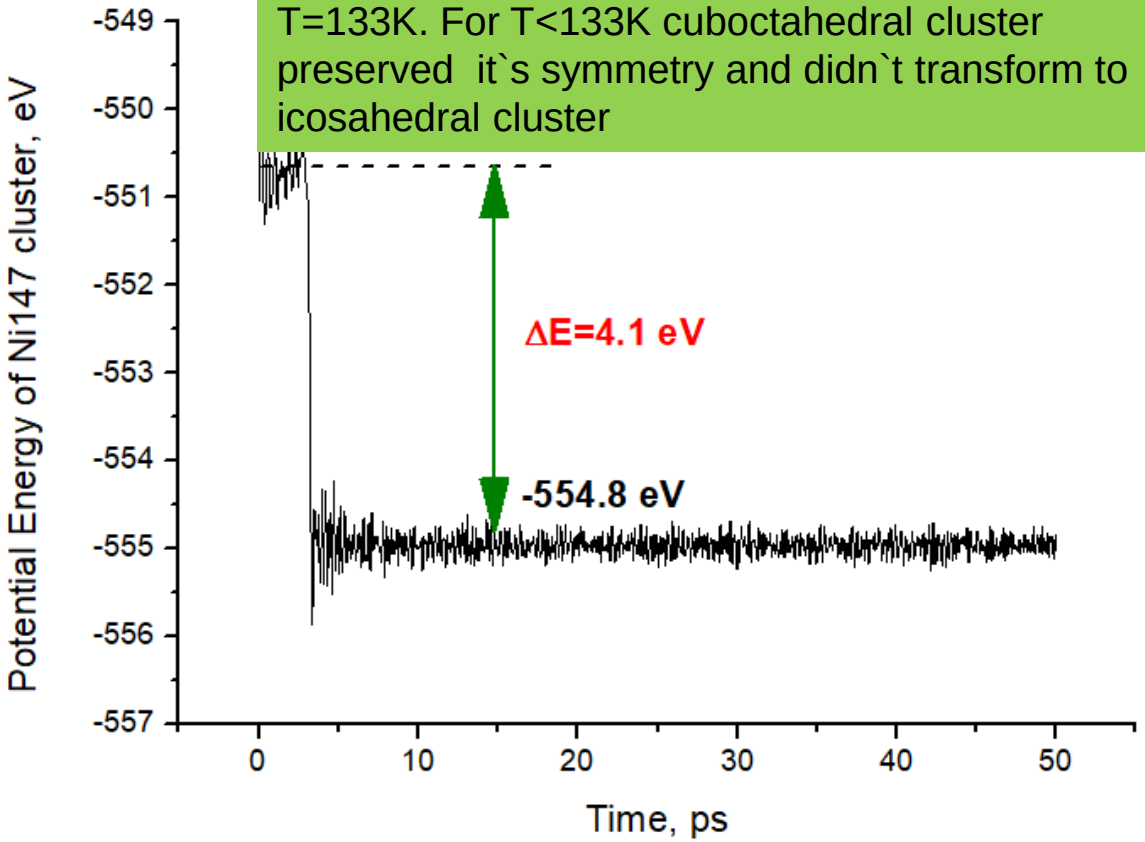

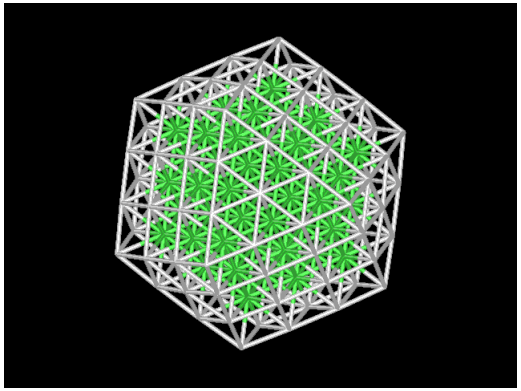

The potential energy of the cuboctahedral phase (-550.7 eV) is larger then for icosahedral phase (-554.8 eV).

Temperature of the Jitterbug Transition for Ni147 cluster. T=133K

For Ni147 Jitterbug transition was observed at T=133K. For T<133K cuboctahedral cluster preserved it`s symmetry and didn`t transform to icosahedral cluster

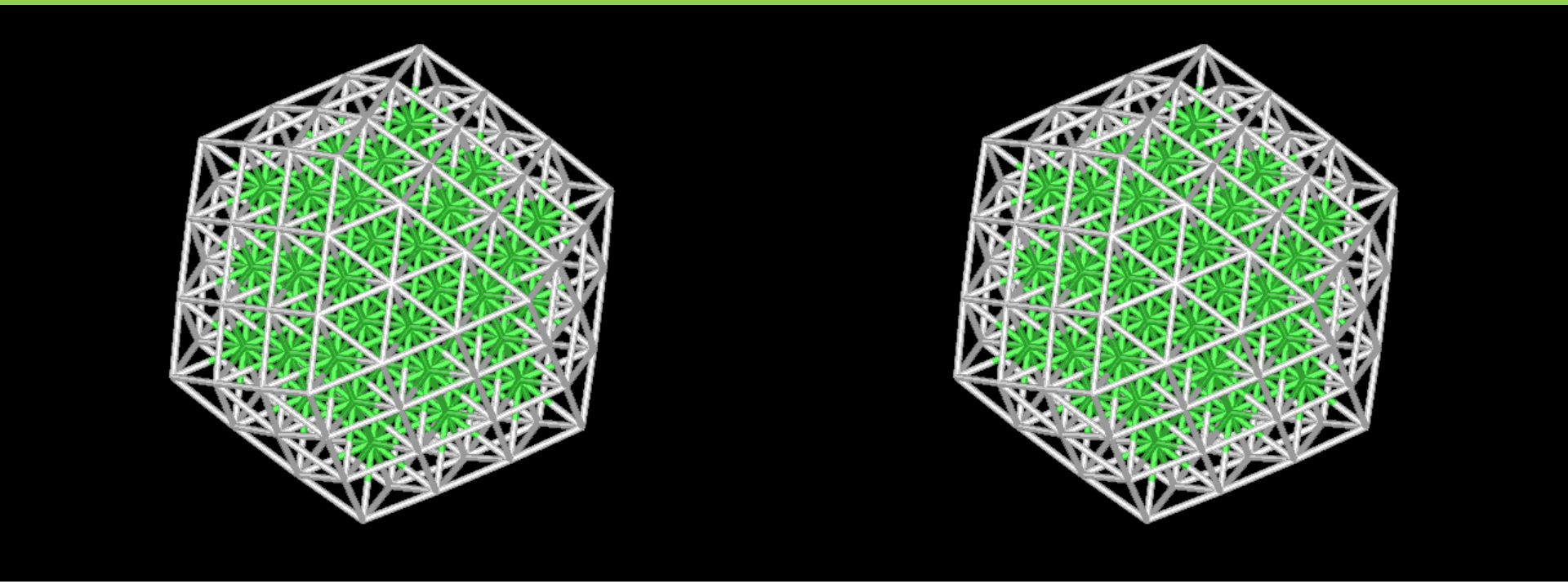

T=132K **T=133K (Jitterbug Transition)**

Jitterbug transformation for Pd13 cluster

Results: It was shown numerically that in Pd clusters a Jitterbug transition occurs.

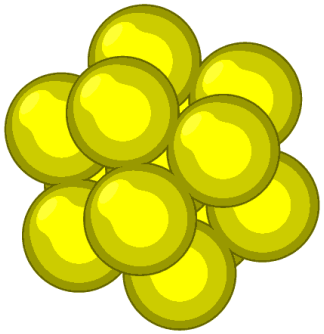

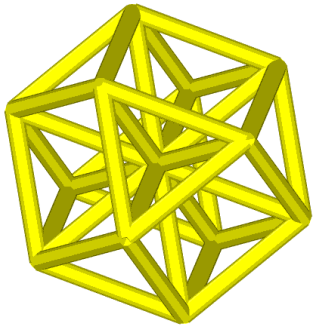

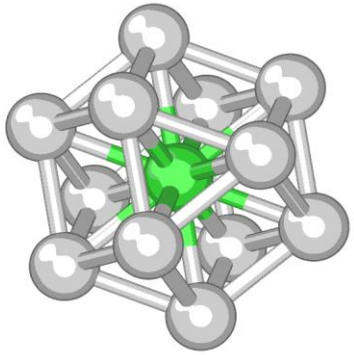

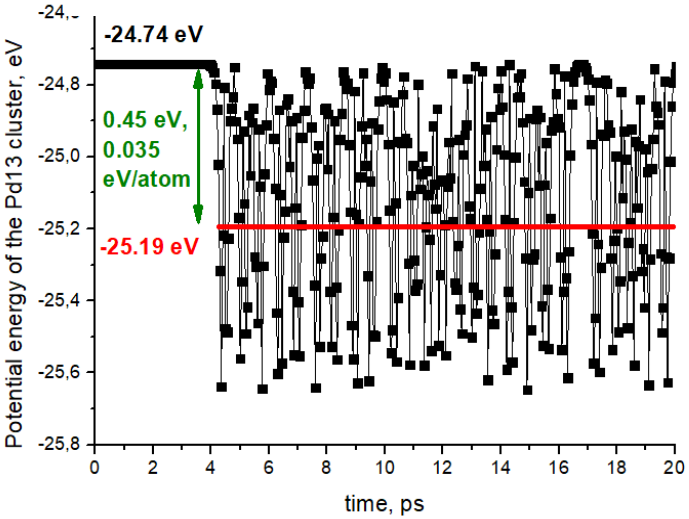

Pd55 cluster, dE=5.84eV

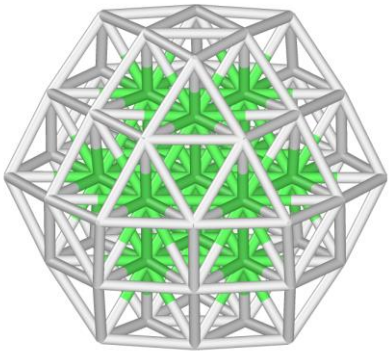

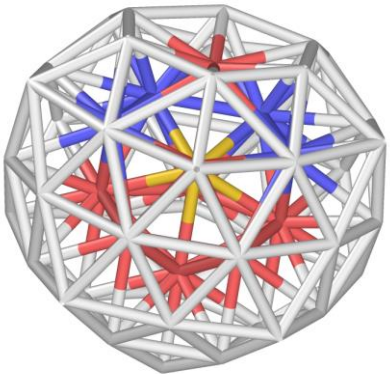

Pd147 cluster, dE=87eV

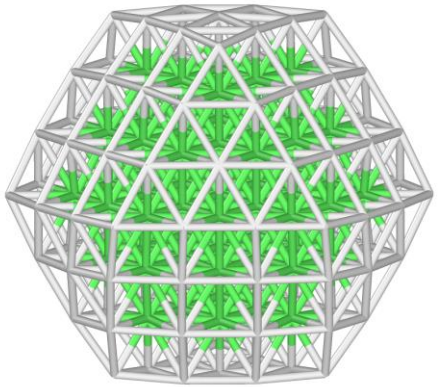

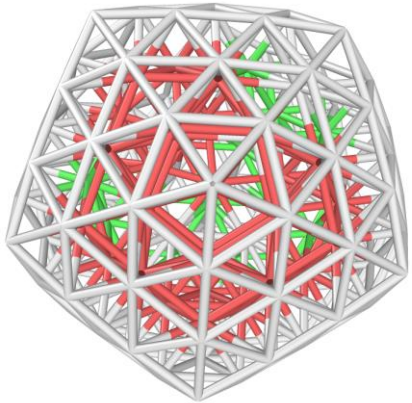

Preliminary Conclusions

- For palladium and nickel clusters with 13, 55 and 147 atoms a Jitterbug transformation (JT) from cuboctahedral to icosahedral morphology has been observed.
- It was shown that icosahedral symmetry is more energetically favorable then cuboctahedral.
- For nickel clusters with 13 and 55 atoms JT was observed for low temperatures (0.1K), for cluster with 147 atoms JT began at T=133K, for lower temperatures cuboctahedral Ni147 cluster preserved it`s symmetry and didn`t transform to icosahedral cluster.
- For palladium clusters with 13 atoms JT was observed for low temperatures (0.1K), for clusters with 55 and 147 atoms JT appeared when cluster was heated to high temperatures and after relaxation these clusters became icosahedral.

Outline of the present experiments

- Interaction of Ni with H and $LiAlH_4$ under heating and gamma irradiation
- Interaction of melt spun amorphous alloy Nd90Fe10 with H/D under heating and gamma irradiation
- Interaction of H/D with guest/host systems: (γ-Al2O3) and zeolites containing Pd nanoparticles.
- Interaction of H/D with Ti-Zr-Ni systems

Schematic picture of the reactor system

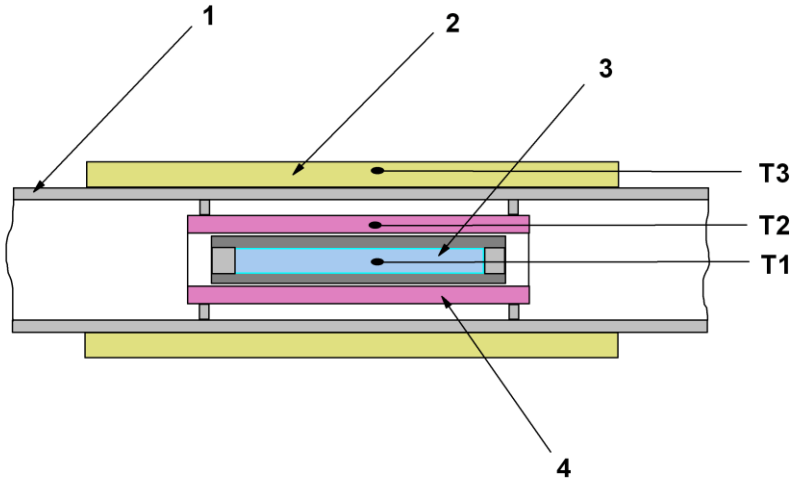

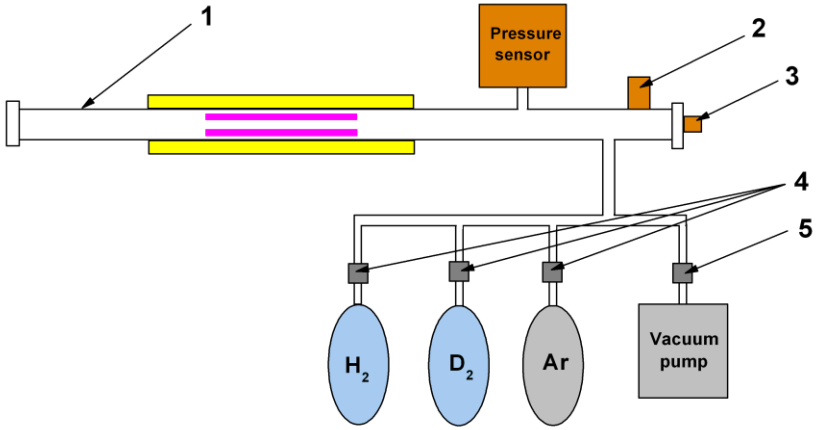

Ceramic tube (1); heat-insulation (2); experimental ‘fuel’ (3); ceramic tube with a heater (4).

Ceramic tube (1); with electric current inputs for the heater (2); flange for entering the thermocouples T1 and T2 (3) gas valves (4); vacuum valve (5)

Photo of the reactor system

Electron accelerator ELIAS at the NCS KIPT

Irradiation of the bremsstrahlung γ-quantum flux with a continuous energy spectrum, received on a tantalum convertor using an electron beam with the current of 160 μA and the energy of 2.5 MeV

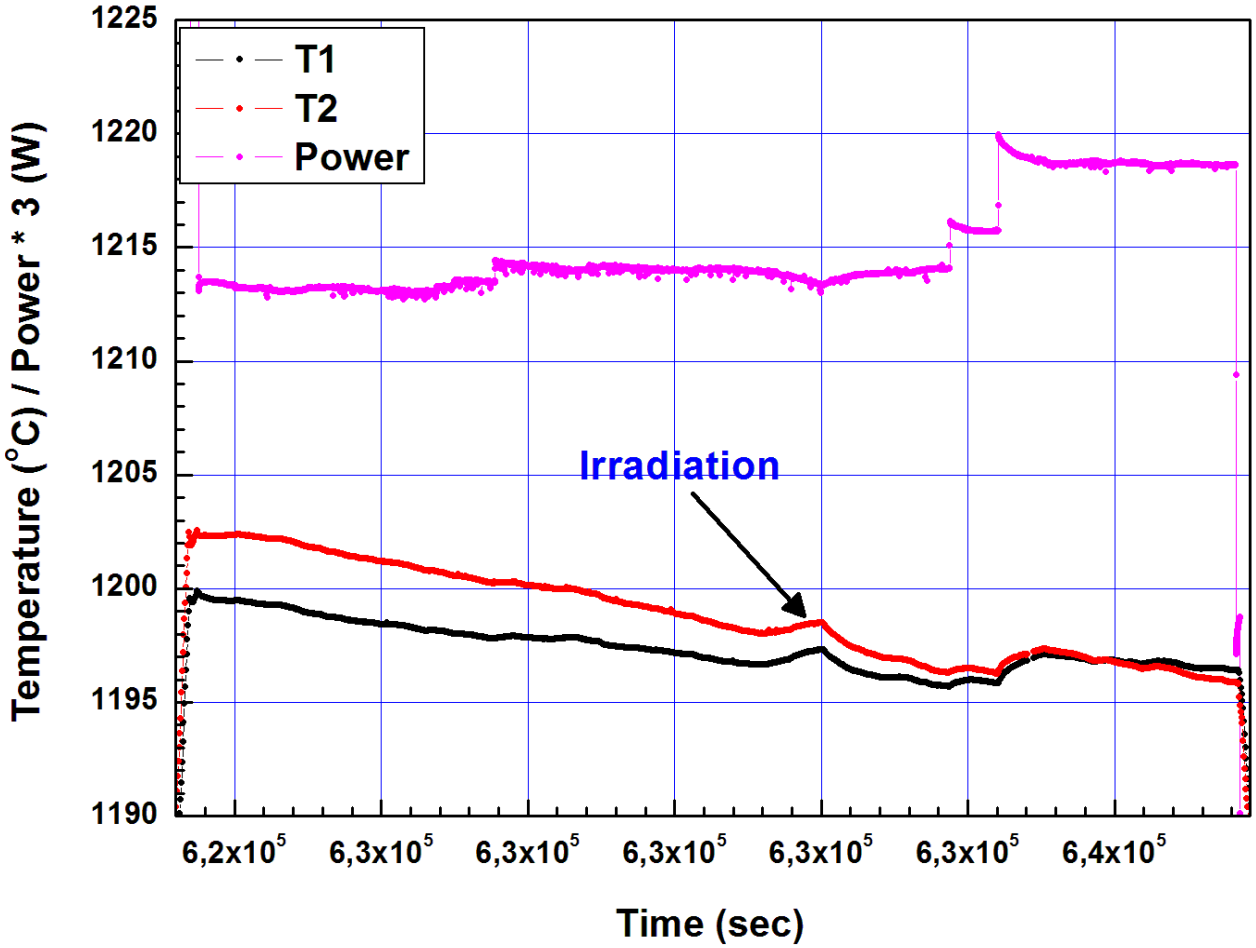

Summary of the heat production due to H/D interaction with samples under investigation

Sample -> _____ Stage	1.28 g of γ- Al_2O_3 + 0.5 wt% Pd_3.1 nm	1 g of γ- Al_2O_3 + 0.5 wt% Pd_3.6 nm	1.5 g of PdLaCaX+ 0.2 wt% Pd_4.0 nm	2 g of LaCaPdY+ 1 wt% Pd_2.9 nm	1.1 g of PdCaX+1 wt% Pd_5.5 nm
1	122 J total 170 kJ /moleD2 1 MJ / molePd	90.7 J total 255 kJ/moleD2 1.85 MJ/mole Pd	45 J total 76 kJ/moleD2 1.6 MJ/molePd + 0/moleH2	153 J total 216 kJ/moleD2 1.36 MJ/molePd	73.5 J total 277 kJ/moleD2 0.71 MJ/molePd
2	18 J total 77 kJ / moleH2 150 kJ /molePd	125 J total 188 kJ/moleH2 2.55 MJ/molePd	13 J total 224 kJ/moleD2 0.46 MJ/molePd + 0/moleH2	50 J total 232 kJ/moleD2 0.44 MJ/molePd	
3	80 J total 132 kJ /moleH2 667 kJ/molePd	218 J total 210 kJ/moleD2 4.45 MJ/molePd			
4	120 J total 174 kJ /moleD2 1 MJ /molePd	74 J total 198 kJ/moleD2 1.51 MJ/molePd			
5	126 J total 203 kJ/moleD2 1.05MJ/molePd				
6	30 J total 100 kJ/moleH2 250 kJ/molePd				

The heat production in Pd/zeolite samples per one absorbed deuterium molecule were in the range of (216÷277) kJ/moleD2, which is close to the heat of hydrogen combustion in oxygen

Conclusions and outlook

New mechanism of catalysis in solids is proposed, based on quasi **time-periodic driving** of the potential landscape induced by **LAV**s.

At high T, LAVs may result in effective lowering of the reaction activation barrier.

At low T, LAVs may result in enhancing the tunneling through the potential barrier

Outstanding problems:

Experimental verification of LENR !!!

Publications

1. V.I. Dubinko, P.A. Selyshchev and F.R. Archilla, *Reaction-rate theory with account of the crystal anharmonicity*, **Phys. Rev**. **E** 83 (2011**),**041124-1-13
2. V.I. Dubinko, F. Piazza, *On the role of disorder in catalysis driven by discrete breathers*, **Letters on Materials** 4 (2014) 273-278.
3. V.I. Dubinko, *Low-energy Nuclear Reactions Driven by Discrete Breathers*, **J. Condensed Matter Nucl. Sci**., 14, (2014) 87-107.
4. V.I. Dubinko, *Quantum tunneling in gap discrete breathers*, **Letters on Materials**, 5 (2015) 97-104.
5. V.I. Dubinko, *Quantum Tunneling in Breather 'Nano-colliders'*, **J. Condensed Matter Nucl. Sci.**, 19, (2016) 1-12.
6. V. I. Dubinko, D. V. Laptev, *Chemical and nuclear catalysis driven by localized anharmonic vibrations*, **Letters on Materials** 6 (2016) 16–21.
7. V. I. Dubinko, *Radiation-induced catalysis of low energy nuclear reactions in solids***, J. Micromechanics and Molecular Physics**, 1 (2016) 165006 -1-12.
8. V. I. Dubinko, D. V. Laptev, A. S. Mazmanishvili, J. F. R. Archilla*, "Quantum dynamics of wave packets in a nonstationary parabolic potential and the Kramers escape rate theory", J. Micromechanics and Molecular Physics*, **1**, 650010 -1-12 (2016)
9. Dubinko V., Laptev D., Irwin K., Catalytic mechanism of LENR in quasicrystals based on localized anharmonic vibrations and phasons, **J. Condensed Matter Nucl. Sci.** -2017.-V. 24.- P. 1-12

THANK YOU
FOR YOUR ATTENTION!